Gregory M. Fahy *Editor-in-Chief*

Michael D. West · L. Stephen Coles
Steven B. Harris *Associate Editors*

The Future of Aging

Pathways to Human Life Extension

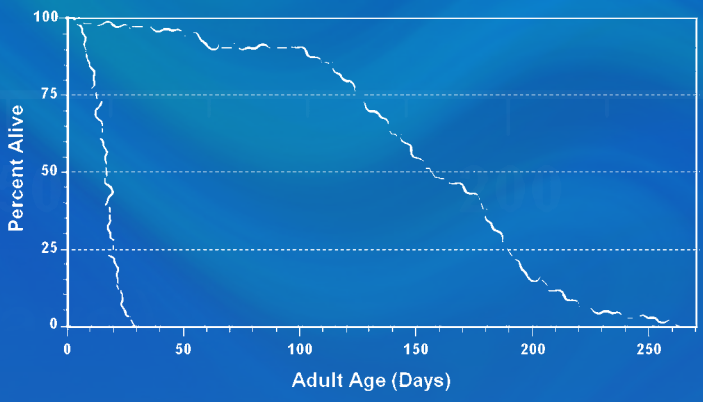

Springer

Editors
Gregory M. Fahy
Intervene Biomedical, LLC
Norco CA 92860
Box 478
USA
gfahy@sbcglobal.net

Dr. Michael D. West
BioTime, Inc.
1301 Harbor Bay Parkway
Alameda CA 94502
USA
mwest@biotimemail.com

L. Stephen Coles
817 Levering Ave.
Los Angeles CA 90024
Apt. 3
USA

Stephen B. Harris
10743 Civic Center Drive
Rancho Cucamonga CA
91730
USA

ISBN 978-90-481-3998-9 e-ISBN 978-90-481-3999-6
DOI 10.1007/978-90-481-3999-6
Springer Dordrecht Heidelberg London New York

Library of Congress Control Number: 2010927444

Cover illustration: On the cover: The small nematode worm, *C. elegans* (wavy lines), can realize some very large gains in lifespan. Compared to the standard N2DRM (wild-type) worm, worms with a strong mutation in a single gene (the age-1 mg44 allele) can live 10 times longer, and can do so in excellent health. This striking result brings into question the very nature of aging, and raises the possibility of someday extending the lifespans of humans in good health as well. The latter subject is the theme taken up in this book.

Printed on acid-free paper

Springer is part of Springer Science+Business Media (www.springer.com)

Chapter 23
Comprehensive Nanorobotic Control of Human Morbidity and Aging

Robert A. Freitas Jr.

Contents

R.A. Freitas Jr. (✉)
The Institute for Molecular Manufacturing, Palo Alto, CA, USA
e-mail: rfreitas@rfreitas.com

G.M. Fahy et al. (eds.), *The Future of Aging*, DOI 10.1007/978-90-481-3999-6_23,

23.1 A Vision of Future Medicine

Mankind is nearing the end of a historic journey. The 19th century saw the establishment of what we think of today as scientific medicine. But human health is fundamentally biological, and biology is fundamentally molecular. As a result, throughout the 20th century scientific medicine began its transformation from a merely rational basis to a fully molecular basis. First, antibiotics that interfered with pathogens at the molecular level were introduced. Next, the ongoing revolutions in genomics, proteomics and bioinformatics (Baxevanis and Ouellette 1998) began to provide detailed and precise knowledge of the workings of the human body at the molecular level. Our understanding of life advanced from organs, to tissues, to cells, and finally to molecules. By the end of the 20th century the entire human genome was finally mapped, inferentially incorporating a complete catalog of all human proteins, lipids, carbohydrates, nucleoproteins and other biomolecules.

By the early 21st century, this deep molecular familiarity with the human body, along with continuing nanotechnological engineering advances, has set the stage for a shift from present-day molecular scientific medicine in which fundamental new discoveries are constantly being made, to a future molecular technologic medicine in which the molecular basis of life, by then well-known, is manipulated to produce specific desired results. The comprehensive knowledge of human molecular structure so painstakingly acquired during the previous century will be extended and employed in this century to design medically-active microscopic machines. These machines, rather than being tasked primarily with voyages of pure discovery, will instead most often be sent on missions of cellular inspection, repair and reconstruction. The principal focus will shift from medical science to medical engineering. Nanomedicine (Freitas 1999, 2003) will involve designing and building a vast proliferation of incredibly efficacious molecular devices, and then deploying these devices in patients to establish and maintain a continuous state of human healthiness.

"Physicians aim to make tissues healthy," wrote one early pioneer (Drexler 1986) in medical nanorobotics, "but with drugs and surgery they can only encourage tissues to repair themselves. Molecular machines will allow more direct repairs, bringing a new era in medicine. Systems based on nanomachines will generally be more compact and capable than those found in nature. Natural systems show us

only lower bounds to the possible, in cell repair as in everything else. By working along molecule by molecule and structure by structure, repair machines will be able to repair whole cells. By working along cell by cell and tissue by tissue, they (aided by larger devices, where need be) will be able to repair whole organs. By working through a [patient], organ by organ, they will restore health. Because molecular machines will be able to build molecules and cells from scratch, they will be able to repair even cells damaged to the point of complete inactivity. Thus, cell repair machines will bring a fundamental breakthrough: they will free medicine from reliance on self-repair as the only path to healing."

23.2 Nanotechnology, Nanomedicine and Medical Nanorobotics

The only important difference between the carbon atoms in a plain lump of coal and the carbon atoms in a stunning crystal of diamond is their molecular arrangement, relative to each other. Future technology currently envisioned will allow us to rearrange atoms the way we want them, consistent with natural laws, thus permitting the manufacture of artificial objects of surpassing beauty and strength that are far more valuable than bulk diamonds. This is the essence of **nanotechnology**: the control of the composition and structure of matter at the atomic level. The prefix "nano-" refers to the scale of these constructions. A nanometer is one-billionth of a meter, the width of about 5 carbon atoms nestled side by side.

Nanotechnology involves the engineering of molecularly precise structures and, ultimately, molecular machines. BCC Research (McWilliams, 2006) estimates the global market for nanotools and nanodevices was $1.3B in 2005 and $1.5B in 2006, projected to reach $8.6B by 2011 and rapidly gaining on the slower-growing nanomaterials market which is estimated at $8.1B (2005), $9.0B (2006) and $16.6B (2011). As distinct from nanoscale materials and today's simple nanotools and nanodevices having nanoscale features, molecular nanotechnology encompasses the concept of engineering functional mechanical systems at the molecular scale – that is, machines at the molecular scale designed and built to atomic precision. Molecular manufacturing (Section 23.4) would make use of positionally-controlled mechanosynthesis (mechanically-mediated chemistry) guided by molecular machine systems to build complex products, including additional nanomachines.

Nanomedicine (Freitas 1999, 2003) is the application of nanotechnology to medicine: the preservation and improvement of human health, using molecular tools and molecular knowledge of the human body. Nanomedicine encompasses at least three types of molecularly precise structures (Freitas 2005a): nonbiological nanomaterials, biotechnology materials and engineered organisms, and nonbiological devices including diamondoid nanorobotics. In the near term, the molecular tools of nanomedicine will include biologically active nanomaterials and nanoparticles having well-defined nanoscale features. In the mid-term (5–10 years), knowledge

gained from genomics and proteomics will make possible new treatments tailored to specific individuals, new drugs targeting pathogens whose genomes have been decoded, and stem cell treatments. Genetic therapies, tissue engineering, and many other offshoots of biotechnology will become more common in therapeutic medical practice. We also may see biological robots derived from bacteria or other motile cells that have had their genomes re-engineered and re-programmed, along with artificial organic devices that incorporate biological motors or self-assembled DNA-based structures for a variety of useful medical purposes.

In the farther term (2020s and beyond), the first fruits of **medical nanorobotics** – the most powerful of the three classes of nanomedicine technology, though clinically the most distant and still mostly theoretical today – should begin to appear in the medical field. Nanotechnologists will learn how to build nanoscale molecular parts like gears, bearings, and ratchets. Each nanopart may comprise a few thousand precisely placed atoms. These mechanical nanoparts will then be assembled into larger working machines such as nanosensors, nanomanipulators, nanopumps, nanocomputers, and even complete nanorobots which may be micron-scale or larger. The presence of onboard computers is essential because in vivo medical nanorobots will be called upon to perform numerous complex behaviors which must be conditionally executed on at least a semiautonomous basis, guided by receipt of local sensor data and constrained by preprogrammed settings, activity scripts, and event clocking, and further limited by a variety of simultaneously executing real-time control protocols and by external instructions sent into the body by the physician during the course of treatment. With medical nanorobots in hand, doctors should be able to quickly cure most diseases that hobble and kill people today, rapidly repair most physical injuries our bodies can suffer, and significantly extend the human healthspan.

The early genesis of the concept of medical nanorobotics sprang from the visionary idea that tiny nanomachines could be designed, manufactured, and introduced into the human body to perform cellular repairs at the molecular level. Although the medical application of nanotechnology was later championed in the popular writings of Drexler (Drexler 1986; Drexler et al. 1991) in the 1980s and 1990s and in the technical writings of Freitas (Freitas 1999, 2003) in the 1990s and 2000s, the first scientist to voice the possibility was the late Nobel physicist Richard P. Feynman, who worked on the Manhattan Project at Los Alamos during World War II and later taught at CalTech for most of his professorial career.

In his prescient 1959 talk "There's Plenty of Room at the Bottom," Feynman proposed employing machine tools to make smaller machine tools, these to be used in turn to make still smaller machine tools, and so on all the way down to the atomic level (Feynman 1960). He prophetically concluded that this is "a development which I think cannot be avoided." After discussing his ideas with a colleague, Feynman offered the first known proposal for a medical nanorobotic procedure of any kind – in this instance, to cure heart disease: "A friend of mine (Albert R. Hibbs) suggests a very interesting possibility for relatively small machines. He says that, although it is a very wild idea, it would be interesting in surgery if you could swallow the surgeon. You put the mechanical surgeon inside the blood vessel and it goes into the heart and looks around. (Of course the information has to be fed out.) It finds out which

valve is the faulty one and takes a little knife and slices it out. Other small machines might be permanently incorporated in the body to assist some inadequately functioning organ." Later in his historic 1959 lecture, Feynman urges us to consider the possibility, in connection with microscopic biological cells, "that we can manufacture an object that maneuvers at that level!" The field had progressed far enough by 2007, half a century after Feynman's speculations, to allow Martin Moskovits, Professor of Chemistry and Dean of Physical Science at UC Santa Barbara, to write (Moskovits 2007) that "the notion of an ultra-small robot that can, for example, navigate the bloodstream performing microsurgery or activating neurons so as to restore muscular activity, is not an unreasonable goal, and one that may be realized in the near future."

23.3 Fundamentals of Medical Nanorobotics

Many skeptical questions arise when one first encounters the idea of micron-scale nanorobots constructed of nanoscale components, operating inside the human body. At the most fundamental level, technical questions about the influence of quantum effects on molecular structures, friction and wear among nanomechanical components, radiation damage, other failure mechanisms, the influence of thermal noise on reliability, and the effects of Brownian bombardment on nanomachines have all been extensively discussed and resolved in the literature (Drexler 1992; Freitas 1999a). Molecular motors consisting of just 50–100 atoms have been demonstrated experimentally (e.g., see Section 23.3.2). Published discussions of technical issues of specific relevance to medical nanorobots include proposed methods for recognizing, sorting and pumping individual molecules (Drexler 1992a; Freitas 1999b), and theoretical designs for mechanical nanorobot sensors (Freitas 1999c), flexible hull surfaces (Freitas 1999d), power sources (Freitas 1999e), communications systems (Freitas 1999f), navigation systems (Freitas 1999g), manipulator mechanisms (Freitas 1999h), mobility mechanisms for travel through bloodstream, tissues and cells (Freitas 1999i), onboard clocks (Freitas 1999j), and nanocomputers (Drexler 1992b; Freitas 1999k), along with the full panoply of nanorobot biocompatibility issues (Freitas 2003) (see also Section 23.5).

The idea of placing semi-autonomous self-powered nanorobots inside of us might seem a bit odd, but the human body already teems with similar natural nanodevices. For instance, more than 40 trillion single-celled microbes swim through our colon, outnumbering our tissue cells almost ten to one (Freitas 1999m). Many bacteria move by whipping around a tiny tail, or flagellum, that is driven by a 30-nanometer biological ionic nanomotor powered by pH differences between the inside and the outside of the bacterial cell. Our bodies also maintain a population of more than a trillion motile biological nanodevices called fibroblasts and white cells such as neutrophils and lymphocytes, each measuring perhaps 10 microns in size (Freitas 1999m). These beneficial natural nanorobots are constantly crawling around inside us, repairing damaged tissues, attacking invading microbes, and

gathering up foreign particles and transporting them to various organs for disposal from the body (Freitas 2003a).

The greatest power of nanomedicine will begin to emerge in a decade or two as we learn to design and construct complete artificial nanorobots using nanometer-scale parts and subsystems such as diamondoid bearings and gears (Section 23.3.1), nanomotors and pumps (Section 23.3.2), nanomanipulators (Section 23.3.3), nanosensors (Section 23.3.4), and nanocomputers (Section 23.3.5).

23.3.1 Nanobearings and Nanogears

In order to establish the foundations for molecular manufacturing and medical nanorobotics, it is first necessary to create and to analyze possible designs for nanoscale mechanical parts that could, in principle, be manufactured. Because these components cannot yet be physically built in 2009, such designs cannot be subjected to rigorous experimental testing and validation. Designers are forced instead to rely upon ab initio structural analysis and computer studies including molecular dynamics simulations. "Our ability to model molecular machines (systems and devices) of specific kinds, designed in part for ease of modeling, has far outrun our ability to make them," notes K. Eric Drexler (Drexler 1992). "Design calculations and computational experiments enable the theoretical studies of these devices, independent of the technologies needed to implement them."

Molecular bearings are perhaps the most convenient class of components to design because their structure and operation is fairly straightforward. One of the simplest classical examples is Drexler's early overlap-repulsion bearing design (Drexler 1992f), shown with end views and exploded views in Fig. 23.1 using both ball-and-stick and space-filling representations. This bearing has exactly 206 atoms including carbon, silicon, oxygen and hydrogen, and is comprised of a small shaft that rotates within a ring sleeve measuring 2.2 nm in diameter. The atoms of the shaft are arranged in a 6-fold symmetry, while the ring has 14-fold symmetry, a combination that provides low energy barriers to shaft rotation. Figure 23.2 shows an exploded view of a 2808-atom strained-shell sleeve bearing designed by Drexler and Merkle (Drexler 1992f) using molecular mechanics force fields to ensure that bond lengths, bond angles, van der Waals distances, and strain energies are reasonable. This 4.8-nm diameter bearing features an interlocking-groove interface which derives from a modified diamond (100) surface. Ridges on the shaft interlock with ridges on the sleeve, making a very stiff structure. Attempts to bob the shaft up or down, or rock it from side to side, or displace it in any direction (except axial rotation, wherein displacement is extremely smooth) encounter a very strong resistance (Drexler 1995). Whether these bearings would have to be assembled in unitary fashion, or instead could be assembled by inserting one part into the other without damaging either part, had not been extensively studied or modeled by 2009. There is some experimental evidence that these bearings, if and when they can be built, should work as expected: In 2000, John Cumings and Alex Zettl at U.C. Berkeley demonstrated experimentally that nested carbon nanotubes

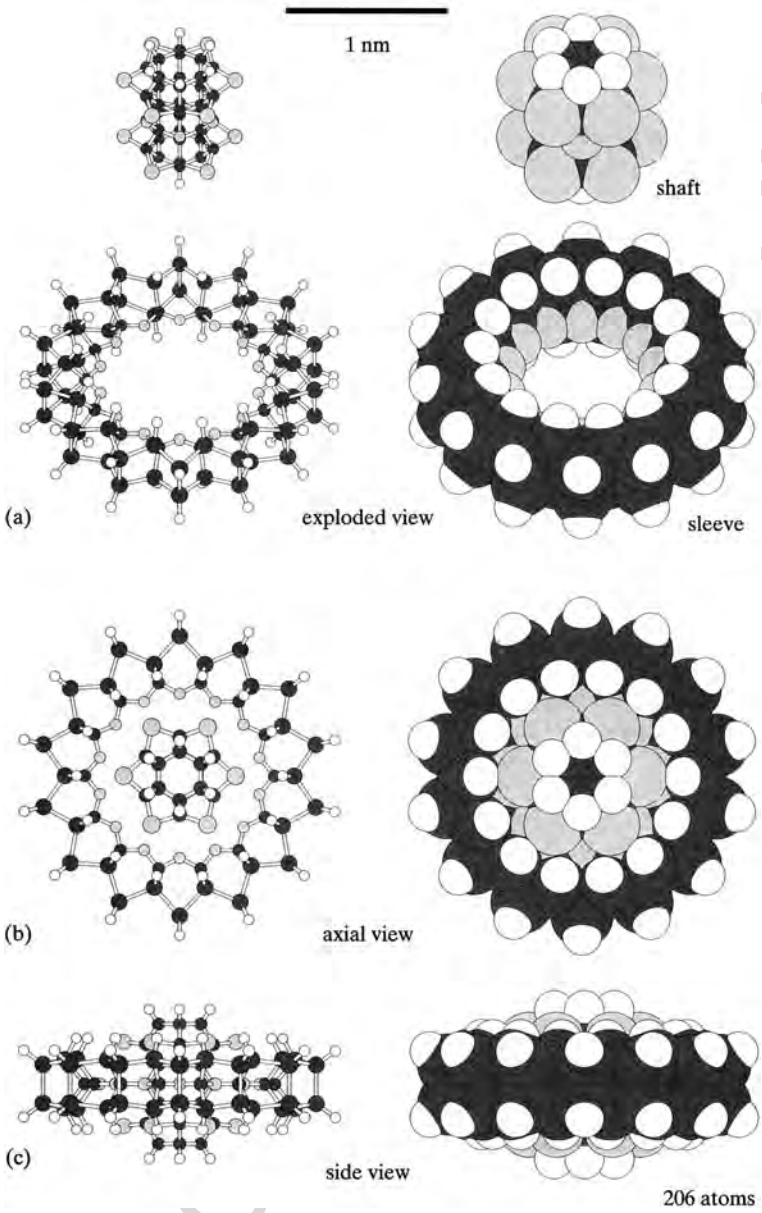

Fig. 23.1 End views and exploded views of a 206-atom overlap-repulsion bearing (Drexler 1992f). Image courtesy of K. Eric Drexler. ©1992 by John Wiley & Sons, Inc. Used with permission

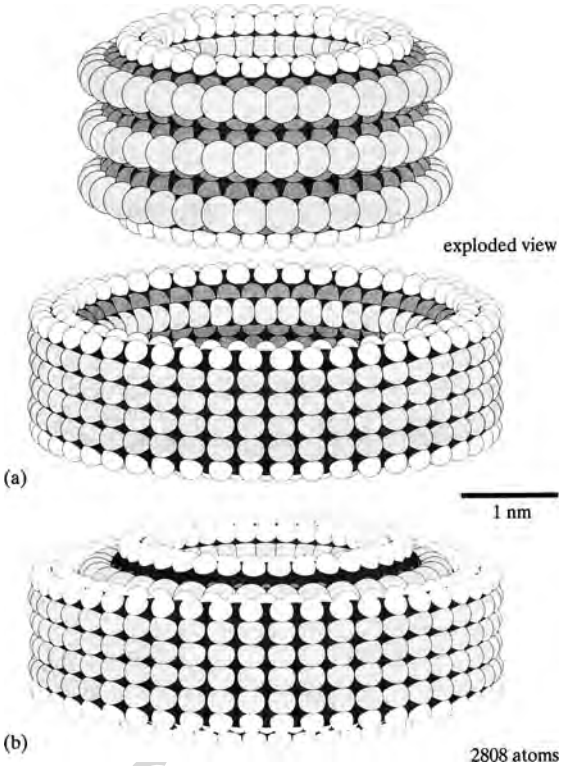

Fig. 23.2 Exploded view of a 2808-atom strained-shell sleeve bearing (Drexler 1992f). Image courtesy of K. Eric Drexler. ©1992 by John Wiley & Sons, Inc. Used with permission

do indeed make exceptionally low-friction nanobearings (Cumings and Zettl 2000).

Molecular gears are another convenient component system for molecular manufacturing design-ahead. For example, in the 1990s Drexler and Merkle (Drexler 1992g) designed a 3557-atom planetary gear, shown in side, end, and exploded views in Fig. 23.3. The entire assembly has twelve moving parts and is 4.3 nm in diameter and 4.4 nm in length, with a molecular weight of 51,009.844 daltons and a molecular volume of 33.458 nm^3. An animation of the computer simulation shows the central shaft rotating rapidly and the peripheral output shaft rotating slowly as intended. The small planetary gears rotate around the central shaft, and they are surrounded by a ring gear that holds the planets in place and ensures that all of the components move in the proper fashion. The ring gear is a strained silicon shell with sulfur atom termination; the sun gear is a structure related to an oxygen-terminated diamond (100) surface; the planet gears resemble multiple hexasterane structures with oxygen rather than CH_2 bridges between the parallel rings; and the planet carrier is adapted from a Lomer dislocation (Lomer 1951) array created by R. Merkle and L. Balasubramaniam, and linked to the planet gears using C–C bonded bearings. View (c) retains the elastic deformations that are hidden in (a) – the gears are bowed.

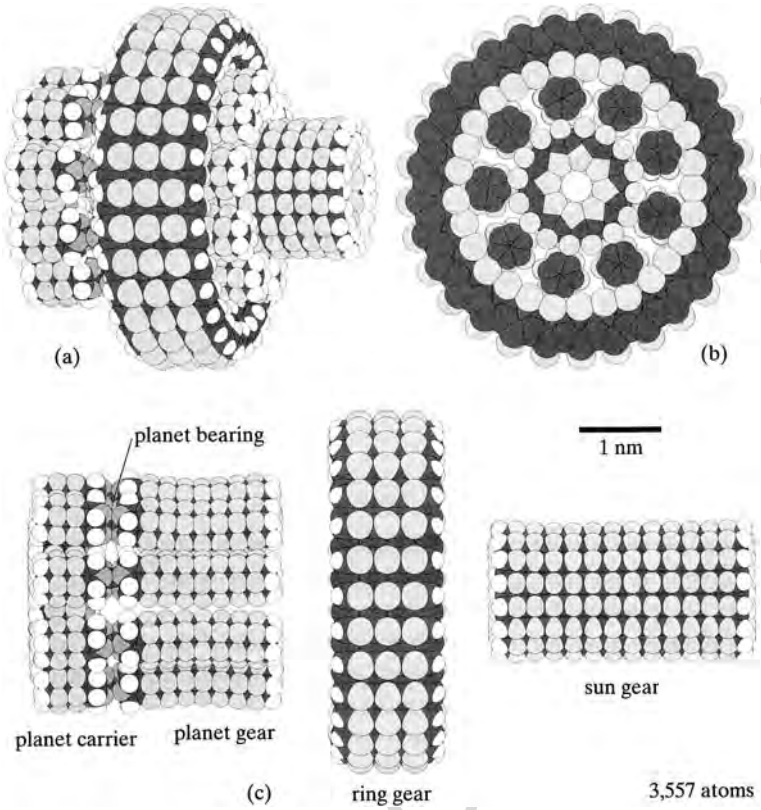

Fig. 23.3 End-, side-, and exploded-view of a 3557-atom planetary gear (Drexler 1992g). Image courtesy of K. Eric Drexler. ©1992 by John Wiley & Sons, Inc. Used with permission

In the macroscale world, planetary gears are used in automobiles and other machines where it is necessary to transform the speeds of rotating shafts.

Goddard and colleagues at CalTech (Goddard 1995; Cagin et al. 1998) performed a rotational impulse dynamics study of this "first-generation" planetary gear. At the normal operational rotation rates for which the component was designed (e.g., <1 GHz for <10 m/sec interfacial velocities), the gear worked as intended and did not overheat (Goddard 1995). However, when the gear was driven to ~100 GHz, significant instabilities appeared although the device still did not self-destruct (Goddard 1995). One run at ~80 GHz showed excess kinetic energy causing gear temperature to oscillate up to 450 K above baseline (Cagin et al. 1998). One animation of the simulation shows that the ring gear wiggles violently because it is rather thin. In an actual nanorobot incorporating numerous mechanical components of this type, the ring gear would be part of a larger wall that would hold it solidly in place and would eliminate these convulsive motions which, in any case, are seen in the simulation only at unrealistically high operating frequencies.

23.3.2 Nanomotors, Nanopumps, and Power Sources

Nanorobots need motors to provide motion, pumps to move materials, and power sources to drive mechanical activities. One important class of theoretical nanodevice that has been designed is a gas-powered molecular motor or pump (Drexler and Merkle 1996). The pump and chamber wall segment shown in Fig. 23.4 contain 6165 atoms with a molecular weight of 88,190.813 daltons and a molecular volume of 63.984 nm^3. The device could serve either as a pump for neon gas atoms or (if run backwards) as a motor to convert neon gas pressure into rotary power. The helical rotor has a grooved cylindrical bearing surface at each end, supporting a screw-threaded cylindrical segment in the middle. In operation, rotation of the shaft moves a helical groove past longitudinal grooves inside the pump housing. There is room enough for small gas molecules only where facing grooves cross, and these crossing points move from one side to the other as the shaft turns, moving the neon atoms along. Goddard (Cagin et al. 1998) reported that preliminary molecular dynamics simulations of the device showed that it could indeed function as a pump, although "structural deformations of the rotor can cause instabilities at low and high rotational frequencies. The forced translations show that at very low perpendicular forces due to pump action, the total energy rises significantly and again the structure deforms." The neon motor/pump is not very energy-efficient, but further refinement or extension of this crude design is clearly warranted. Almost all such design research in diamondoid nanorobotics is restricted to theory and computer simulation. This allows the design and testing of large structures or complete nanomachines and the compilation of growing libraries of molecular designs.

Although the neon pump cannot yet be built, proof-of-principle motors for nanoscale machines have already received a great deal of experimental attention

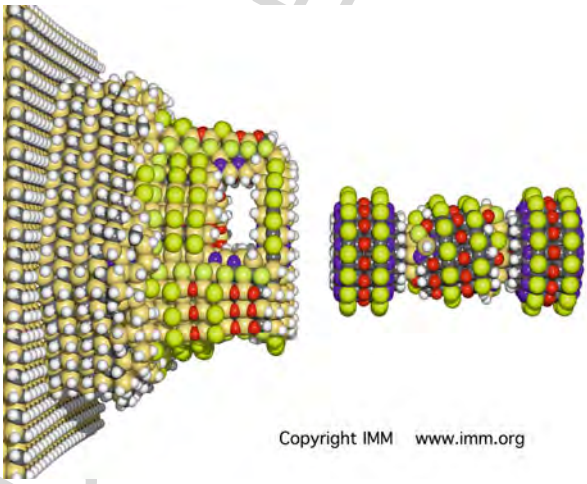

Fig. 23.4 Side views of a 6165-atom neon gas pump/motor (Drexler and Merkle, 1996). © Institute for Molecular Manufacturing (www.imm.org). Used with permission

This figure will be printed in b/w

including the 78-atom chemically-powered rotating nanomotor synthesized in 1999 by Kelly (Kelly et al. 1999), a chemically-powered rotaxane-based linear motor exerting ~100 pN of force with a 1.9 nm throw and a ~250 sec contraction cycle by Stoddart's group (Huang et al. 2003), a UV-driven catenane-based ring motor by Wong and Leigh (Leigh et al. 2003), an artificial 58-atom motor molecule that spins when illuminated by solar energy by Feringa (Koumura et al. 1999), and a great variety of additional synthetic molecular motor motifs as excellently reviewed by Browne and Feringa (Browne and Feringa 2006) and by Kay et al. (Kay et al. 2007). Zettl's group at U.C. Berkeley has experimentally demonstrated an essentially frictionless bearing made from two co-rotating nested nanotubes (Cumings and Zettl 2000), which can also serve as a mechanical spring because the inner nanotube "piston" feels a restoring force as it is extracted from the outer nanotube "jacket". Zettl's group then fabricated a nanomotor mounted on two of these nanotube bearings, demonstrating the first electrically powered nanoscale motor (Fennimore et al. 2003).

In 2005, Tour's group at Rice University reported (Shirai et al. 2005) constructing a tiny molecular "nanocar" measuring 3–4 nm across that consists of a chassis, two freely rotating axles made of well-defined rodlike acetylenic structures with a pivoting suspension, and wheels made of C_{60} buckyball (or, later, spherical carborane) molecules that can turn independently because the bond between them and the axle is freely rotatable (Fig. 23.5). Placed on a warmed gold surface held at 170°C, the nanocar spontaneously rolls on all four wheels, but only along its long axis in a direction perpendicular to its axles (a symmetrical three-wheeled variant just spins in place). When pulled with an STM tip, the nanocar cannot be towed sideways – the wheels dig in, rather than rolling. A larger, more functionalized version of the nanocar might carry other molecules along and dump them at will. Indeed, the Rice team (Shirai et al. 2006) has reportedly "followed up the nanocar work by designing a [motorized] light-driven nanocar and a nanotruck that's capable of carrying a payload" (Shirai et al. 2005).

Nanorobots working inside the body could most conveniently be powered by ambient glucose and oxygen found in the blood and tissues, which could be

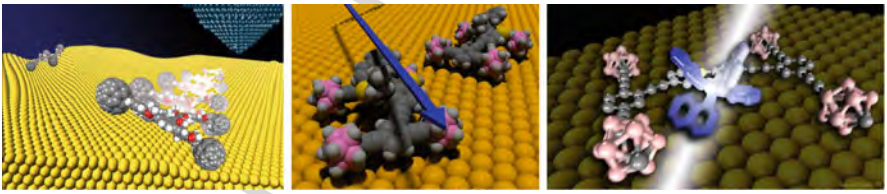

Fig. 23.5 Tour molecular nanocar (Shirai et al. 2005, 2006). *Left*: Original nanocar is depicted on gold surface. *Middle*: Two motorized nanocars are shown on a gold surface; each nanocar consists of a rigid chassis and four alkyne axles that spin freely and swivel independently of one another, with wheels made of p-carborane (spherical molecules of carbon, hydrogen and boron). *Right*: The nanocar's light-powered motor is attached mid-chassis; when struck by light, it rotates in one direction, pushing the car along like a paddlewheel. Used with permission.

This figure will be printed in b/w

converted to mechanical energy using a nanoengine (Freitas 1999aq) or to electrical energy using a nanoscale fuel cell (Freitas 1999ar). The first glucose-oxygen fuel cell was demonstrated experimentally by Nishizawa's group (Satoa et al. 2005) in 2005, who used a Vitamin K3-immobilized polymer with glucose dehydrogenase on one side as the anode and a polydimethylsiloxane-coated Pt cathode to yield an open circuit voltage of 0.62 volts and a maximum power density of 14.5 $\mu W/cm^2$ at 0.36 volts in an air-saturated phosphate buffered saline solution (pH 7.0) at 37°C containing 0.5 mM NADH and 10 mM glucose.

Another well-known proposal is for medical nanorobotic devices to receive all power (and some control) signals acoustically (Freitas 1999n; Drexler 1992c). Externally generated ultrasonic pressure waves would travel through the aqueous in vivo environment to the medical nanodevice, whereupon a piston on the device is driven back and forth in a well-defined manner, mechanically passing energy and information simultaneously into the device. Although an acoustically-actuated nanoscale piston has not yet been demonstrated experimentally, we know that pressure applied, then released, on carbon nanotubes causes fully reversible compression (Chesnokov et al. 1999), and experiments have shown very low frictional resistance between nested nanotubes that are externally forced in and out like pistons (Cumings and Zettl 2000). Masako Yudasaka, who studies C_{60} molecules trapped inside carbon nanotubes or "peapods" at NEC (Nippon Electric Corp.), expects that "the buckyball can act like a piston" (Schewe et al. 2001). In 2007, a prototype nanometer-scale generator that produces continuous direct-current electricity by harvesting mechanical energy from ultrasonic acoustic waves in the environment was demonstrated by Wang et al. (Wang et al. 2007).

Yet another important nanorobot component is the molecular sorting rotor (Freitas 1999o; Drexler 1992a) (see also Fig. 23.6a), which would provide an active means for pumping, say, individual gas molecules into, and out of, pressurized onboard microtanks, one molecule at a time. Sorting pumps are typically envisioned as ~1000 nm^3-size devices that can transfer ~10^6 molecules/sec and would be embedded in the hull of the nanorobot. Each pump employs reversible artificial binding sites (Freitas 1999p) mounted on a rotating structure that cycles between the interior and exterior of the nanorobot, allowing transport of a specific molecule even against concentration gradients up to ~20,000 atm. Sorting rotors are conceptually similar to the biological transporter pumps (Freitas 1999as) which are found in nature for conveying numerous ions (Gouaux and Mackinnon 2005), amino acids, sugars (Olson and Pessin 1996), and other small biomolecules (Sharom 1997) across cell membranes. The molecular structures of natural enzymatic binding sites for small molecules like oxygen, carbon dioxide, nitrogen, water and glucose have been known since the 1990s, and the design (Kapyla et al. 2007), simulation (Rohs et al. 2005), and fabrication (Bracci et al. 2002; Subat et al. 2004; Franke et al. 2007) of artificial binding sites for more complex molecules is an active field of research. Sequential cascades of sorting rotors (Fig. 23.6b) (Drexler 1992d; Freitas 1999o) could achieve high fidelity purification and a contaminant fraction of $<10^{-15}$ for transporting small molecules of common types.

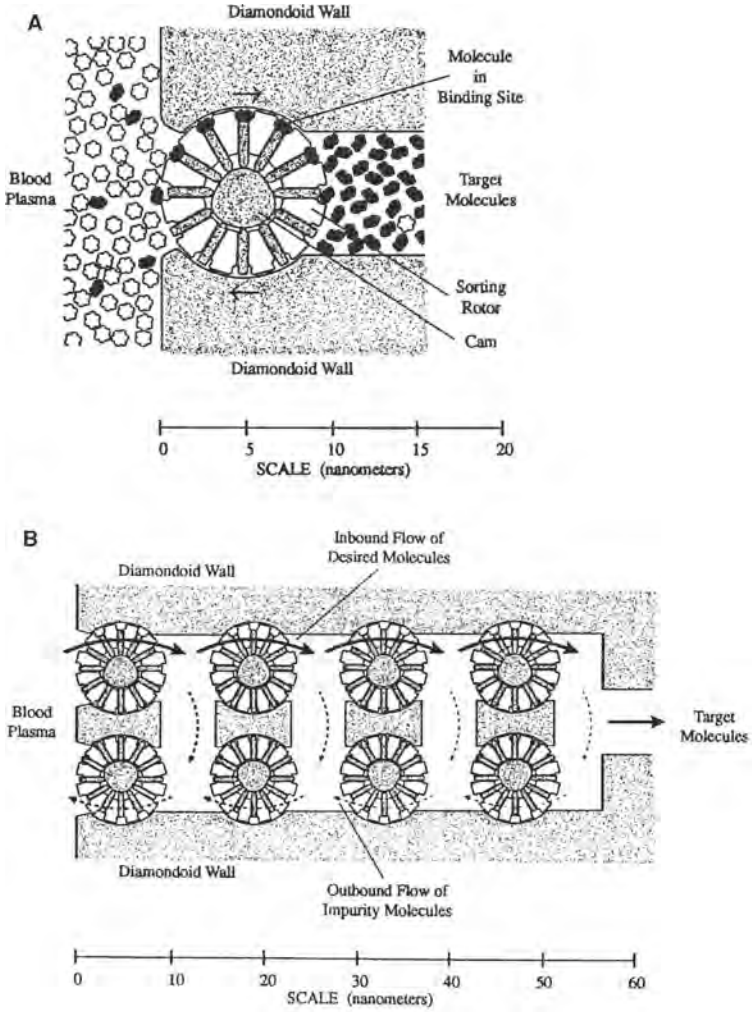

Fig. 23.6 (**a**) Individual sorting rotor and (**b**) a sorting rotor cascade, redrawn from Drexler (1992)

23.3.3 Nanomanipulators

Nanorobots require manipulators to perform grasping and manipulation tasks, and also to provide device mobility. One well-known telescoping nanomanipulator design (Fig. 23.7) features a central telescoping joint whose extension and retraction is controlled by a 1.5-nm diameter drive shaft (Drexler 1992e). The rapid rotation of this drive shaft (up to ~1 m/sec tangential velocity) forces a transmission gear to quickly execute a known number of turns, causing the telescoping joint to

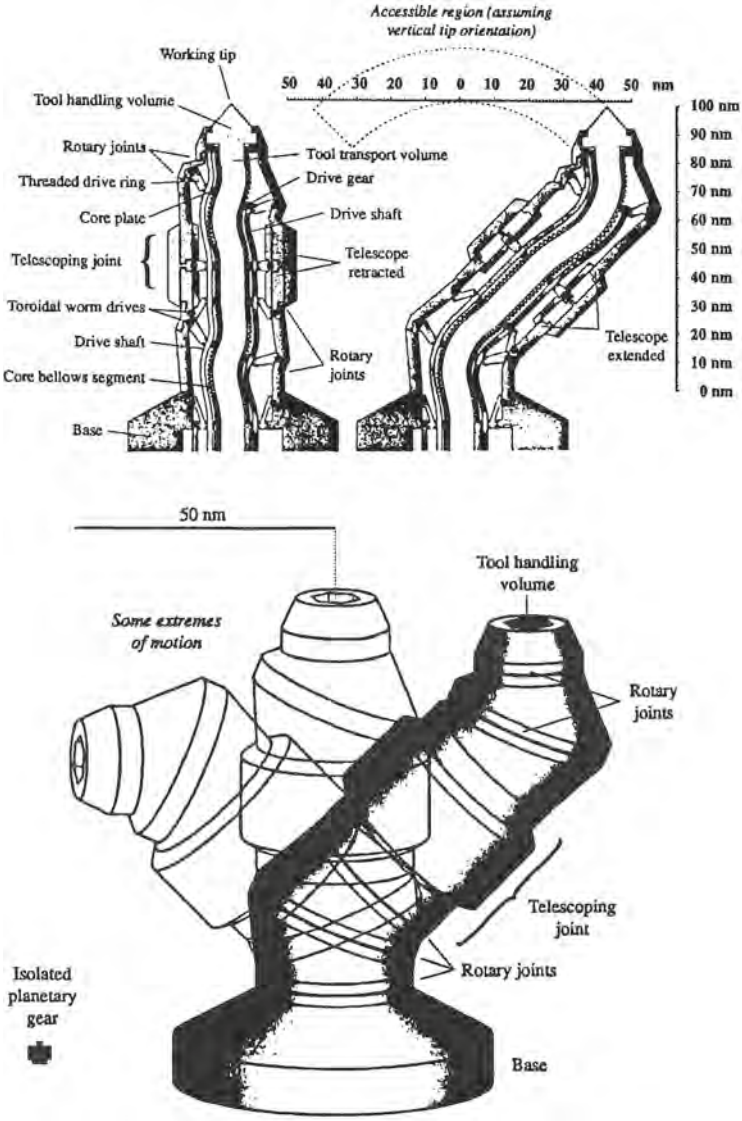

Fig. 23.7 Telescoping nanomanipulator design (Drexler 1992e). Image courtesy of K. Eric Drexler. ©1992 by John Wiley & Sons, Inc. Used with permission

slowly unscrew or screw in the axial direction, thus lengthening or contracting the manipulator. These shafts can be made to turn through a known number of rotations between locked states giving odometer-like control of manipulator joint rotations. Additionally, two pairs of canted rotary joints – one pair between the telescoping section and the base, the other pair between the telescoping section and the working

tip – are controlled by toroidal worm drives. These joints enable a wide variety of complex angular motions and give full 6-DOF (degrees of freedom) access to the work envelope. The manipulator is approximately cylindrical in shape with an outside diameter of ~35 nm and an extensible length from 90 nm to 100 nm measured from top of base to working tip. The mechanism includes a hollow circular channel 7 nm in diameter to allow tool tips and materials to be moved from below the manipulator through the base up to the working tip. At the tip, a slightly larger region is reserved for a mechanism to allow positioning and locking of tool tips. This ~10^{-19} kg manipulator would be constructed of ~4×10^6 atoms excluding the base and external power and control structures, and is hermetically sealed to maintain a controlled internal environment while allowing leakproof operation in vivo.

Experimentally, a DNA-based robot arm has been inserted into a 2D array substrate by Seeman's group (Ding and Seeman 2006), and this simple rotary mechanism was then verified by atomic force microscopy to be a fully functional nanomechanical device.

23.3.4 Nanosensors

Medical nanorobots will need to acquire information from their environment to properly execute their assigned tasks. Such acquisition can be achieved using onboard nanoscale sensors, or nanosensors, of various types which are currently the subject of much experimental research (Nagahara et al. 2008). More advanced nanosensors to be used in medical nanorobots will allow monitoring environmental states including internal nanorobot states and local and global somatic states inside the human body. Theoretical designs for advanced nanosensors to detect chemical substances (Freitas 1999q), displacement and motion (Freitas 1999r), force and mass (Freitas 1999s), and acoustic (Freitas 1999t), thermal (Freitas 1999u), and electromagnetic (Freitas 1999v) stimuli have been described elsewhere.

For instance, medical nanorobots which employ onboard tankage will need various nanosensors to acquire external data essential in regulating gas loading and unloading operations, tank volume management, and other special protocols. Sorting rotors (Section 23.3.2) can be used to construct quantitative concentration sensors for any molecular species desired. One simple two-chamber design (Freitas 1999cj) uses an input sorting rotor running at 1% normal speed synchronized with a counting rotor (linked by rods and ratchets to the computer) to assay the number of molecules of the desired type that are present in a known volume of fluid. At typical blood concentrations, this sensor, which measures $45 \times 45 \times 10$ nm comprising ~500,000 atoms (~10^{-20} kg), should count, for example, ~100,000 molecules/sec of glucose, ~30,000 molecules/sec of arterial or venous CO_2, or ~2000 molecules/sec of arterial or venous O_2. It is also convenient to include internal pressure sensors to monitor O_2 and CO_2 gas tank loading, ullage (container fullness) sensors for ballast and glucose fuel tanks, and internal/external temperature sensors to help monitor and regulate total system energy output.

As another example of nanosensors, the attending physician could broadcast signals to nanorobotic systems deployed inside the human body most conveniently using modulated compressive pressure pulses received by mechanical transducers embedded in the surface of the nanorobot. Converting a pattern of pressure fluctuations into mechanical motions that can serve as input to a mechanical nanocomputer (Section 23.3.5) requires transducers that function as pressure-driven actuators (Drexler 1992c; Freitas 1999t, ck). Broadcast mechanisms similar to medical pulse-echo diagnostic ultrasound systems can transmit data into the body acoustically at ~10 MHz (~10^7 bits/sec) using peak-to-trough 10-atm pressure pulses that can be received onboard the nanorobot by nanosensors ~$(21\ \text{nm})^3$ in size comprising ~10^5 atoms. Such signals attenuate only ~10% per 1 cm of travel (Drexler 1992c), so whole-body broadcasts should be feasible even in emergency field situations. Pressure transducers will consume minimal power because the input signal drives the motion.

23.3.5 Nanocomputers

Many important medical nanorobotic tasks will require computation (Freitas 1999k) during the acquisition and processing of sensor data, the control of tools, manipulators, and motility systems, the execution of navigation and communication tasks, and during the coordination of collective activities with neighboring nanorobots, and also to allow a physician to properly monitor and control the work done by nanorobots. *Ex vivo* computation has few theoretical limits, but computation by in vivo nanorobots will be subject to a number of constraints such as physical size, power consumption, onboard memory and processing speed.

The memory required onboard a medical nanorobot will be strongly mission dependent. Simple missions involving basic process control with limited motility may require no more than ~10^5-10^6 bits of memory, comparable to an old Apple II computer (including RAM plus floppy disk drive). At the other extreme, a complex cell repair mission might require the onboard storage of the equivalent of a substantial fraction of the patient's genetic code, representing perhaps 10^9–10^{10} bits of memory which would be in the same range as the 1985 Cray-2 (2×10^{10} bits) or the 1989 Cray-3 (6×10^8 bits) supercomputers. Computational speed will also be strongly mission dependent. Simple process control systems in basic factory settings may only require speeds as slow as 10^4 bit/sec. At the other extreme, a processing speed of 10^9 bits/sec allows a ~10^9 bit genome-sized information store to be processed in ~1 sec, about the same as the small-molecule diffusion time across an average 20-micron wide cell.

Perhaps the best-characterized (though not yet built) mechanical nanocomputer is Drexler's rod logic design (Drexler 1992b). In this theoretical design, one sliding rod with a knob (Fig. 23.8a) intersects a second knobbed sliding rod at right angles to the first. Depending upon the position of the first rod, the second may be free to move, or unable to move. This simple blocking interaction serves as the basis for logical operations. One implementation of a nanomechanical Boolean NAND

This figure will be printed in b/w

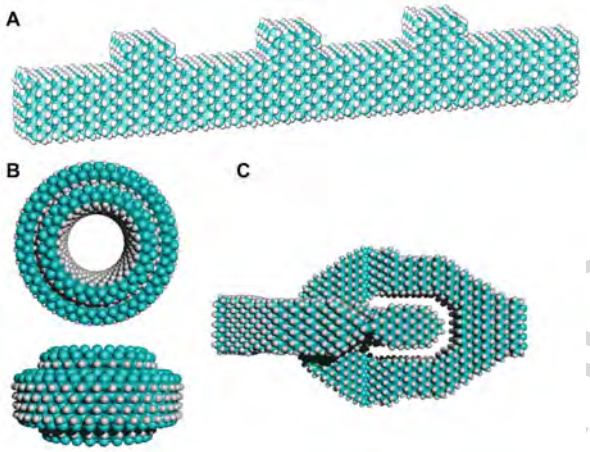

Fig. 23.8 (**a**) hydrocarbon logic rod, (**b**) hydrocarbon bearing, and (**c**) hydrocarbon universal joint (Nanofactory Collaboration 2007a)

"interlock" gate uses clock-driven input and output logic rods 1 nm wide which interact via knobs that prevent or enable motion, all encased in a housing, allowing ~16 nm^3/interlock. (Any logic function, no matter how complicated, can be built from NAND or NOR gates alone.) Similarly, a thermodynamically efficient class of register capable of mechanical data storage would use rods ~1 nm in width with 0.1-nanosec switching speeds, allowing ~40 nm^3/register. The benchmark mechanical nanocomputer design fits inside a 400 nm cube, consumes ~60 nW of power, and has 10^6 interlock gates, 10^5 logic rods, 10^4 registers, and an energy-buffering flywheel. Power dissipation is ~2 $\times$ 10^4 operations/sec-pW with a processing speed of ~10^9 operations/sec (~1 gigaflop), similar to a typical desktop PC in 2007.

Biocomputers (Freitas 1999ai; Guet et al. 2002; Yokobayashi et al. 2002; Basu et al. 2004, 2005) and both electronic (Heath 2000; Tseng and Ellenbogen 2001; Das et al. 2005) and mechanical (Blick et al. 2007) nanocomputers are active areas of current research and development. There has been progress toward nanotube- and nanorod-based molecular electronics (Collins et al. 2001; Reed and Lee 2003) and nanoscale-structured quantum computers (Stegner et al. 2006), possibly using diamond lattice (Dutt et al. 2007). A 160-kilobit memory device smaller than a white blood cell was fabricated by Stoddart's group in 2007 (Green et al. 2007) by laying down a series of perpendicular crossing nanowires with 400 bottom wires and 400 crossing top wires. (Sitting at each intersection of the tic-tac-toe structure and serving as the storage element were approximately 300 bistable rotaxane molecules that could be switched between two different states, and each junction of a crossbar could be addressed individually by controlling the voltages applied to the appropriate top and bottom crossing wires, forming a bit at each nanowire crossing.) A simple DNA-based molecular machine capable of translating "coded" information

from one DNA strand to another, another basic nanocomputational activity, was demonstrated experimentally in 2007 by Seeman's group (Garibotti et al. 2007).

23.4 Manufacturing Medical Nanorobots

The development pathway for diamondoid medical nanorobots will be long and arduous. First, theoretical scaling studies (Freitas 1998, 2000a, b, 2005b, 2006a, 2007; Freitas and Phoenix 2002) are used to assess basic concept feasibility. These initial studies must then be followed by more detailed computational simulations of specific nanorobot components and assemblies, and ultimately full systems simulations, all thoroughly integrated with additional simulations of massively parallel manufacturing processes from start to finish consistent with a design-for-assembly engineering philosophy. Once nanofactories implementing molecular manufacturing capabilities become available, experimental efforts may progress from fabrication of components (from small-molecule or atomic precursors) and testing, to the assembly of components into nanomechanical devices and nanomachine systems, and finally to prototypes and mass manufacture of medical nanorobots, ultimately leading to clinical trials. By 2009 there was some limited experimental work with microscale-component microscopic microrobots (Ishiyama et al. 2002; Chrusch et al. 2002; Mathieu et al. 2005; Yesin et al. 2005; Monash University 2006) (see also Section "Endoscopic Nanosurgery and Surgical Nanorobots") but progress on nanoscale-component microscopic nanorobots today is largely at the concept feasibility and preliminary design stages and will remain so until experimentalists develop the capabilities required for molecular manufacturing, as reviewed below.

23.4.1 Positional Assembly and Molecular Manufacturing

Complex medical nanorobots probably cannot be manufactured using the conventional techniques of self-assembly. As noted in the final report (Committee 2006) of the 2006 Congressionally-mandated review of the U.S. National Nanotechnology Initiative by the National Research Council (NRC) of the National Academies and the National Materials Advisory Board (NMAB): "For the manufacture of more sophisticated materials and devices, including complex objects produced in large quantities, it is unlikely that simple self-assembly processes will yield the desired results. The reason is that the probability of an error occurring at some point in the process will increase with the complexity of the system and the number of parts that must interoperate."

The opposite of self-assembly processes is positionally controlled processes, in which the positions and trajectories of all components of intermediate and final product objects are controlled at every moment during fabrication and assembly. Positional processes should allow more complex products to be built with high

quality and should enable rapid prototyping during product development. Positional assembly is the norm in conventional macroscale manufacturing (e.g., cars, appliances, houses) but is only recently (Kenny 2007; Nanofactory Collaboration 2007a) starting to be seriously investigated experimentally for nanoscale manufacturing. Of course, we already know that positional fabrication will work in the nanoscale realm. This is demonstrated in the biological world by ribosomes, which positionally assemble proteins in living cells by following a sequence of digitally encoded instructions (even though ribosomes themselves are self-assembled). Lacking this positional fabrication of proteins controlled by DNA-based software, large, complex, digitally-specified organisms would probably not be possible and biology as we know it would not exist.

The most important materials for positional assembly may be the rigid covalent or "diamondoid" solids, since these could potentially be used to build the most reliable and complex nanoscale machinery. Preliminary theoretical studies have suggested great promise for these materials in molecular manufacturing. The NMAB/NRC Review Committee recommended (Committee 2006) that experimental work aimed at establishing the technical feasibility of positional molecular manufacturing should be pursued and supported: "Experimentation leading to demonstrations supplying ground truth for abstract models is appropriate to better characterize the potential for use of bottom-up or molecular manufacturing systems that utilize processes more complex than self-assembly." Making complex nanorobotic systems requires manufacturing techniques that can build a molecular structure by positional assembly (Freitas 2005c). This will involve picking and placing molecular parts one by one, moving them along controlled trajectories much like the robot arms that manufacture cars on automobile assembly lines. The procedure is then repeated over and over with all the different parts until the final product, such as a medical nanorobot, is fully assembled using, say, a desktop nanofactory (see Fig. 23.17).

23.4.2 Diamond Mechanosynthesis (DMS)

Theorists believe that the most reliable and durable medical nanorobots will be built using diamondoid materials. What is diamondoid? First and foremost, diamondoid materials include pure diamond, the crystalline allotrope of carbon. Among other exceptional properties, diamond has extreme hardness, high thermal conductivity, low frictional coefficient, chemical inertness, a wide electronic bandgap, and is the strongest and stiffest material presently known at ordinary pressures. Diamondoid materials also may include any stiff covalent solid that is similar to diamond in strength, chemical inertness, or other important material properties, and possesses a dense three-dimensional network of bonds. Examples of such materials are carbon nanotubes and fullerenes, several strong covalent ceramics such as silicon carbide, silicon nitride, and boron nitride, and a few very stiff ionic ceramics such as sapphire (monocrystalline aluminum oxide) that can be covalently bonded to pure covalent structures such as diamond. Of course, large pure crystals of diamond are brittle

and easily fractured. The intricate molecular structure of a diamondoid nanofactory macroscale product will more closely resemble a complex composite material, not a brittle solid crystal. Such products, and the nanofactories that build them, should be extremely durable in normal use.

Mechanosynthesis, involving molecular positional fabrication, is the formation of covalent chemical bonds using precisely applied mechanical forces to build, for example, diamondoid structures. Mechanosynthesis employs chemical reactions driven by the mechanically precise placement of extremely reactive chemical species in an ultra-high vacuum environment. Mechanosynthesis may be automated via computer control, enabling programmable molecular positional fabrication. Molecularly precise fabrication involves holding feedstock atoms or molecules, and a growing nanoscale workpiece, in the proper relative positions and orientations so that when they touch they will chemically bond in the desired manner. In this process, a mechanosynthetic tool is brought up to the surface of a workpiece. One or more transfer atoms are added to, or removed from, the workpiece by the tool. Then the tool is withdrawn and recharged. This process is repeated until the workpiece (e.g., a growing nanopart) is completely fabricated to molecular precision with each atom in exactly the right place. Note that the transfer atoms are under positional control at all times to prevent unwanted side reactions from occurring. Side reactions are also prevented using proper reaction design so that the reaction energetics help us avoid undesired pathological intermediate structures.

The positional assembly of diamondoid structures, some almost atom by atom, using molecular feedstock has been examined theoretically (Drexler 1992h; Merkle 1997; Merkle and Freitas 2003; Mann et al. 2004; Allis and Drexler 2005; Freitas 2005d; Peng et al. 2006; Temelso et al. 2006; Freitas et al. 2007; Temelso et al. 2007; Freitas and Merkle 2008) via computational models of diamond mechanosynthesis (DMS). DMS is the controlled addition of individual carbon atoms, carbon dimers (C_2), single methyl (CH_3) or like groups to the growth surface of a diamond crystal lattice workpiece in a vacuum manufacturing environment. Covalent chemical bonds are formed one by one as the result of positionally constrained mechanical forces applied at the tip of a scanning probe microscope (SPM) apparatus. Programmed sequences of carbon dimer placement on growing diamond surfaces *in vacuo* appear feasible in theory (Peng et al. 2006; Freitas and Merkle 2008), as illustrated by the hypothetical DCB6Ge tooltip which is shown depositing two carbon atoms on a diamond surface in Fig. 23.9.

The first experimental proof that individual atoms could be manipulated was obtained by IBM scientists in 1989 when they used a scanning tunneling microscope to precisely position 35 xenon atoms on a nickel surface to spell out the corporate logo "IBM" (Fig. 23.10). However, this feat did not involve the formation of covalent chemical bonds. One important step toward the practical realization of DMS was achieved in 1999 by Ho and Lee (Lee and Ho 1999), who achieved the first site-repeatable site-specific covalent bonding operation of two diatomic carbon-containing molecules (CO), one after the other, to the same atom of iron on a crystal surface, using an SPM. The first experimental demonstration of true mechanosynthesis, establishing covalent bonds using purely mechanical forces – albeit on silicon

This figure will be printed in b/w

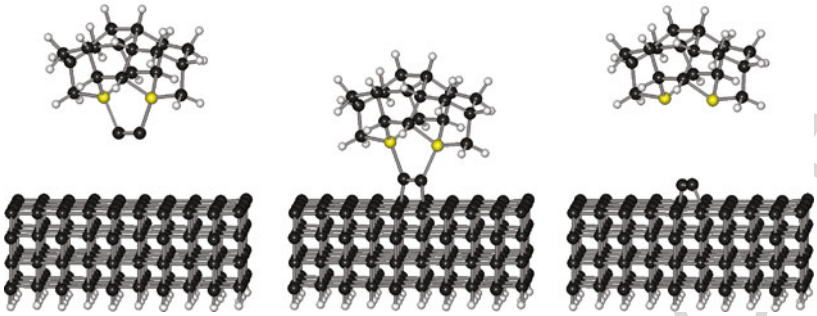

Fig. 23.9 DCB6Ge tooltip shown depositing two carbon atoms on a diamond surface (Nanofactory Collaboration 2007a)

This figure will be printed in b/w

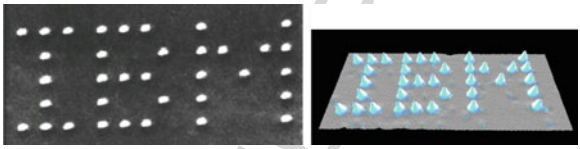

Fig. 23.10 IBM logo spelled out using 35 xenon atoms arranged on a nickel surface by an STM (courtesy of IBM Research Division)

atoms, not carbon atoms – was reported in 2003 by Oyabu and colleagues (Oyabu et al. 2003) in the Custance group. In this landmark experiment, the researchers vertically manipulated single silicon atoms from the Si(111)–(7×7) surface, using a low-temperature near-contact atomic force microscope to demonstrate (1) removal of a selected silicon atom from its equilibrium position without perturbing the (7×7) unit cell and (2) the deposition of a single Si atom on a created vacancy, both via purely mechanical processes.

Following prior theoretical proposals (Freitas 2005d; Freitas and Merkle 2008) for experimental investigations, participants in the Nanofactory Collaboration (Nanofactory Collaboration 2007a) are now planning work designed to achieve DMS with carbon and hydrogen atoms using an SPM apparatus (Section 23.4.4).

23.4.3 Designing a Minimal Toolset for DMS

It is already possible to synthesize bulk diamond today. In a process somewhat reminiscent of spray painting, layer after layer of diamond can be built up by holding a cloud of reactive hydrogen atoms and hydrocarbon molecules over a deposition surface. When these molecules bump into the surface they change it by adding, removing, or rearranging atoms. By carefully controlling the pressure, temperature, and the exact composition of the gas in this process – called chemical vapor deposition or CVD – conditions can be created that favor the growth of diamond on the surface. But randomly bombarding a surface with reactive molecules does not offer

fine control over the growth process and lacks atomic-level positional control. To achieve molecularly precise fabrication, the first challenge is to make sure that all chemical reactions will occur at precisely specified places on the surface. A second problem is how to make the diamond surface reactive at the particular spots where we want to add another atom or molecule. A diamond surface is normally covered with a layer of hydrogen atoms. Without this layer, the raw diamond surface would be highly reactive because it would be studded with unused (or "dangling") bonds from the topmost plane of carbon atoms. While hydrogenation prevents unwanted reactions, it also renders the entire surface inert, making it difficult to add carbon (or anything else) to it.

To overcome these problems, we're trying to use a set of molecular-scale tools that would, in a series of well-defined steps, prepare the surface and create hydrocarbon structures on a layer of diamond, atom by atom and molecule by molecule. A mechanosynthetic tool typically has two principal components – a chemically active tooltip and a chemically inert handle to which the tooltip is covalently bonded. The tooltip is the part of the tool where chemical reactions are forced to occur. The much larger handle structure is big enough to be grasped and positionally manipulated using an SPM or similar macroscale instrumentality. At least three types of basic mechanosynthetic tools (Fig. 23.11) have already received considerable theoretical (and some experimental) study and are likely among those required to build molecularly precise diamond via positional control:

(1) *Hydrogen Abstraction Tools.* The first step in the process of mechanosynthetic fabrication of diamond might be to remove a hydrogen atom from each of one or two specific adjacent spots on the diamond surface, leaving behind one or two reactive dangling bonds or a penetrable C=C double bond. This could be done using a hydrogen abstraction tool (Temelso et al. 2006) that has a high chemical affinity for hydrogen at one end but is elsewhere inert (Fig. 23.11a). The tool's unreactive region serves as a handle or handle attachment point. The

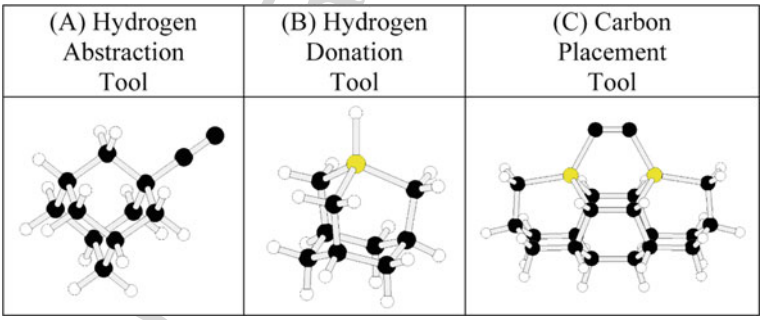

This figure will be printed in b/w

Fig. 23.11 Examples of three basic mechanosynthetic tooltypes that are required to build molecularly precise diamond via positional control (*black* = C atoms, *grey* = Ge atoms, *white* = H atoms) (Freitas and Merkle 2008)

tool would be held by a molecular positional device, initially perhaps a scanning probe microscope tip but ultimately a molecular robotic arm, and moved directly over particular hydrogen atoms on the surface. One suitable molecule for a hydrogen abstraction tool is the acetylene or "ethynyl" radical, comprised of two carbon atoms triply bonded together. One carbon of the two serves as the handle connection, and would bond to a nanoscale positioning tool through a much larger handle structure perhaps consisting of a lattice of adamantane cages as shown in Fig. 23.12. The other carbon of the two has a dangling bond where a hydrogen atom would normally be present in a molecule of ordinary acetylene (C_2H_2). The working environment around the tool would be inert (e.g., vacuum or a noble gas such as neon).

(2) *Hydrogen Donation Tools.* After a molecularly precise structure has been fabricated by a succession of hydrogen abstractions and carbon depositions, the fabricated structure must be hydrogen-terminated to prevent additional unplanned reactions. While the hydrogen abstraction tool is intended to make an inert structure reactive by creating a dangling bond, the hydrogen donation tool (Temelso et al. 2007) does the opposite. It makes a reactive structure inert by terminating a dangling bond. Such a tool would be used to stabilize reactive surfaces and help prevent the surface atoms from rearranging in unexpected and undesired ways. The key requirement for a hydrogen donation tool is that it include a weakly attached hydrogen atom. Many molecules fit that description, but the bond between hydrogen and germanium is sufficiently weak so that a Ge-based hydrogen donation tool (Fig. 23.11b) should be effective.

This figure will be printed in b/w

Fig. 23.12 Recyclable DCB6Ge tooltip with crossbar handle motif (Peng et al. 2006)

(3) *Carbon Placement Tools.* After the abstraction tool has created adjacent reactive spots by selectively removing hydrogen atoms from the diamond surface but before the surface is re-terminated by hydrogen, carbon placement tools may be used to deposit carbon atoms at the desired reactive surface sites. In this way a diamond structure would be built on the surface, molecule by molecule, according to plan. The first *complete* tool ever proposed for this carbon deposition function is the "DCB6Ge" dimer placement tool (Merkle and Freitas 2003) – in this example, a carbon (C_2) dimer having two carbon atoms connected by a triple bond with each carbon in the dimer connected to a larger unreactive handle structure through two germanium atoms (Fig. 23.11c). This dimer placement tool, also held by a molecular positional device, is brought close to the reactive spots along a particular trajectory, causing the two dangling surface bonds to react with the ends of the carbon dimer. The dimer placement tool would then withdraw, breaking the relatively weaker bonds between it and the C_2 dimer and transferring the carbon dimer from the tool to the surface, as illustrated in Fig. 23.9. A positionally controlled dimer could be bonded at many different sites on a growing diamondoid workpiece, in principle allowing the construction of a wide variety of useful nanopart shapes. As of 2009, the DCB6Ge dimer placement tool remains the most intensively studied of any mechanosynthetic tooltip to date (Merkle and Freitas 2003; Mann et al. 2004; Freitas 2005d; Peng et al. 2006; Freitas et al. 2007; Freitas and Merkle 2008), having had more than 150,000 CPU-hours of computation invested thus far in its analysis, and it remains the only DMS tooltip motif that has been successfully simulated and validated for its intended function on a full 200-atom diamond surface model (Peng et al. 2006). Other proposed dimer (and related carbon transfer) tooltip motifs (Drexler 1992h; Merkle 1997; Merkle and Freitas 2003; Allis and Drexler 2005; Freitas et al. 2007; Freitas and Merkle 2008) have received less extensive study but are also expected to perform well.

In 2007, Freitas and Merkle (Freitas and Merkle 2008) completed a three-year project to computationally analyze a comprehensive set of DMS reactions and an associated minimal set of tooltips that could be used to build basic diamond, graphene (e.g., carbon nanotubes), and all of the tools themselves including all necessary tool recharging reactions. The research defined 65 DMS reaction sequences incorporating 328 reaction steps, with 354 pathological side reactions analyzed and with 1,321 unique individual DFT-based (Density Functional Theory) quantum chemistry reaction energies reported. (These mechanosynthetic reaction sequences range in length from 1 to 13 reaction steps (typically 4) with 0–10 possible pathological side reactions or rearrangements (typically 3) reported per reaction step.) For the first time, this toolset provides clear developmental targets for a comprehensive near-term DMS implementation program (Nanofactory Collaboration 2007a).

23.4.4 Building the First Mechanosynthetic Tools

The first practical proposal for building a DMS tool experimentally was published by Freitas in 2005 and was the subject of the first mechanosynthesis patent ever filed (Freitas 2005d). According to this proposal, the manufacture of a complete DCB6Ge positional dimer placement tool would require four distinct steps: synthesizing a capped tooltip molecule, attaching it to a deposition surface, attaching a handle to it via CVD, then separating the tool from the deposition surface. The workability of the proposed process has already received valuable criticism from the scientific community and may be sufficiently viable to serve as a vital stepping-stone to more sophisticated DMS approaches.

An even simpler practical proposal for building DMS tools experimentally, also using only experimental methods available today, was published in 2008 by Freitas and Merkle as part of their minimal toolset work (Freitas and Merkle 2008) (see also Section 23.4.3). Processes are identified for the experimental fabrication of a hydrogen abstraction tool, a hydrogen donation tool, and two alternative carbon placement tools (other than DCB6Ge), and these processes and tools are part of the second mechanosynthesis patent ever filed and the first to be filed by the Nanofactory Collaboration (Nanofactory Collaboration 2007a). At this writing, Collaboration participants are undertaking preparatory steps (including equipment assessment and securing of funding) leading to direct experimental tests of these proposals.

Other practical proposals for building the first DMS tooltips, using existing technology, are eagerly sought by the Nanofactory Collaboration.

23.4.5 Next Generation Tools and Components

After the ability to fabricate the first primitive DMS tooltips has been demonstrated experimentally and repeatable sub-Angstrom positional placement accuracy for SPM tips has been developed, then-existing primitive tooltips could be manipulated to build the next generation of more precise, more easily rechargeable, and generally much improved mechanosynthetic tools. These more capable tools may include more stable handles of standardized dimensions, such as the rechargeable DCB6Ge dimer placement tool with the more reliable crossbar design (Peng et al. 2006) shown in Fig. 23.12, or tools with more complex handles incorporating moving components (Fig. 23.13). The end result of this iterative development process will be a mature set of efficient, positionally controlled mechanosynthetic tools that can reliably build molecularly precise diamondoid structures – including more DMS tools.

These more sophisticated tools also will be designed to allow building more complex components such as the all-hydrocarbon diamond logic rod (Fig. 23.8a), hydrocarbon bearing (Fig. 23.8b) and diamond universal joint (Fig. 23.8c), and related devices already described in Section 23.3. Once mechanosynthetic tooltips are developed for additional element types, a still wider variety of nanomachines

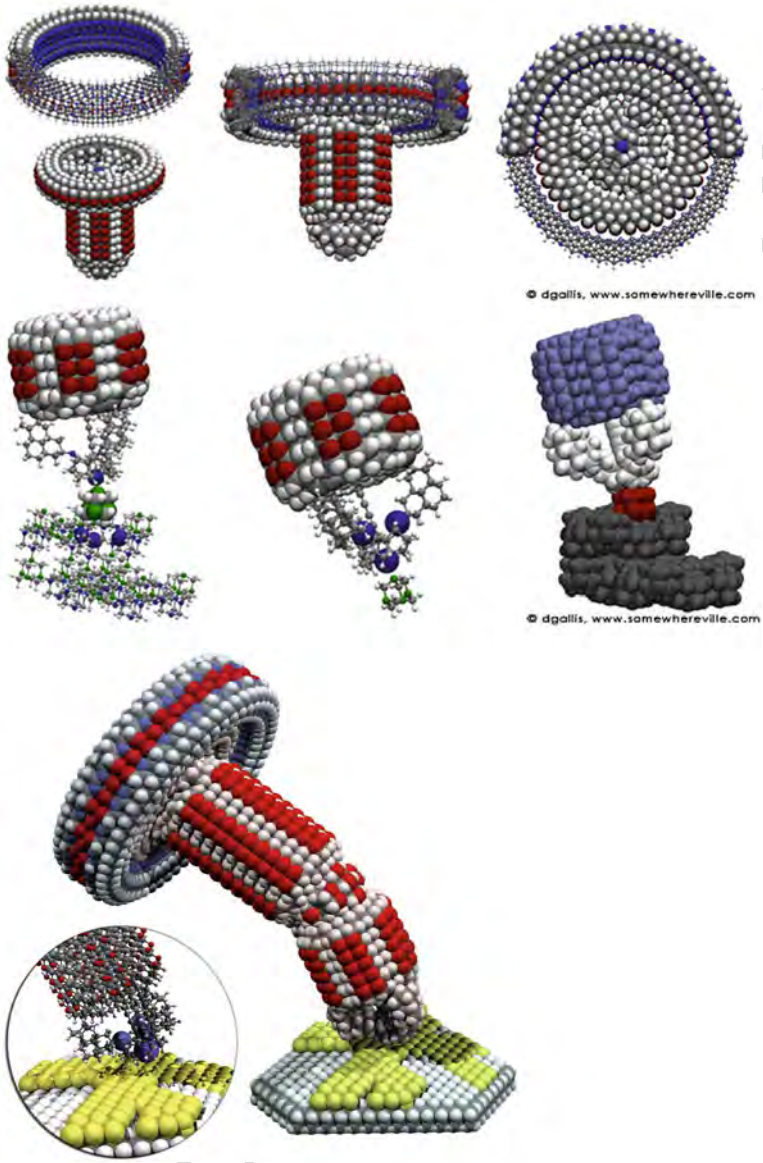

This figure will be printed in b/w

Fig. 23.13 Mechanosynthetic tooltip incorporating moving components (courtesy of Damian Allis). Used with permission

can be fabricated incorporating atoms other than hydrogen, carbon and germanium (e.g., silicon, oxygen, and sulfur). Examples of these diamondoid nanomachines include the speed reduction gear (Fig. 23.14a), in which the train of gears reduces the speed from the high-speed one on the left to the half-speed one on the right, and the differential gear (Fig. 23.14b) that smoothly converts mechanical rotation in one

This figure will be printed in b/w

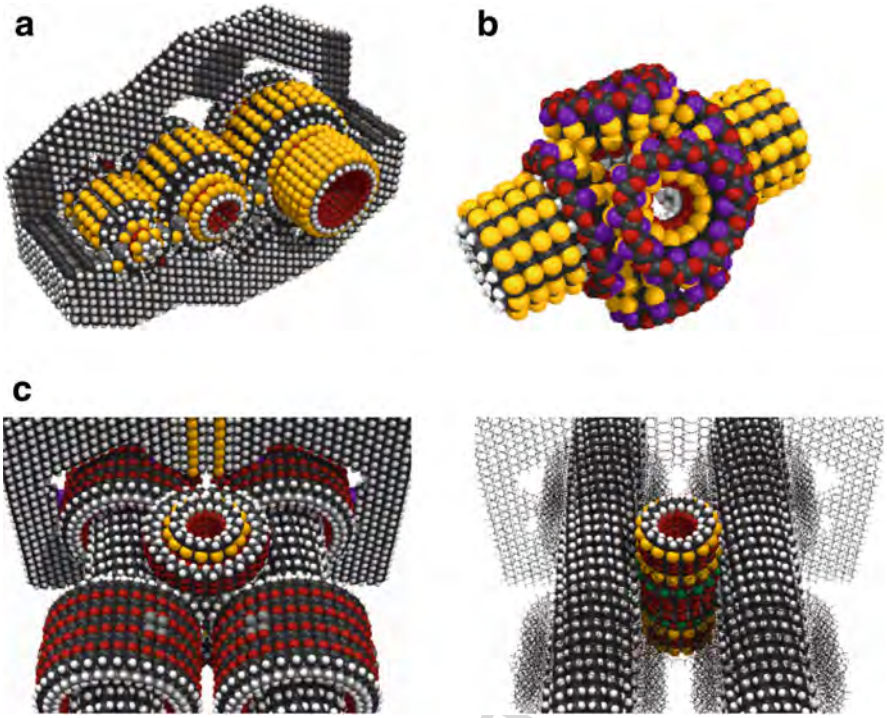

Fig. 23.14 (**a**) speed reduction gear, *above left*; (**b**) interior workings of differential gear, *above right*; (**c**) worm drive, *below* (*black* = silicon, *white* = hydrogen, *light grey* = sulfur, *dark grey* = oxygen). Images courtesy of Nanorex, used with permission

direction into mechanical rotation in the opposite direction. The largest molecular machine model that had been simulated as of 2009 using molecular dynamics was the worm drive assembly (Fig. 23.14c), consisting of 11 separate components and over 25,000 atoms; the two tubular worm gears progress in opposite directions, converting rotary into linear motion. Note that the magnitude of quantum effects is only ~10% of the classical (nonquantum) magnitudes for ~1 nm objects at 300 K, and even less significant for larger objects (Drexler 1992j).

Using computer-automated tooltips performing positionally-controlled DMS in lengthy programmed sequences of reaction steps, we should be able to fabricate simple diamondoid nanomechanical parts such as bearings, gears, struts, springs, logic rods and casings to atomic precision. Early tools would progress from single DMS tools manipulated by SPM-like mechanisms, to more complex multitip tools and jigs which the simple tools could initially fabricate, one at a time. In a factory production line (Fig. 23.15), individual DMS tooltips can be affixed to rigid moving support structures and guided through repeated contact events with workpieces, recharging stations, and other similarly-affixed apposable tooltips. These "molecular mills" could then perform repetitive fabrication steps using simple, efficient

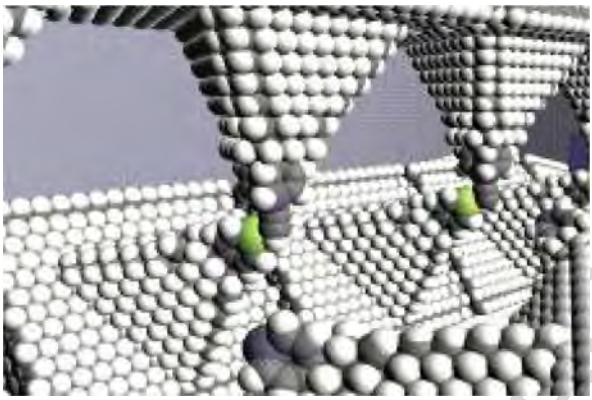

This figure will be printed in b/w

Fig. 23.15 Fabrication of nanoparts using DMS tooltips affixed to rigid moving support structures and guided through repeated contact events with workpieces under computer control in a nanofactory production line (courtesy of John Burch). Used with permission

mechanisms. Such mills can, in principle, be operated at high speeds – with positionally constrained mechanosynthetic encounters possibly occurring at up to megahertz frequencies.

The Nanofactory Collaboration has identified a large number of technical challenges (Nanofactory Collaboration 2007b) that must be solved before we can progress to building the kinds of complex nanoscale machinery described above. Among the theoretical and design challenges are: (1) nanopart gripper design, (2) nanopart manipulator actuator design, (3) design and simulation of nanopart feedstock presentation systems, (4) design and simulation of workpiece release surfaces, (5) design and simulation of nanopart assembly sequences, and (6) atomic rearrangements in juxtaposed nanoparts. Some experimental challenges include: (1) development of SPM technology to enable nanopart assembly work, (2) fabrication and testing of workpiece release surfaces, and (3) experimental proof-of-principle and early positional assembly demonstration benchmarks.

23.4.6 Strategies for Molecular Manufacturing

The ultimate goal of molecular nanotechnology is to develop a manufacturing technology able to inexpensively manufacture most arrangements of atoms that can be specified in molecular detail – including complex arrangements involving millions or billions of atoms per product object, as in the hypothesized medical nanorobots. This will provide the ultimate manufacturing technology in terms of precision, flexibility, and low cost. But to be practical, molecular manufacturing must also be able to assemble very large numbers of identical medical nanorobots very quickly. Two central technical objectives thus form the core of our current strategy for diamondoid molecular manufacturing: (1) programmable positional assembly including fabrication of diamondoid structures using molecular feedstock, as discussed above,

and (2) massive parallelization of all fabrication and assembly processes, briefly described below.

Molecular manufacturing systems capable of massively parallel fabrication (Freitas and Merkle 2004a) might employ, at the lowest level, large arrays of DMS-enabled scanning probe tips all building similar diamondoid product structures in unison. Analogous approaches are found in present-day larger-scale systems. For example, simple mechanical ciliary arrays consisting of 10,000 independent microactuators on a 1 cm^2 chip have been made at the Cornell National Nanofabrication Laboratory for microscale parts transport applications, and similarly at IBM for mechanical data storage applications (Vettiger et al. 2002). Active probe arrays of 10,000 independently-actuated microscope tips have been developed by Mirkin's group at Northwestern University for dip-pen nanolithography (Bullen et al. 2002) using DNA-based "ink". Almost any desired 2D shape can be drawn using 10 tips in concert. Another microcantilever array manufactured by Protiveris Corp. has millions of interdigitated cantilevers on a single chip (Protiveris, 2003). Martel's group has investigated using fleets of independently mobile wireless instrumented microrobot manipulators called NanoWalkers to collectively form a nanofactory system that might be used for positional manufacturing operations (Martel and Hunter 2002).

Zyvex Corp. (www.zyvex.com) of Richardson TX received a $25 million, five-year, National Institute of Standards and Technology (NIST) contract to develop prototype microscale assemblers using microelectromechanical systems (Freitas and Merkle 2004d).

Eventually this research can lead to the design of production lines in a nanofactory, both for diamondoid mechanosynthesis and for component assembly operations. Ultimately, medical nanorobots will be manufactured in desktop nanofactories efficiently designed for this purpose. The nanofactory system will include a progression of fabrication and assembly mechanisms at several different physical scales (Fig. 23.16). At the smallest scale, molecular mills will manipulate individual molecules to fabricate successively larger submicron-scale building blocks. These are passed to larger block assemblers that assemble still larger microblocks, which are themselves passed to even larger product assemblers that put together the final product. The microblocks are placed in a specific pattern and sequence following construction blueprints created using a modern "design for assembly" philosophy. As plane after plane is completed, the product extrudes outward through the surface of the nanofactory output platform (Fig. 23.17).

23.4.7 R&D Timeline, Costs, and Market Value of Medical Nanorobots

The Nanofactory Collaboration (Nanofactory Collaboration 2007a) is establishing a combined experimental and theoretical program to explore the feasibility of nanoscale positional manufacturing techniques, starting with the positionally controlled mechanosynthesis of diamondoid structures using simple molecular

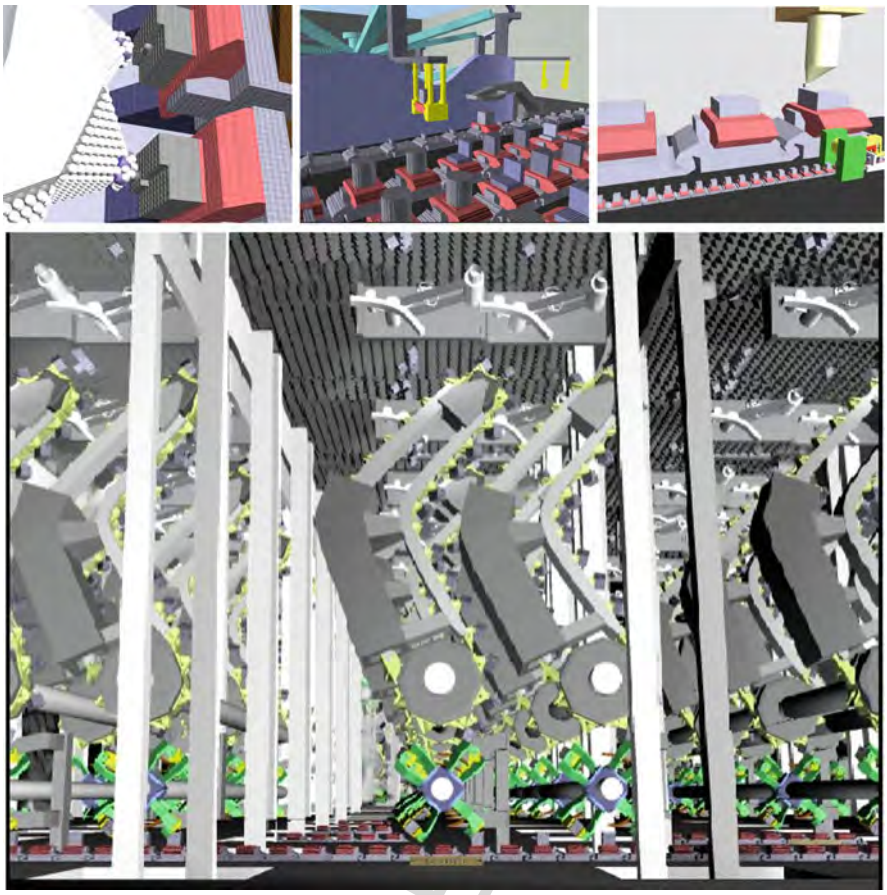

This figure will be printed in b/w

Fig. 23.16 Assembly of nanoparts into larger components and product structures using mechanical manipulators at various size scales on interconnected production lines inside a diamondoid nanofactory (courtesy of John Burch). Used with permission

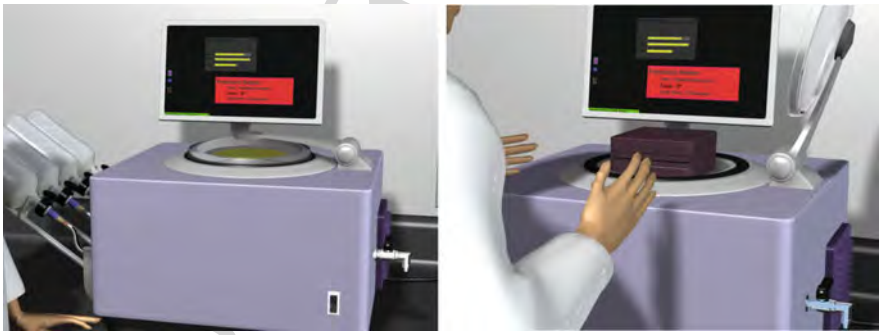

This figure will be printed in b/w

Fig. 23.17 Diamondoid desktop nanofactory (courtesy of John Burch). Used with permission

feedstock and progressing to the ultimate goal of a desktop nanofactory appliance able to manufacture macroscale quantities of molecularly precise product objects according to digitally-defined blueprints. The Collaboration was initiated by Freitas and Merkle in 2001 and has led to continuing efforts involving direct collaborations among 23 researchers and others, including 17 PhD's or PhD candidates, at 9 organizations in 4 countries – the U.S., U.K., Russia, and Belgium – as of 2009.

What will it cost to develop a nanofactory? Let's assume research funds are spent in a completely focused manner toward the goal of a primitive diamondoid nanofactory that could assemble rigid diamondoid structures involving carbon, hydrogen, and perhaps a few other elements. In this case, we estimate that an ideal research effort paced to make optimum use of available computational, experimental, and human resources would probably run at a $1–5 M/yr level for the first 5 years of the program, ramp up to $20–50 M/yr for the next 6 years, then finish off at a ~$100 M/yr rate culminating in a simple working desktop nanofactory appliance in year 16 of a ~$900 M effort. Of course the bulk of this work, after the initial 5 year period, would be performed by people, companies, and university groups recruited from outside the Nanofactory Collaboration. The key early milestone is to demonstrate positionally-controlled carbon placement on a diamond surface by the end of the initial 5 year period. We believe that successful completion of this key experimental milestone would make it easier to recruit significant additional financial and human resources to undertake the more costly later phases of the nanofactory development work.

Some additional costs would also be required to design, build, test, and obtain FDA approval for the many specific classes of nanorobots to be employed in various therapeutic medical applications (Sections 23.6 and 23.7). Medical nanorobots will certainly be among the first consumer products to be made by nanofactories because: (1) even relatively small (milligram/gram) quantities of medical nanorobots could be incredibly useful; (2) nanorobots can save lives and extend the human healthspan, thus will be in high demand once available; (3) manufacturers of such high value products (or of the nanofactories, depending on the economic model) can command a high price from healthcare providers, which means nanorobots should be worth building early, even though early-arriving nanomedical products are likely to be more expensive (in $/kg) than later-arriving products; and (4) the ability to extract, re-use and recycle nanorobots may allow the cost per treatment to the individual patient to be held lower than might be expected, with treatment costs also declining rapidly over time.

Is it worth spending billions of dollars to develop and begin deploying medical nanorobots? The billion-dollar R&D expense should be compared to the cost of doing nothing. Every year humanity suffers the death of ~55 million people, of which about 94% or 52 million of these deaths were not directly caused by human action – that is, not accidents, suicides, homicides or war – and thus all, in principle, are directly preventable by future nanomedical interventions (Section 23.6). We can crudely calculate the annual opportunity cost of a failure to intervene, as follows.

According to the Lasker Foundation (Lasker Foundation 2000), a dozen or so studies since the mid-1970s have found the value for human life is in the range

of $3 to $7 million constant dollars, using many different methodologies. More recently, data from Murphy and Topel (Murphy and Topel 1999) at the University of Chicago, updated to Year 2000 dollars, show the value of human life at every age for white males (Fig. 23.18). It recognizes that fewer years remain to us at older ages. The chart in Fig. 23.19 gives an estimate of the number of people that died in the United States in the Year 2000, in each age cohort, year by year, again for white males. This estimate is computed by multiplying the estimated U.S. population of

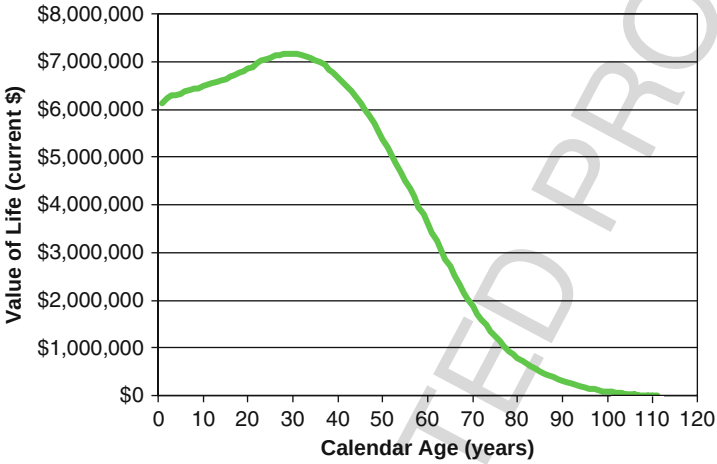

This figure will be printed in b/w

Fig. 23.18 U.S. Value of Human Life, by Age, for White Males in the Year 2000 (modified from Murphy and Topel 1999))

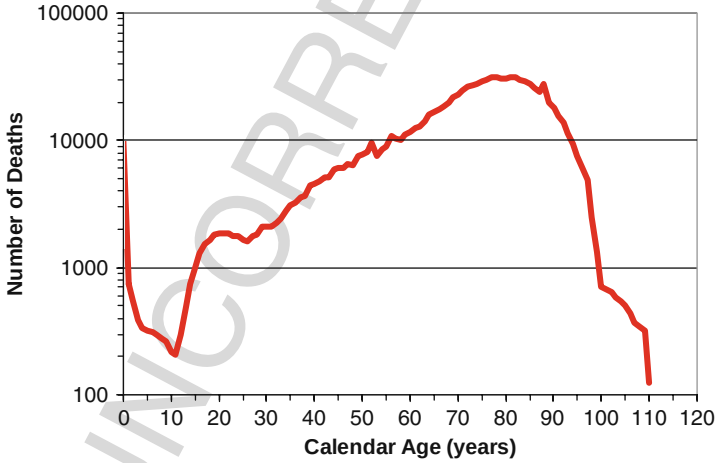

This figure will be printed in b/w

Fig. 23.19 U.S Number of Human Deaths in U.S., by Age, for White Males in the Year 2000 (values estimated using data from U.S. Census Bureau (Day 1993, Census Bureau 2001a) and from Vaupel et al. (1998))

while males (by age group, 0–110 years) (Day 1993) by the death rate by age for U.S. white males (ages 0–80 from Census Bureau (Census Bureau, 2001a), ages 81–110 estimated from Vaupel (Vaupel et al. 1998)). If we multiply the death rate at each age, from the chart in Fig. 23.19, by the dollar value at each age, from the previous chart in Fig. 23.18, we get the economic loss at each calendar age, due to human death. The sum of these economic losses divided by the total number of deaths gives the average economic value of a human life lost, across all the ages of a natural lifespan. The result is an average value of about $2.05 million dollars for each (white male) human life lost, with similar conclusions for either gender and for other races. If we assume that the population age structure, the age-specific mortality, and the value of human life is the same worldwide as in the United States, then the worldwide medically-preventable death toll of 52 million people in the Year 2000 represents an economic loss of about $104 trillion dollars per year, or ~$140T/year in 2007 dollars.

For comparison, taking Federal Reserve figures for the total tangible net wealth of the United States ($80.3T), which includes all household and business financial assets, all real estate, and all consumer durables, net of debt for 2007 (Federal Reserve System 2007), and applying the ratio (~29.4%, circa Year 2000) of U.S. GDP ($9.9T) (Census Bureau 2001b) to world GDP ($33.2T) (Department of Energy 1999) gives us a crude estimate of total global tangible net worth of $269 trillion dollars for the Year 2007. Thus every year, nanomedically preventable deaths deplete human capital by an amount exceeding half of the entire tangible wealth of the world. This ongoing *annual* capital loss is many of orders of magnitude greater than the entire likely *multi-decade* R&D expense of developing medical nanorobotics, whose deployment could spare us this great loss of human capital.

23.5 Medical Nanorobot Biocompatibility

The safety, effectiveness, and utility of medical nanorobotic devices will critically depend upon their biocompatibility with human organs, tissues, cells, and biochemical systems. An entire technical book published in 2003 (*Nanomedicine, Vol. IIA* (Freitas 2003)) describes the many biocompatibility issues surrounding the use of diamond-based nanorobots inside the human body, and broadens the definition of nanomedical biocompatibility to include all of the mechanical, physiological, immunological, cytological, and biochemical responses of the human body to the introduction of artificial medical nanodevices (Table 23.1). A large part of this work is an examination of the classical biocompatibility challenges including issues such as immune system reactions (Section 23.5.1), complement activation, inflammation (Section 23.5.2), thrombogenesis, and carcinogenesis that might be caused by medical nanorobots. But this study of classical challenges suggested a number of new biocompatibility issues that must also be addressed in medical nanorobotics including, most importantly, the areas of mechanocompatibility, particle biodynamics and distribution, and phagocyte avoidance protocols (Section 23.5.3). Readers interested

Table 23.1 Issues in nanorobot biocompatibility

Classical nanorobot biocompatibility issues	New nanorobot biocompatibility issues
• Adhesive Interactions with Nanorobot Surfaces	• Geometrical Trapping of Bloodborne Medical Nanorobots
• Nanorobot Immunoreactivity	• Phagocytosis of Bloodborne Microparticles
• Complement Activation	• Particle Clearance from Tissues or Lymphatics
• Immunosuppression, Tolerization, and Camouflage	• Phagocyte Avoidance and Escape
• Immune Privilege and Immune Evasion	• Nanorobotic Thermocompatibility and Electrocompatibility
• General and Nonspecific Inflammation	• Biofouling of Medical Nanorobots
• Coagulation and Thrombogenicity	• Biocompatibility of Nanorobot Effluents and Leachates
• Allergic and Other Sensitivity Reactions	• Biocompatibility of Nanorobot Fragments in vivo
• Sternutogenesis, Nauseogenesis and Emetogenesis	• Nanorobot Mechanocompatibility
• Nanoid Shock	• Mechanical Peristaltogenesis and Mucosacompatibility
• Nanopyrexia	• Nanorobotic Mechanical Vasculopathies
• Nanorobot Mutagenicity and Carcinogenicity	• Mechanocompatibility with Extracellular Matrix and Tissue Cells
• Protein Adsorption on Diamondoid Surfaces	• Mechanocompatibility with Nontissue Cells
• Cell Response to Diamondoid Surfaces	• Cytomembrane and Intracellular Mechanocompatibility
• Chemical Stability and Corrosion Degradation Effects	• Disruption of Molecular Motors and Vesicular Transport
• Nanorobot Hemolysis, Thrombocytolysis, and Leukocytolysis	• Mechanical Disruption of Intracellular Microzones
	• Mechanically-Induced Proteolysis, Apoptosis, or Prionosis

in biocompatibility issues not covered below can find a more comprehensive list of topics in the book *Nanomedicine, Vol. IIA* (Freitas 2003).

23.5.1 Immune System Reactions

Whether the human immune system can recognize medical nanorobots may depend largely upon the composition of the nanorobot exterior surfaces. Pure diamond is generally considered nonimmunogenic – e.g., chemical vapor deposition (CVD) diamond coatings for artificial joints are considered to have "low immunoreactivity", and as of 2009 there were no reports in the literature of antibodies having been raised to diamond. However, concerted experimental searches for antibodies to diamondoid materials have yet to be undertaken, and experimental failures rarely find their way into the literature. It is conceivable that different antibodies may recognize distinct faces of a crystal (possibly including diamond or sapphire crystal faces exposed at the surfaces of medical nanorobots) in an interaction similar to that

of antibodies for repetitive epitopes present on protein surfaces – for instance, one monoclonal antibody (MAb) to 1,4-dinitrobenzene crystals was shown to specifically interact with the molecularly flat, aromatic, and polar (101) face of these crystals, but not with other faces of the same crystal (Kessler et al. 1999). Another concern is that antibodies may be raised against binding sites that are positioned on the nanorobot exterior, e.g., sorting rotor pockets (Freitas 1999o) which may be similar to traditional bioreceptors, and that these antibodies could then act as antagonists (Fauque et al. 1985; Wright et al. 2000) for such sites, since MAbs specific to biological binding sites are well known.

If antibodies to nanorobot exteriors are found to exist in the natural human antibody specificity repertoire, then to avoid immune recognition many techniques of immune evasion (Freitas 2003b) may be borrowed from biology, for example:

(1) *Camouflage.* Coat the nanorobot with a layer of "self" proteins and carbohydrate moieties resembling fibroblast, platelet, or even RBC (red blood cell) plasma membrane.
(2) *Chemical Inhibition.* Nanorobots may slowly secrete chemical substances into the perirobotic environment to make it difficult for Ig molecules to adhere to an otherwise immunogenic nanorobot surface.
(3) *Decoys.* Release a cloud of soluble nanorobot-epitope antigens in the vicinity of the nanorobot (though this method has limited utility because sending out decoys will only expand the number of attacking elements to overwhelm the decoys).
(4) *Active Neutralization.* Equip the nanorobot with molecular sorting rotors designed with binding sites similar or identical to the nanorobot epitopes that raised the target antibodies.
(5) *Tolerization.* Using only traditional methods, nanorobots introduced into a newborn may train the neonatal immune system to regard these foreign materials as "native," thus eliminating nanorobot-active antibodies via natural clonal deletion. However, it now appears possible to tolerize an adult to any antigen by regenerating the adult's thymus (the source of the newborn effect) and placing the antigen into the thymus where self-reactive clones are then deleted or anergized (Fahy 2003, 2007, 2010; Aspinall 2010).
(6) *Clonal Deletion.* Once the paratopes of antibodies that bind nanorobots are known, immunotoxin molecules can be engineered that display those paratopes, and upon injection into the patient, these targeted immunotoxins would bind to all T cell receptors that display this paratope, killing the nanorobot-sensitive T cells.

23.5.2 Inflammation

Could medical nanorobots trigger general inflammation in the human body? One early experiment (Royer et al. 1982) to determine the inflammatory effects of various implant substances placed subdermally into rat paws found that an injection

of 2–10 mg/cm^3 (10- to 20-micron particles at 10^5–10^6 particles/cm^3) of natural diamond powder suspension caused a slight increase in volume of the treated paw relative to the control paw. However, the edematous effect subsided after 30–60 minutes at both concentrations of injected diamond powder that were tried, so this swelling could have been wholly caused by mechanical trauma of the injection and not the diamond powder. Another experiment (Delongeas et al. 1984) at the same laboratory found that intraarticulate injection of diamond powder was not phlogistic (i.e., no erythematous or edematous changes) in rabbit bone joints and produced no inflammation. Diamond particles are traditionally regarded as biologically inert and noninflammatory for neutrophils (Tse and Phelps 1970; Higson and Jones 1984; Hedenborg and Klockars 1989; Aspenberg et al. 1996) and are typically used as experimental null controls (Delongeas et al. 1984).

Since the general inflammatory reaction is chemically mediated, it should also be possible to employ nanorobot surface-deployed molecular sorting rotors to selectively absorb kinins or other soluble activation factors such as HMGB1 (High Mobility Group Box Protein 1) (Scaffidi et al. 2002), thus short-circuiting the inflammatory process. Active semaphores consisting of bound proteases such as gelatinase A could be deployed at the nanorobot surface to cleave and degrade monocyte chemoattractant molecules (McQuibban et al. 2000) or other chemokines, suppressing the cellular inflammatory response. Conversely, key inflammatory inhibitors could be locally released by nanorobots. For instance, Hageman factor contact activation inhibitors such as the 22.5-kD endothelial cell-secreted protein HMG-I (Donaldson et al. 1998), surface-immobilized unfractionated heparin (Elgue et al. 1993), and C1 inhibitor (Cameron et al. 1989) would probably require lower release dosages than for aspirin or steroids, and therapeutic blockade of factor XII activation has been demonstrated (Fuhrer et al. 1990). As yet another example, platelet activating factor (PAF) is a cytokine mediator of immediate hypersensitivity which produces inflammation. PAF is produced by many different kinds of stimulated cells such as basophils, endothelial cells, macrophages, monocytes, and neutrophils. It is 100–10,000 times more vasoactive than histamine and aggregates platelets at concentrations as low as 0.01 pmol/cm^3 (Mayes 1993). Various PAF antagonists and inhibitors are known (Freitas 2003c) – and these or related inhibitory molecules, if released or surface-displayed by medical nanorobots, may be useful in circumventing a general inflammatory response.

23.5.3 Phagocytosis

Invading microbes that readily attract phagocytes and are easily ingested and killed are generally unsuccessful as parasites. In contrast, most bacteria that are successful as parasites interfere to some extent with the activities of phagocytes or find some way to avoid their attention (Todar 2003). Bacterial pathogens have devised numerous diverse strategies to avoid phagocytic engulfment and killing. These strategies are mostly aimed at blocking one or more of the steps in phagocytosis, thereby halting the process (Todar 2003).

Similarly, phagocytic cells presented with any significant concentration of medical nanorobots may attempt to internalize these nanorobots. Virtually every medical nanorobot placed inside the human body will physically encounter phagocytic cells many times during its mission. Thus all nanorobots that are of a size capable of ingestion by phagocytic cells must incorporate physical mechanisms and operational protocols for avoiding and escaping from phagocytes (Freitas 2003d). Engulfment may require from many seconds to many minutes to go to completion (Freitas 2003e), depending upon the size of the particle to be internalized, so medical nanorobots should have plenty of time to detect, and to actively prevent, this process. Detection by a medical nanorobot that it is being engulfed by a phagocyte may be accomplished using (1) hull-mounted chemotactic sensor pads equipped with artificial binding sites that are specific to phagocyte coat molecules, (2) continuous monitoring of the flow rates of nanorobot nutrient ingestion or waste ejection mechanisms (e.g., blocked glucose or O_2 import), (3) acoustic techniques (Freitas 1999w), (4) direct measurement of mechanical forces on the hull, or (5) various other means.

The basic anti-phagocyte strategy is first to avoid phagocytic contact (Freitas 2003f), recognition (Freitas 2003g), or binding and activation (Freitas 2003h), and secondly, if this fails, then to inhibit phagocytic engulfment (Freitas 2003i) or enclosure and scission (Freitas 2003j) of the phagosome. If trapped, the medical nanorobot can induce exocytosis of the phagosomal vacuole in which it is lodged (Freitas 2003k) or inhibit both phagolysosomal fusion (Freitas 2003m) and phagosome metabolism (Freitas 2003n). In rare circumstances, it may be necessary to kill the phagocyte (Freitas 2003o) or to blockade the entire phagocytic system (Freitas 2003p). Of course, the most direct approach for a fully-functional medical nanorobot is to employ its motility mechanisms to locomote out of, or away from, the phagocytic cell that is attempting to engulf it. This may involve reverse cytopenetration (Freitas 1999x), which must be done cautiously (e.g., the rapid exit of nonenveloped viruses from cells can be cytotoxic (Oh 1985)). It is possible that frustrated phagocytosis may induce a localized compensatory granulomatous reaction. Medical nanorobots therefore may also need to employ simple but active defensive strategies to forestall granuloma formation (Freitas 2003q).

23.6 Control of Human Morbidity using Medical Nanorobots

Morbidity is the state of being unhealthy, sick, diseased, possessing genetic or anatomic pathologies or injuries, or experiencing physiological malfunctions, and also generally refers to conditions that are potentially medically treatable. Here we'll examine how human morbidity can be controlled and prevented by employing medical nanorobots to cure disease, reverse trauma, and repair individual cells. The descriptions of nanorobots suggested for each treatment are representative of the powerful new capabilities that are expected to be available some decades hence, but we do not provide an exhaustive summary of all devices that may be needed during each treatment as that would be beyond the scope of this chapter.

23.6.1 Advantages of Medical Nanorobots

Although biotechnology makes possible a greatly increased range and efficacy of treatment options compared to traditional approaches, with medical nanorobotics the range, efficacy, comfort and speed of possible medical treatments further expands enormously. Medical nanorobotics will be essential whenever the damage to the human body is extremely subtle, highly selective, or time-critical (as in head traumas, burns, or fast-spreading diseases), or when the damage is very massive, overwhelming the body's natural defenses and repair mechanisms – pathological conditions from which it is often difficult or impossible to recover at all using current or easily foreseeable biotechnological techniques.

While it is true that many classes of medical problems may be at least partially resolved using existing treatment alternatives, it is also true that as the chosen medical technology becomes more precise, active, and controllable, the range of options broadens and the quality of the options improves. Thus the question is not whether medical nanorobotics is absolutely required to accomplish a given medical objective. In many cases, it is not – though of course there are some things that only biotechnology and nanotechnology can do, and some other things that only nanotechnology can do. Rather, the important question is which approach offers a superior outcome for a given medical problem, using any reasonable metric of treatment efficacy. For virtually every class of medical challenge, a mature medical nanorobotics offers a wider and more effective range of treatment options than any other solution. A few of the most important advantages of medical nanorobotics over present-day and future biotechnology-based medical and surgical approaches include (Freitas 1999ct):

1. *Speed of Treatment.* Doctors may be surprised by the incredible quickness of nanorobotic action when compared to methods relying on self-repair. We expect that mechanical nanorobotic therapeutic systems can reach their targets up to ~1,000 times faster, all else equal, and treatments which require ~10^5 sec (~days) for biological systems to complete may require only ~10^2 sec (~minutes) using nanorobotic systems (Freitas 2005b).
2. *Control of Treatment.* Present-day biotechnological entities are not programmable and cannot easily be switched on and off conditionally (while following complex multidecision trees) during task execution. Even assuming that a digital biocomputer (Freitas 1999ai; Guet et al. 2002; Yokobayashi et al. 2002; Basu et al. 2004, 2005) could be installed in, for example, a fibroblast, and that appropriate effector mechanisms could be attached, such a biorobotic system would necessarily have slower clock cycles (Basu et al. 2004), less capacious memory per unit volume, and longer data access times, implying less diversity of action, poorer control, and less complex executable programs than would be available in diamondoid nanocomputer-controlled nanorobotic systems (Section 23.3.5). The mechanical or electronic nanocomputer approach (Freitas 1999k) emphasizes precise control of action (Freitas 2009), including control of physical placement, timing, strength, structure, and interactions with other (especially biological) entities.

3. *Verification of Treatment.* Nanorobotic-enabled endoscopic nanosurgery (Section "Endoscopic Nanosurgery and Surgical Nanorobots") will include comprehensive sensory feedback enabling full VR telepresence permitting real-time surgery into cellular and subcellular tissue volumes. Using a variety of communication modalities (Freitas 1999f), nanorobots will be able to report back to the attending physician, with digital precision and ~MHz bandwidth (Freitas 1999ah), a summary of diagnostically- or therapeutically-relevant data describing exactly what was found prior to treatment, what was done during treatment, and what problems were encountered after treatment, in every cell or tissue visited and treated by the nanorobot. A comparable biological-based approach relying primarily upon chemical messaging must necessarily be slow and have only limited signaling capacity and bandwidth.
4. *Minimal Side Effects.* Almost all drugs have significant side effects, such as conventional cancer chemotherapy which causes hair loss and vomiting, although computer-designed drugs can have higher specificity and fewer side effects than earlier drugs. Carefully tailored cancer vaccines under development starting in the late 1990s were expected unavoidably to affect some healthy cells. Even well-targeted drugs are distributed to unintended tissues and organs in low concentrations (Davis 1996), although some bacteria can target a few organs fairly reliably without being able to distinguish individual cells. By contrast, mechanical nanorobots may be targeted with virtually 100% accuracy to specific organs, tissues, or even individual cellular addresses within the human body (Freitas 1999g, 2006a). Such nanorobots should have few if any side effects, and will remain safe even in large dosages because their actions can be digitally self-regulated using rigorous control protocols (Freitas 2009) that affirmatively prohibit device activation unless all necessary preconditions have been met, and remain continuously satisfied. More than a decade ago, Fahy (1993) observed that these possibilities could transform "drugs" into "programmable machines with a range of sensory, decision-making, and effector capabilities [that] might avoid side effects and allergic reactions...attaining almost complete specificity of action.... Designed smart pharmaceuticals might activate themselves only when, where, and if needed." Additionally, nanorobots may be programmed to harmlessly remove themselves from the site of action, or conveniently excrete themselves from the body, after a treatment is completed. By contrast, spent biorobotic elements containing ingested foreign materials may have more limited post-treatment mobility, thus lingering at the worksite causing inflammation when naturally degraded in situ or removed. (It might be possible to design artificial eukaryotic biorobots having an apoptotic pathway (Freitas 1999ag) that could be activated to permit clean and natural self-destruction, but any indigestible foreign material that had been endocytosed by the biorobot could still cause inflammation in surrounding tissues when released).
5. *Faster and More Precise Diagnosis.* The analytic function of medical diagnosis requires rapid communication between the injected devices and the attending physician. If limited to chemical messaging, biotechnology-based devices such as biorobots will require minutes or hours to complete each diagnostic loop.

Nanomachines, with their more diverse set of input-output mechanisms, will be able to outmessage complete results (both aggregated and individual outliers) of in vivo reconnaissance or testing to the physician, literally in seconds (Freitas 1999f). Such nanomachines could also run more complex tests of greater variety in far less time. Nanomechanical nanoinstrumentation will make comprehensive rapid cell mapping and cell interaction analysis possible. For example, new instances of novel bacterial resistance could be assayed at the molecular level in real time, allowing new treatment agents to be quickly composed using an FDA-approved formulary, then manufactured and immediately deployed on the spot.

6. *More Sensitive Response Threshold for High-Speed Action.* Unlike natural systems, an entire population of nanorobotic devices could be triggered globally by just a single local detection of the target antigen or pathogen. The natural immune system takes $>10^5$ sec to become fully engaged after exposure to a systemic pathogen or other antigen-presenting intruder. A biotechnologically enhanced immune system that could employ the fastest natural unit replication time ($\sim 10^3$ sec for some bacteria) would thus require at least $\sim 10^4$ sec for full deployment post-exposure. By contrast, an artificial nanorobotic immune system (Freitas 2005b) could probably be fully engaged (though not finished) in at most two blood circulation times, or $\sim 10^2$ sec.
7. *More Reliable Operation*. Individual engineered macrophages would almost certainly operate less reliably than individual mechanical nanorobots. For example, many pathogens, such as *Listeria monocytogenes* and *Trypanosoma cruzi*, are known to be able to escape from phagocytic vacuoles into the cytoplasm (Stenger et al. 1998). While biotech drugs or cell manufactured proteins could be developed to prevent this (e.g., cold therapy drugs are entry-point blockers), nanorobotic trapping mechanisms could be more secure (Freitas 1999y, 2005b). Proteins assembled by natural ribosomes typically incorporate one error per $\sim 10^4$ amino acids placed; current gene and protein synthesizing machines utilizing biotechnological processes have similar error rates. A molecular nanotechnology approach should decrease these error rates by at least a millionfold (Drexler 1992i). Nanomechanical systems will also incorporate onboard sensors to determine if and when a particular task needs to be done, or when a task has been completed. Finally, and perhaps most importantly, it is highly unlikely that natural microorganisms will be able to infiltrate rigid watertight diamondoid nanorobots or to co-opt their functions. By contrast, a biotech-based biorobot more readily could be diverted or defeated by microbes that would piggyback on its metabolism, interfere with its normal workings, or even incorporate the device wholesale into their own structures, causing the engineered biomachine to perform some new or different – and possibly pathological – function that was not originally intended. There are many examples of such co-option in natural biological systems, including the protozoan mixotrichs found in the termite gut that have assimilated bacteria into their bodies for use as motive engines (Cleveland and Grimstone 1964; Tamm 1982), and the nudibranch mollusks (marine snails without shells) that steal nematocysts (stinging cells) away from

coelenterates such as jellyfish (i.e. a Portuguese man-of-war) and incorporate the stingers as defensive armaments in their own skins (Thompson and Bennett 1969) – a process which Vogel (Vogel 1998) calls "stealing loaded guns from the army."

8. *Nonbiodegradable Treatment Agents.* Diagnostic and therapeutic agents constructed of biomaterials generally are biodegradable in vivo, although there is a major branch of pharmacology devoted to designing drugs that are moderately non-biodegradable – e.g., anti-sense DNA analogs with unusual backbone linkages and peptide nucleic acids (PNAs) are difficult to break down. An engineered fibroblast may not stimulate an immune response when transplanted into a foreign host, but its biomolecules are subject to chemical attack in vivo by free radicals, acids, and enzymes. Even "mirror" biomolecules or "Doppelganger proteins" comprised exclusively of unnatural D-amino acids have a lifetime of only ~5 days inside the human body (Robson 1998). In contrast, suitably designed nanorobotic agents constructed of nonbiological materials will not be biodegradable. Nonbiological diamondoid materials are highly resistant to chemical breakdown or leukocytic degradation in vivo, and pathogenic biological entities cannot easily evolve useful attack strategies against these materials (Freitas 1999z). This means that medical nanorobots could be recovered intact from the patient and recycled, reducing life-cycle energy consumption and treatment costs.
9. *Superior Materials*. Typical biological materials have tensile failure strengths in the 10^6–10^7 N/m^2 range, with the strongest biological materials such as wet compact bone having a failure strength of ~10^8 N/m^2, all of which compare poorly to ~10^9 N/m^2 for good steel, ~10^{10} N/m^2 for sapphire, and ~10^{11} N/m^2 for diamond and carbon fullerenes (Freitas 1999aa), again showing a 10^3–10^5 fold strength advantage for mechanical systems that use nonbiological, and especially diamondoid, materials. Nonbiological materials can be much stiffer, permitting the application of higher forces with greater precision of movement, and they also tend to remain more stable over a larger range of relevant conditions including temperature, pressure, salinity and pH. Proteins are heat sensitive in part because much of the functionality of their structure derives from the noncovalent bonds involved in folding, which are broken more easily at higher temperatures. In diamond, sapphire, and many other rigid materials, structural shape is covalently fixed, hence is far more temperature-stable. Most proteins also tend to become dysfunctional at cryogenic temperatures, unlike diamond-based mechanical structures (Freitas 1999ab), so diamondoid nanorobots could more easily be used to repair frozen cells and tissues. Biomaterials are not ruled out for all nanomechanical systems, but they represent only a small subset of the full range of materials that can be employed in nanorobots. Nanorobotic systems may take advantage of a wider variety of atom types and molecular structures in their design and construction, making possible novel functional forms that might be difficult to implement in a purely biological-based system (e.g., steam engines (Freitas 1999ac) or nuclear power (Freitas 1999ad)). As another example, an application requiring the most effective bulk thermal conduction possible

should use diamond, the best conductor available, not some biomaterial having inferior thermal performance.

23.6.2 Curing Disease

Nanorobots should be able to cure most common diseases in a manner more akin to the directness and immediacy of surgery, fixing a given problem in minutes or hours, than to current treatment regimens for treating most disease conditions which typically involve (a) the injection or ingestion of slow-acting medications of relatively poor efficacy, (b) dietary and lifestyle changes, (c) psychological factors, and so forth, often taking weeks, months, or even years to provide what is sometimes only an incomplete cure. We focus here on the disease conditions that presently pose the greatest risk of death, most of which are, not surprisingly, presently associated with aging and include microbial infections (Section 23.6.2.1), cancer (Section 23.6.2.2), heart disease (Section 23.6.2.3), stroke (Section 23.6.2.4), and hormonal, metabolic and genetic disease (Section 23.6.2.5).

Bear in mind that each of the nanorobotic treatment devices described below has been subjected to a rigorous design and scaling study, most of which have been published in peer reviewed journals. Thus the proposed nanomachines are not cartoons or simplistic speculations but rather are genuine engineering constructs believed to be thoroughly feasible and likely to function as described once they (or similar devices) can be manufactured (Section 23.4).

23.6.2.1 Bacterial, Viral, and Other Parasitic Infection

Perhaps the most widely recognized form of disease is when the human body is under attack by invading viruses, bacteria, protozoa, or other microscopic parasites. One general class of medical nanorobot will serve as the first-line nanomedical treatment for pathogen-related disease. Called a "microbivore" (Fig. 23.20), this artificial nanorobotic white cell substitute, made of diamond and sapphire, would seek out and harmlessly digest unwanted bloodborne pathogens (Freitas 2005b). One main task of natural white cells is to phagocytose and kill microbial invaders in the bloodstream. Microbivore nanorobots would also perform the equivalent of phagocytosis and microbial killing, but would operate much faster, more reliably, and under human control.

The baseline microbivore is designed as an oblate spheroidal nanomedical device measuring 3.4 microns in diameter along its major axis and 2.0 microns in diameter along its minor axis, consisting of 610 billion precisely arranged structural atoms in a gross geometric volume of 12.1 micron^3 and a dry mass of 12.2 picograms. This size helps to ensure that the nanorobot can safely pass through even the narrowest of human capillaries and other tight spots in the spleen (e.g., the interendothelial splenofenestral slits (Freitas 2003r)) and elsewhere in the human body (Freitas 2003s). The microbivore has a mouth with an irising door, called the ingestion port, where microbes are fed in to be digested, which is large enough to

This figure will be printed in b/w

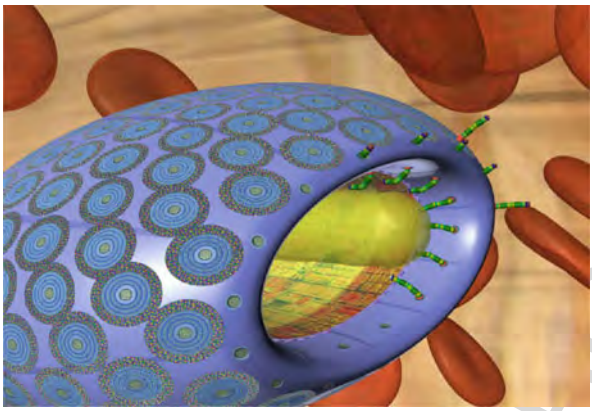

Fig. 23.20 An artificial white cell – the microbivore (Freitas 2005a). Designer Robert A. Freitas Jr., additional design Forrest Bishop. ©2001 Zyvex Corp. Used with permission

internalize a single microbe from virtually any major bacteremic species in a single gulp. The microbivore also has a rear end, or exhaust port, where the completely digested remains of the pathogen are harmlessly expelled from the device. The rear door opens between the main body of the microbivore and a tail-cone structure. According to this author's scaling study (Freitas 2005b), the device may consume up to 200 pW of continuous power (using bloodstream glucose and oxygen for energy) while completely digesting trapped microbes at a maximum throughput of 2 micron^3 of organic material per 30-second cycle. This "digest and discharge" protocol (Freitas 1999aj) is conceptually similar to the internalization and digestion process practiced by natural phagocytes, except that the artificial process should be much faster and cleaner. For example, it is well-known that macrophages release biologically active compounds during bacteriophagy (Fincher et al. 1996), whereas well-designed microbivores need only release biologically inactive effluent.

The first task for the bloodborne microbivore is to reliably acquire a pathogen to be digested. If the correct bacterium bumps into the nanorobot surface, reversible species-specific binding sites on the microbivore hull can recognize and weakly bind to the bacterium. A set of 9 distinct antigenic markers should be specific enough (Freitas 1999ak), since all 9 must register a positive binding event to confirm that a targeted microbe has been caught. There are 20,000 copies of these 9-marker receptor sets, distributed in 275 disk-shaped regions across the microbivore surface. Inside each receptor ring are more rotors to absorb ambient glucose and oxygen from the bloodstream to provide nanorobot power. At the center of each 150-nm diameter receptor disk is a grapple silo. Once a bacterium has been captured by the reversible receptors, telescoping robotic grapples (Freitas 1999am) rise up out of the microbivore surface and attach to the trapped bacterium, establishing secure anchorage to the microbe's cell wall, capsid, or plasma membrane (Fig. 23.21). The microbivore grapple arms are about 100 nm long and have various rotating and telescoping joints that allow them to change their position, angle, and length. After

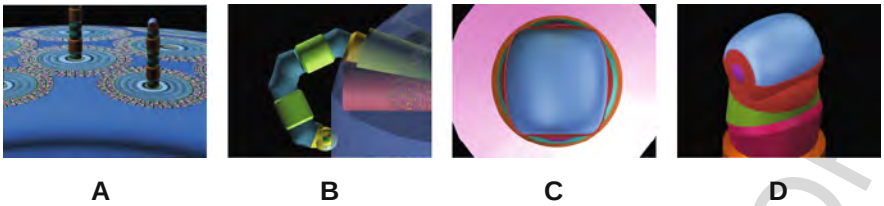

Fig. 23.21 Telescoping grapple manipulators for the microbivore (Freitas 2005a) help to capture and manipulate target pathogens into the interior of the device for digestion, and to assist in device mobility; (**a**) fully extended grapple, (**b**) grapple work envelope, (**c**) top view of grapple in silo with iris cover mechanism retracted, (**d**) grapple footpad covered by protective cowling. Images © 2001 Forrest Bishop, used with permission

This figure will be printed in b/w

rising out of its silo, a grapple arm could execute complex twisting motions, and adjacent grapple arms can physically reach each other, allowing them to hand off bound objects as small as a virus particle. Grapple handoff motions could transport a large rod-shaped bacterium from its original capture site forward to the ingestion port at the front of the device. The captive organism would be rotated into the proper orientation as it approaches the open microbivore mouth, where the pathogen is internalized into a 2 micron^3 morcellation chamber under continuous control of mouth grapples and an internal mooring mechanism.

There are two concentric cylinders inside the microbivore. The bacterium will be minced into nanoscale pieces in the morcellation chamber (Freitas 1999an), the smaller inner cylinder, then the remains are pistoned into a separate 2 micron^3 digestion chamber, a larger outer cylinder. In a preprogrammed sequence, ~40 different engineered digestive enzymes will be successively injected and extracted six times during a single digestion cycle, progressively reducing the morcellate to monoresidue amino acids, mononucleotides, glycerol, free fatty acids and simple sugars, using an appropriate array of molecular sorting rotors. These basic molecules are then harmlessly discharged back into the bloodstream through the exhaust port at the rear of the device, completing the 30-second digestion cycle. When treatment is finished, the doctor may transmit an ultrasound signal to tell the circulating microbivores that their work is done. The nanorobots then exit the body through the kidneys and are excreted with the urine in due course (Weatherbee and Freitas 2010).

A human neutrophil, the most common type of leukocyte or white cell, can capture and engulf a microbe in a minute or less, but complete digestion and excretion of the organism's remains can take an hour or longer. Our natural white cells – even when aided by antibiotics – can sometimes take weeks or months to completely clear bacteria from the bloodstream. By comparison, a single terabot (10^{12}-nanorobot) dose of microbivores should be able to fully eliminate bloodborne pathogens in just minutes, or hours in the case of locally dense infections. This is accomplished without increasing the risk of sepsis or septic shock because all bacterial components (including all cell-wall lipopolysaccharide) will be internalized and fully digested

into harmless nonantigenic molecules prior to discharge from the device. And no matter that a bacterium has acquired multiple drug resistance to antibiotics or to any other traditional treatment – the microbivore will eat it anyway. Microbivores would be up to ~1000 times faster-acting than antibiotic-based cures which often need weeks or months to work. The nanorobots would digest ~100 times more microbial material than an equal volume of natural white cells could digest in any given time period, and would have far greater maximum lifetime capacity for phagocytosis than natural white blood cells.

Besides intravenous bacterial, viral, fungal, and parasitic scavenging, microbivores or related devices could also be used to help clear respiratory or cerebrospinal bacterial infections, or infections in other nonsanguinous fluid spaces such as pleural (Strange and Sahn 1999), synovial (Perez 1999), or urinary fluids. They could eliminate bacterial toxemias; eradicate viral, fungal, and parasitic infections; patrol tissues to remove pathological substances and organisms; disinfect surfaces, foodstuffs, or organic samples; and even help clean up biohazards and toxic chemicals.

Slightly modified microbivores are envisioned (Freitas 2005b) that could attack biofilms (Costerton et al. 1999) or small tumor masses (Section 23.6.2.2). A targeted cell-rich surface would be detected via receptor binding, then grapple arms would rotate the entire nanorobot perpendicular to the stationary biofilm. After positioning the nanorobot's mouth over the film and establishing watertight contact via lipophilic semaphores (Freitas 1999cu), operation of the vacuum piston draws biofilm contents into the morcellation chamber and the regular digestion cycle begins. The geometry of the nanorobot mouth can be altered (e.g., to square or hexagonal cross-section) to allow closer packing of a sufficient number of adjacent microbivores to avoid significant leakage of cell contents as the biofilm or tumor is planarly digested.

Bloodborne microbivores alone are not a complete solution to microbial disease – pathogens also accumulate in reservoirs inside organs, tissues, and even cells, and thus would need to be extirpated by more sophisticated tissue-mobile (Freitas 1999at) and even cytopenetrating (Freitas 1999x) microbivores. Similarly, viruses can insert alien genetic sequences into native DNA that must be rooted out using chromallocyte-class devices (Section 23.6.4.3), and so forth. But microbivore-class devices will be the foundation of our future first-line treatment against microbiological pathogens.

23.6.2.2 Cancer

A cell that has lost its normal control mechanisms and thus exhibits unregulated growth is called a cancer. Cancer cells can arise from normal cells in any tissue or organ, and during this process their genetic material undergoes change. As these cells grow and multiply, they form a mass of cancerous tissue that invades adjacent tissues and can metastasize around the body. Near-term alternatives to traditional chemotherapy (that kills not just cancer cells but healthy cells as well and causes fatigue, hair loss, nausea, depression, and other side effects) are being developed

such as angiogenesis inhibitors (Bergers et al. 1999), autologous vaccines (Berd et al. 1998), and WILT (Section 23.7.1.7).

The healthy human body can use phagocytosis to dispose of many isolated cancer cells (Shankaran et al. 2001; Dunn et al. 2002; Street et al. 2004; Swann and Smyth 2007) before they can replicate and become established as a growing tumor – which happens more frequently in people with abnormally functioning immune systems (e.g., patients with autoimmune disease or on immunosuppressive drugs) – though some cancers can evade immune system surveillance even when that system is functioning normally. No such evasion is possible, however, if we use microbivore-class nanodevices, some with enhanced tissue mobility, that could patrol the bloodstream or body tissues, seeking out the clear antigenic signature of cancerous cells or tumors (see below) and then digesting these cancers into harmless effluvia, leaving healthy cells untouched. For example, active microbivores crowding on the exterior surface of a tumor mass could each excavate and digest the tumor mass beneath it at ~1 micron/min, requiring ~1 hour for ~4000 devices to digest a 100 micron diameter tumor mass or ~400,000 devices and ~10 hours for a 1 mm diameter tumor. Larger tumors could be infiltrated by tissue-mobile microbivores along numerous parallel strata or more tortuous vascular paths and then be rapidly consumed from multiple foci, from the inside out.

A more organized treatment protocol would begin with a comprehensive whole-body mapping of all tissue-borne cancer cells and tumors based on detection of specific biomarkers (Box 23.1) or other thermographic (Freitas 1999av) or chemographic (Freitas 1999aw) techniques. A trillion-nanorobot survey fleet that spends 100 seconds examining the chemical surface signatures of the plasma membranes of all ~10 trillion tissue cells in the body (Freitas 1999m) nominally would require ~1000 sec to complete the survey. Each device could reach the vicinity of most organs and tissues in the body in about one circulation time or ~60 sec, and could then reach most cells which lie well within ~40 microns (~2 cell widths) of a capillary exit point within ~40 sec even traveling at a very slow ~1 micron/sec through the tissues (comparable to leukocyte and fibroblast speeds (Freitas 1999au)). Adding this travel time increases survey time to ~1520 seconds for infusion, travel to 10 adjacent target cells, examination of target cells, and return to the bloodstream, so we should perhaps allow ~1 hour for the entire mapping process (Freitas 2007) which must also include ingress and egress of nanorobots from the body.

Once the locations of all cancerous cells in the body have been mapped, tissue-mobile microbivores can employ precise in vivo positional navigation (Freitas 1999cj) to return to the address of each isolated cancer cell or small cancer cell aggregate and destroy them. Tumor masses larger than 0.1–1 mm in diameter may be more practical to remove via endoscopic nanosurgery (Section "Endoscopic Nanosurgery and Surgical Nanorobots") in which a specialized nanomechanical probe instrument such as a nanosyringoscope (Section "Nanosyringoscopy") (whose intelligent tip is mobile and guided by continuous sensor readings to detect the perimeter of the cancerous region) would be inserted into the diseased tissue which is then excised and either digested or vacuumed out in a few minutes, much

like fatty deposits during present-day atherectomies (Mureebe and McKinsey 2006), malignant tumors during endoscopic tumor microdebridement (Simoni et al. 2003), or less-precise laser-based tumor debulking procedures (Paleri et al. 2005). In principle, cell repair nanorobots called chromallocytes (Section 23.6.4.3) that are capable of in situ chromosome replacement therapy could be used to effect a complete genetic cure of diseased cancer cells, but this is not practical for large tumors (treatment time too long, cell population too protean) and because most tumors consist of surplus tissue that is more convenient to excise than to repair.

Box 23.1 Biochemical markers for cancer cell mapping

Cancer cells may display below-normal concentrations of β_4 integrins and above-normal concentrations of β_1 integrins, survivin, sialidase-sensitive cancer mucins, and leptin receptors such as galectin-3 (Dowling et al. 2007). Other cancer cell biomarkers are GM2 ganglioside, a glycolipid present on the surface of ~95% of melanoma cells with the carbohydrate portion of the molecule conveniently jutting out on the extracellular side of the melanoma cell membrane, and fucosyl GM1, which is only detected on small cell lung cancers (Zhang et al. 1997). GM2 and another ganglioside, GD2, are expressed on the surface of several types of cancer cells involved in small-cell lung, colon, and gastric cancer, sarcoma, lymphoma, and neuroblastoma (Zhang et al. 1997). Recognition of surface GM2 is the basis of anticancer vaccines currently under development (Livingston 1998; Knutson 2002). The membranes of cancer cells in gastrointestinal stromal tumors express CD117 (aka. Kit) 95% of the time, heavy caldesmon (80%) and CD34 (70%) (Miettinen and Lasota 2006). Other cancer cell membrane biomarkers include ERBB2 oncoprotein (aka. p185) in breast cancer (Wu 2002), DDR1 and CLDN3 in epithelial ovarian cancer (Heinzelmann-Schwarz et al. 2004), the cell surface glycoprotein CD147 (aka. emmprin) on the surface of malignant tumor cells (Yan et al. 2005), and the transmembrane protein EDFR in various human carcinomas (Normanno et al. 2006). Helpfully, expression of some cancer cell surface biomarkers is differentially related to tumor stage (Roemer et al. 2004) – for example, MMP-26 and TIMP-4 are strongly expressed in high-grade prostatic intraepithelial neoplasia but their expression significantly declines as the cancer progresses to invasive adenocarcinoma in human prostate (Lee et al. 2006). Many tumor-associated antigens are already known (Malyankar 2007) and the search for new membrane-bound (Liang et al. 2006, Alvarez-Chaver et al. 2007) and other (Zhang et al. 2007; Feng et al. 2007) cancer cell biomarkers is very active.

23.6.2.3 Heart and Vascular Disease

Perhaps the most common form of heart disease – and the leading cause of illness and death in most Western countries – is atherosclerosis, a condition in which the endothelial cell-lined artery wall becomes thicker and less elastic due to the presence of fatty-material-accumulating white cells under the inner lining of the arterial wall, creating a deposit called an atheroma. As the atheromas grow, the arterial lumens narrow. In time, the atheromas may collect calcium deposits, become brittle, and rupture, spilling their fatty contents and triggering the formation of a blood clot. The clot can further narrow or even occlude the artery, possibly leading to heart attack, or it may detach and float downstream, producing a vascular embolism.

By the era of nanomedicine in the 2020s and beyond, the incidence of heart disease in Western countries may be somewhat diminished compared to today because atherosclerosis is already partially reversible by controlling blood lipids (Wissler and Vesselinovitch 1990; Schell and Myers 1997; Grobbee and Bots 2004; Tardif et al. 2006), and future nanorobotic control of gene expression (Section 23.6.4.4) or stem cell treatments as already demonstrated in rodents (Lu et al. 2007) may prove even more effective as preventive measures. However, the regression of atherosclerotic plaque is generally accompanied by a decrease in total vessel size without an increase in luminal dimensions (Tardif et al. 2006), so restoring original luminal dimensions will likely still require a capability for direct vascular remodeling. Prevention is also likely to be underutilized by asymptomatic hyperlipidemic patients in wealthy countries, and may not be sufficiently available to less affluent patients or to patients in nonindustrialized countries.

The "vasculocyte" (Fig. 23.22) may be the nanorobotic treatment of choice for the limited vascular repair of primarily intimal arteriosclerotic lesions prior to complete arterial occlusion (Freitas 1996a). The device is designed as a squat, hexagonal-shaped nanorobot with rounded corners, measuring 2.7 microns across and 1 micron tall, that walks the inside surface of blood vessels atop telescoping

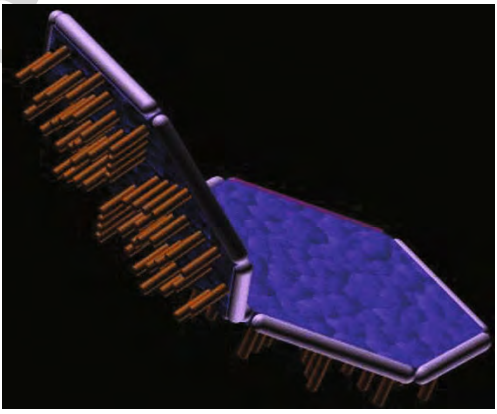

Fig. 23.22 The vasculocyte (Freitas 1996), nanorobotic treatment of choice for repairing atherosclerotic lesions on the vascular surface of arteries (courtesy of Forrest Bishop. Used with permission)

This figure will be printed in b/w

appendages arranged on its underbelly. Its 400-billion atom structure would weigh about 8 picograms. The machine is scaled so that its longest cross-body diagonal (Freitas 1999ax) is shorter than 4 microns, the diameter of the narrowest capillaries in the human body (Freitas 1999ay). The slightly-curved topmost surface will be almost completely tiled with 174,000 molecular sorting rotors (Section 23.3.2) to allow rapid exchange of specific molecules between the interior of the nanorobot and the patient's bloodstream.

On its six side walls the vasculocyte will be enveloped by an extensible "bumper" surface (Freitas 1999az) which cycles between 100 and 300 nm of thickness as internally-stored piston-pumped ballast fluid inflates and deflates the surface about once every second (Freitas 1999ba). This cycling will allow a nanorobot situated on an arterial wall to continuously adjust its girth by up to 15% to match the regular distensions of arterial wall circumference that occur during each systolic pulse of the heart (Freitas 1999bb), thus maintaining watertight contact with similarly-cycling neighboring devices all of which are stationkeeping over a particular section of vascular tissue.

On its bottom face, the vasculocyte will have 625 stubby telescoping appendages (Section 23.3.3), each capable of 1 cm/sec movements. Limbs are similar to those in the microbivore and are spaced out along a regular grid about 100 nm apart, with only 10% of them used at any one time both to preserve tenfold redundancy and to avoid any possibility of leg-leg collisions. Each leg walks on a "footpad" tool tip (Freitas 1999bc) that is 10 nm in diameter. Acting like a snowshoe, the footpad will distribute leg motion forces widely enough to avoid disrupting cell membranes (Freitas 1999bd).

Many different tool tips (Freitas 1999be) might be deployed up through the interior hollows of the 625 nanorobotic limbs. Appendages on the underbelly may be used as manipulator arms for blood clot and foam cell disassembly, endothelial cell herding, adhesive glycoprotein removal, and so forth. Syringe tips will allow suction or drug injection by penetrating the 10-nm thick cellular membranes over which the device is walking. Other specialized tips will be used for bulk tissue disposal (a rotating cutting annulus), molecular absorption (using binding sites keyed to the molecules that make up plaque), cell peeling (specialized grippers), and as sensors for biomarker detection, chemotactic mapping, and other physical measurements.

After injection, the vasculocytes will circulate freely in the patient's bloodstream for a few minutes, finally dropping out onto a capillary wall and beginning to crawl upstream (or downstream, if in the pulmonary bed) along the vessel surface. Each device moves past the precapillary sphincters, through the metarterioles to the wide end of the terminal arterioles, then up the terminal arterial branches (150 microns in diameter) and into the arteries, where it joins up with others, forming into traveling circumferential scanning rings consisting of millions of individual nanorobots walking side by side. Eventually these traveling bands (Lapidus and Schiller 1978) will enter the 25,000-micron diameter aorta, leading, ultimately, to the heart. Upon reaching the heart uneventfully, each device would release its grip on the arterial wall and return to the bloodstream, allowing removal from the body either by

nanapheresis centrifugation (Freitas 1999bm) or by excretion through the kidneys (Weatherbee and Freitas 2010). Creeping along the arterial tree at a fairly modest speed of 100 microns/sec (Freitas 1999bf), a vasculocyte ring could travel the 70 cm mean distance from capillaries to heart in about 2 hours if uninterrupted.

However, if disease is present the nanorobots will detect sclerotic tissue based on surface plaque temperature heterogeneity (Stefanadis et al. 1999), directly sampled tissue biomarkers (Schönbeck and Libby 2001; Lipinski et al. 2004; Koenig and Khuseyinova 2007), observation of ultrastructural alterations in endothelial cell morphology (Walski et al. 2002), thinning of endothelial glycocalyx (Gouverneur et al. 2006) or other evidence of endothelial dysfunction (Hadi et al. 2005), and circumferential vasculometric variations. Upon such detection, enough vasculocytes would collect over the affected area to entirely cover the lesion. The nanorobots aggregate into a watertight arterial "bandage" by locking themselves together side by side through their inflatable bumpers, then establish mutual communications links (Freitas 1999bg) and anchor themselves securely to the underlying tissue to begin repair operations which may be externally supervised and directed by the physician in real time.

The total computational power inherent in each bandage would be fairly impressive: a 1 cm^2 patch of linked vasculocytes each running a tenfold-redundant 1 MB/sec nanocomputer having 5 MB of memory represents a 10-million nanorobot parallel computer with 100 terabit/sec processing capacity (crudely equivalent to the human brain) with 50 terabits of memory. Within each bandage, nanorobots would complete all repairs within 24 hours or less, faster than hemangioblast precursor cells derived from human stem cells that show robust reparative function of damaged rat/mouse vasculature in 24–48 hours (Lu et al. 2007). Repairs would occur in eight sequenced mission steps including: (1) reconnoiter, (2) clean the site, (3) strip the existing endothelial layer, (4) rebuild endothelial cell population, (5) remove lesions, (6) halt aberrant vascular muscle cell growth, (7) rebuild basement structure, and (8) reposition endothelial cells. A 1 cm^3 injection of 70 billion vasculocytes would be a large enough treatment dosage to entirely coat 50% of the entire human arterial luminal surface with these active, healing nanorobots. Supplemental endothelial cells may be manufactured exogenously (Section "Tissue Printers, Cell Mills and Organ Mills") and transported to active repair sites as required.

If complete arterial occlusion has occurred, the patient may require emergency endoscopic nanosurgery (Section "Endoscopic Nanosurgery and Surgical Nanorobots"), analogous to mechanical thrombectomy (Kasirajan et al. 2001) today, to quickly clear the obstruction, plus a local injection of respirocytes (Section 23.6.3.1) to reduce ischemic damage to the affected tissues; or, alternatively, a population of burrowing tissue-mobile microbivore-class devices could rapidly digest the embolus (Section 23.6.2.4). Nanorobotic devices can also be used to treat non-atheroma lesions of the vasculature, such as those caused by viral invaders that attack and damage the vascular endothelium (Sahni 2007), e.g., in viral hemorrhagic fevers (Marty et al. 2006).

23.6.2.4 Stroke and Cerebrovascular Disease

Strokes are the most common cause of disabling neurologic damage in the industrialized countries. In an ischemic stroke, a large fatty deposit (atheroma) can develop in a carotid artery, greatly reducing its blood flow feeding the brain. If fatty material breaks off from the carotid artery wall it can travel with the blood and become stuck in a smaller brain artery, blocking it completely. Also, a clot formed in the heart or on one of its valves can break loose, travel up through the arteries to the brain, and lodge there. When blood flow to the brain is disrupted, brain cells can die or become damaged from lack of oxygen. If the blood supply is not restored within a few hours, brain tissue dies, resulting in stroke. Insufficient blood supply to parts of the brain for brief periods causes transient ischemic attacks (TIAs), temporary disturbances in brain function, and brain cells can also be damaged if bleeding occurs in or around the brain, producing various cerebrovascular disorders. In a future nanomedical era the incidence of this form of disease should be somewhat reduced, but prevention may not be universally practiced or available for all patients.

Nanorobotic treatments might be applied as follows. First, in the case of partial occlusions of the carotid or lesser cranial arteries that are not immediately life threatening, vasculocytes (Section 23.6.2.3) could be employed to clear partial obstructions, repair the vascular walls, and to enlarge the vessel lumen to its normal diameter in a treatment lasting perhaps several hours. Second, in the case of small solid emboli blocking capillaries or small metarterioles, burrowing tissue-mobile microbivore-class devices could digest the obstructions in minutes (e.g., 8 minutes to clear an 8 micron diameter capillary, digesting an embolus at the ~1 micron/min rate; Section 23.6.2.2) with respirocytes added to the therapeutic cocktail to help maintain oxygenation of the affected tissues via diffusion from devices passing through adjacent capillaries. Finally, endoscopic nanosurgery (Section "Endoscopic Nanosurgery and Surgical Nanorobots") could be used to quickly clear a life-threatening total occlusion on an emergency basis, and intracranial hemorrhages may be dealt with using a combination of endoscopic nanosurgery (Section "Endoscopic Nanosurgery and Surgical Nanorobots"), vascular gates (Section "Vascular Gates") and clottocytes (Section 23.6.3.3).

23.6.2.5 Hormonal, Metabolic and Genetic Disease

Diabetes mellitus is a hormonal disorder that is the tenth leading cause of death in the United States and the leading cause of blindness with complications including kidney and nerve damage, cataracts, impairment of skin health and white cell function, and cardiovascular damage. In Type I diabetes, >90% of the insulin producing beta cells in the pancreas have been destroyed by the immune system, requiring regular insulin injections; in Type II, the pancreas continues to manufacture insulin but the body develops resistance to its effects, creating a relative insulin deficiency. Both forms have a genetic component. By the 2020s and beyond, as in the

cases of heart disease (Section 23.6.2.3) and stroke (Section 23.6.2.4) conventional biotechnology-based cures for diabetes may exist. The immune disorder that causes type I diabetes might be eliminated by proper immunoengineering, perhaps using techniques that have already proven successful in animals, and the changes in gene expression with aging that give rise to type II diabetes occur not in the pancreas but in the tissues that normally use insulin but stop doing so with aging, and this may also be prevented.

Even if these methods prove unsuccessful or have drawbacks (e.g., side effects, excessive treatment time), in the era of medical nanorobotics cell repair devices called chromallocytes (Section 23.6.4.3) could permanently correct any genetic susceptibilities at their source, e.g., by rebuilding any missing pancreatic beta cells via genomic replacement in existing cells, creating healthy new beta cells that can be made more resistant to autoimmune destruction by editing out pancreatic antigens resembling those of the pancreas-destroying virus to which the immune system is responding, thus curing diabetes. Microbivore-class devices could also delete immune cells that recognize the self-antigens. Additional cell repair nanorobots could be used to correct aberrant or unreliable gene expression (Section 23.6.4.4) in tissue cells to eliminate any lingering insulin resistance effects. As a temporary stopgap measure, pharmacyte-class nanorobots (Section 23.6.3.2) or artificial implanted nanorobotic organs will comprehensively control serum levels of any small molecule such as insulin on a real time basis. Other endocrine disorders such as hypopituitarism, hyperthyroidism, and adrenal malfunction, metabolic diseases such as obesity, hyperlipidemia, and Tay-Sachs, and any of the thousands of known genetic diseases similarly could be permanently cured using chromallocytes (Section 23.6.4.3).

Another metabolic condition known as glycation, which may accumulate even when glucose levels are held in the normal range because glucose is chemically reactive and can combine with myelin and other biological components over time, may cause autoimmune conditions and other problems such as increased tissue stiffness. Unless the body already has adequate endogenous defenses against this problem that are not normally marshaled – not currently known one way or the other – glycation would eventually become serious enough to require attention. Nanorobotic deglycation of cell surfaces is briefly discussed in Section 23.7.1.2.

23.6.3 Reversing Trauma

Trauma is a physical injury or wound caused by external force or violence to the human body. In the United States, trauma is the leading cause of death between the ages of 1 and 38 years. The principal sources of trauma are motor vehicle accidents, suicide, homicide, falls, burns, and drowning, with most deaths occurring within the first several hours after the event. However, nanomedical interventions should be able to correct a great deal of the damage resulting from such events.

In this short Chapter we can only briefly summarize a few representative nanorobotic responses to some familiar situations involving traumatic injury,

including suffocation and drowning (Section 23.6.3.1), poisoning (Section 23.6.3.2), hemostasis (Section 23.6.3.3), wound healing (Section 23.6.3.4), and internal injury requiring surgery (Section 23.6.3.5).

23.6.3.1 Suffocation and Drowning

The principal effect of a suffocation or drowning trauma is hypoxemic damage to tissues and organs. The first theoretical design study of a medical nanorobot ever published in a peer-reviewed medical journal (in 1998) described an artificial mechanical red blood cell or "respirocyte" (Freitas 1998) to be made of 18 billion precisely arranged atoms (Fig. 23.23) – a bloodborne spherical 1-micron diamondoid 1000-atmosphere pressure vessel (Freitas 1999bh) with active pumping (Freitas 1999o) powered by endogenous serum glucose (Freitas 1999bi), able to deliver 236 times more oxygen to the tissues per unit volume than natural red cells and to manage acidity caused by carbonic acid formation, controlled by gas concentration sensors (Freitas 1999bj) and an onboard nanocomputer (Drexler 1992b; Freitas 1999k). The basic operation of respirocytes will be straightforward. These nanorobots, still entirely theoretical, would mimic the action of the natural hemoglobin-filled red blood cells, while operating at 1000 atm vs. only 0.1–0.5 atm equivalent for natural Hb. In the tissues, oxygen will be pumped out of the device by the sorting rotors on one side. Carbon dioxide will be pumped into the device by the sorting rotors on the other side, one molecule at a time. Half a minute later, when the respirocyte reaches the patient's lungs in the normal course of the circulation of the blood, these same rotors may reverse their direction of rotation, recharging the device with fresh oxygen and dumping the stored CO_2, which diffuses into the

This figure will be printed in b/w

Fig. 23.23 The respirocyte (Freitas 1998), an artificial mechanical red cell. Designer Robert A. Freitas Jr. ©1999 Forrest Bishop. Used with permission

lungs and can then be exhaled by the patient. Each rotor requires little power, only ~0.03 pW to pump ~10^6 molecules/sec in continuous operation.

In the exemplar respirocyte design (Freitas 1998), onboard pressure tanks can hold up to 3 billion oxygen (O_2) and carbon dioxide (CO_2) molecules. Molecular sorting rotors (Section 23.3.2) are arranged on the surface to load and unload gases from the pressurized tanks. Tens of thousands of these individual pumps cover a large fraction of the hull surface of the respirocyte. Molecules of oxygen or carbon dioxide may drift into their respective binding sites on the exterior rotor surface and be carried into the respirocyte interior as the rotor turns in its casing. The sorting rotor array is organized into 12 identical pumping stations laid out around the equator of the respirocyte, with oxygen rotors on the left, carbon dioxide rotors on the right, and water rotors in the middle of each station. Temperature (Freitas 1999u) and concentration (Freitas 1999q) sensors tell the devices when to release or pick up gases. Each pumping station will have special pressure sensors (Freitas 1999t) to receive ultrasonic acoustic messages (Freitas 1999bk) so the physician can (a) tell the devices to turn on or off, or (b) change the operating parameters of the devices, while the nanorobots are inside a patient. The onboard nanocomputer enables complex device behaviors also remotely reprogrammable by the physician via externally applied ultrasound acoustic signals. Internal power will be transmitted mechanically or hydraulically using an appropriate working fluid, and can be distributed as required using rods and gear trains (Freitas 1999ao) or using pipes and mechanically operated valves, controlled by the nanocomputer. There is also a large internal void surrounding the nanocomputer which can be a vacuum, or can be filled with or emptied of water. This will allow the device to control its buoyancy very precisely and provides a crude but simple method for removing respirocytes from the body using a blood centrifuge, a future procedure now called nanapheresis (Freitas 1999bm).

A 5 cc therapeutic dose of 50% respirocyte saline suspension containing 5 trillion nanorobots would exactly replace the gas carrying capacity of the patient's entire 5.4 l of blood. If up to 1 l of respirocyte suspension can safely be added to the human bloodstream (Freitas 2003t), this could keep a patient's tissues safely oxygenated for up to 4 hours even if a heart attack caused the heart to stop beating, or if there was a complete absence of respiration or no external availability of oxygen. Primary medical applications of respirocytes would include emergency revival of victims of carbon monoxide suffocation at the scene of a fire, rescue of drowning victims, and transfusable preoxygenated blood substitution – respirocytes could serve as "instant blood" at an accident scene with no need for blood typing, and, thanks to the dramatically higher gas-transport efficiency of respirocytes over natural red cells, a mere 1 cm^3 infusion of the devices would provide the oxygen-carrying ability of a full liter of ordinary blood. Larger doses of respirocytes could also: (1) be used as a temporary treatment for anemia and various lung and perinatal/neonatal disorders, (2) enhance tumor therapies and diagnostics and improve outcomes for cardiovascular, neurovascular, or other surgical procedures, (3) help prevent asphyxia and permit artificial breathing (e.g., underwater, high

altitude, etc.), and (4) have many additional applications in sports, veterinary medicine, military science, and space exploration.

23.6.3.2 Poisoning

Poisoning is the harmful effect that occurs when toxic substances are ingested, inhaled, or come into contact with the skin. To deliver antidote or to clear such substances from the bloodstream in the era of nanorobotic medicine, a modified respirocyte-class device called a "pharmacyte" (Freitas 2006a) could be used. The pharmacyte was originally designed as an ideal drug delivery vehicle with near-perfect targeting capability (Section 23.6.1(4)). In that capacity, the device would be targetable not just to specific tissues or organs, but to individual cellular addresses within a tissue or organ. Alternatively, it could be targetable to all individual cells within a given tissue or organ that possessed a particular characteristic (e.g., all cells showing evidence of a particular poison). It would be biocompatible and virtually 100% reliable, with all drug molecules being delivered only to the desired target cells and none being delivered elsewhere so that unwanted side effects are eliminated. (Sensors on the surface of the nanorobot would recognize the unique biochemical signature of specific vascular and cellular addresses (Freitas 1999ak), simultaneously testing encountered biological surfaces for a sufficiently reliable combination (at least 5–10 in number) of positive-pass and negative-pass molecular markers to ensure virtually 100% targeting accuracy.) It would remain under the continuous post-administration supervisory control of the supervising physician – even after the nanorobots had been injected into the body, the doctor would still be able to activate or inactivate them remotely, or alter their mode of action or operational parameters. Once treatment was completed, all of the devices could be removed intact from the body.

The exemplar 1–2 μm diameter pharmacyte would be capable of carrying up to ~1 μm^3 of pharmaceutical payload stored in onboard tanks that are mechanically offloaded using molecular sorting pumps (Section 23.3.2) mounted in the hull, operated under the proximate control of an onboard computer. Depending on mission requirements, the payload alternatively could be discharged into the proximate extracellular fluid (Freitas 1999bn) or delivered directly into the cytosol using a transmembrane injector mechanism (Freitas 1999bo, bp, bj, 2003u). If needed for a particular application, deployable mechanical cilia (Freitas 1999ae) and other locomotive systems (Freitas 1999i) could be added to the pharmacyte to permit transvascular (Freitas 1999bq) and transcellular (Freitas 1999x) mobility, thus allowing delivery of pharmaceutical molecules to specific cellular and even intracellular addresses.

Because sorting pumps can be operated reversibly, pharmacytes could just as easily be used to selectively extract specific molecules from targeted locations as well as deposit them. Thus in the case of poison control, these nanorobots might act in reverse to retrieve a specific chemical substance from the body, just as they can be used for targeted delivery of an antidote. Whole-body clearance rates for

systemic poisons can be quite rapid. For example, a population of 10^{12} bloodborne pharmacytes having aggregate storage volume ~6 cm^3 could reduce serum alcohol from 0.2% in a seriously intoxicated 70 kg patient to 0.005% in ~1 second by prompt onboard sequestration, followed by catabolization of the entire inventory in ~10 minutes within a ~200 watt systemic caloric budget for waste heat production. Of course, continuing outflows from ethanol-soaked body tissues into the bloodstream and other factors complicate the process, e.g., such extremely rapid reduction of blood alcohol levels could be counterproductive because it might produce osmotic brain swelling in which water enters the brain (which still contains more alcohol than the blood) faster than alcohol can leave the brain.

23.6.3.3 Hemostasis

A major form of trauma occurs when the skin and underlying tissues are lacerated by violence, causing bleeding from broken capillaries or somewhat larger blood vessels. Total natural bleeding time, as experimentally measured from initial time of injury to cessation of blood flow, may range from 2–5 minutes (Kumar et al. 1978) up to 9–10 minutes (Hertzendorf et al. 1987; Lind 1995) if even small doses of anticoagulant aspirin are present (Ardekian et al. 2000), with 2–8 minutes being typical in clinical practice. Hemostasis is also a major challenge during surgery, as up to 50% of surgical time can be spent packing wounds to reduce or control bleeding and there are few effective methods to stop it without causing secondary damage. Modern surgical fibrin sealants (e.g., Crosseal, American Red Cross) composed of human clottable proteins and human thrombin can reduce mean hemostasis time to 282 seconds in clinical settings (Schwartz et al. 2004), and there is one report of a laboratory demonstration of artificial hemostasis in 15 seconds for multiple tissues and wound types in animal models using synthetic self-assembling peptides (Ellis-Behnke et al. 2007).

A medical nanorobot theoretical design study (Freitas 2000a) has described an artificial mechanical platelet or "clottocyte" that would allow complete hemostasis in ~1 second, even in moderately large wounds. This response time is on the order of 100–1000 times faster than the natural hemostatic system and 10–100 times faster than the best current artificial agents.

The baseline clottocyte is conceived as a serum oxyglucose-powered spherical nanorobot ~2 microns in diameter (~4 $micron^3$ volume) containing a fiber mesh that is compactly folded onboard. Upon command from its control computer, the device promptly unfurls its mesh packet (Fig. 23.24) in the immediate vicinity of an injured blood vessel – following, say, a cut through the skin. Soluble thin films coating certain parts of the mesh would dissolve upon contact with plasma water, revealing sticky sections (e.g., complementary to blood group antigens unique to red cell surfaces (Freitas 1999br)) in desired patterns. To stop flow, the net must be well anchored to avoid being swept along with the trapped red cells. A cut blood vessel has exposed collagen to which platelets normally adhere – the clottocyte netting may recognize collagen or even intact endothelial cells (or the junctions between endothelial cells) to provide the needed anchoring function. Blood cells

This figure will be printed in b/w

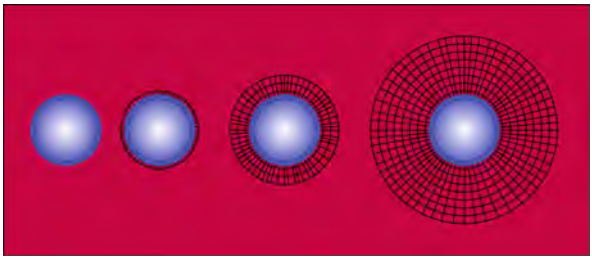

Fig. 23.24 The clottocyte (Freitas 2000a), an artificial mechanical platelet, rapidly unfurls its netting at the wound site, halting bleeding in ~1 second. Designer Robert A. Freitas Jr. © 2008 Robert A. Freitas Jr. (www.rfreitas.com). All Rights Reserved. Used with permission

are immediately trapped in the overlapping artificial nettings released by multiple neighboring activated clottocytes, and bleeding halts at once. The required blood concentration n_{bot} of clottocyte nanorobots required to stop capillary flow at velocity v_{cap} ~1 mm/sec (Freitas 1999bs) in a response time $t_{stop} = 1$ sec, assuming $n_{overlap} = 2$ fully overlapped nets each of area $A_{net} = 0.1$ mm^2, is $n_{bot} \sim n_{overlap} / (A_{net}\, t_{stop}\, v_{cap}) = 20$ mm^{-3}, or just ~110 million clottocytes in the entire 5.4-l human body blood volume possessing ~11 m^2 of total deployable mesh surface. This would be a total dose of ~0.4 mm^3 of clottocytes, producing a negligible serum nanocrit (nanorobot/blood volume ratio) (Freitas 1999bt) of ~0.00001%.

Clottocytes may perform a clotting function that is equivalent in its essentials to that performed by biological platelets – possibly including the release of vasoactive mediators, clotting factor cascade activators, etc. if needed – but at only ~0.01% of the bloodstream concentration of those cells. Hence clottocytes would be ~10,000 times more effective as clotting agents than an equal volume of natural platelets. While 1–300 platelets might be broken and still be insufficient to initiate a self-perpetuating clotting cascade, even a single clottocyte, upon reliably detecting a blood vessel break, could rapidly communicate this fact to its neighboring devices, immediately triggering a progressive controlled mesh-release cascade. Of course, onboard computerized control systems must ensure extremely safe and reliable operation (Freitas 2009).

23.6.3.4 Wound Healing

Once bleeding is stopped, the wound must be closed. Natural processes that rely solely upon wound self-repair often take months for completion and can leave unsightly, dense, shiny white fibrous scars – skin never heals into a condition that is "as good as new," and healed tissue is typically 15–20% weaker than the original tissue. There are a few notable counterexamples. Among mammals, the MRL/MpJ mouse displays accelerated healing and tissue regeneration with an extraordinary capacity to scarlessly heal ear-punch and other surgical wounds. Excision ear-punch wounds 2 mm wide close via regeneration after 30 days (Clark et al. 1998) with full re-epithelialization in just 5 days followed by blastema-like formation, dermal

extension, blood vessel formation, chondrogenesis, folliculogenesis, and skeletal muscle and fat differentiation (Rajnoch et al. 2003); another MRL mouse study (Leferovich et al. 2001) found that even a severe cardiac wound healed in 60 days with reduced scarring and with full restoration of normal myocardium and function.

The goal in medical nanorobotics is to provide an equally effective alternative to wound healing that can work >1000 fold faster than the natural process, e.g., in minutes or hours. No comprehensive nanorobot design study has yet been published but a theoretical scaling study (Freitas 1996b) concentrating on nanomechanical activity requirements for minor dermal excision wound repair describes the dermal zipper or "zippocyte" as a roughly cubical nanorobotic device measuring $40 \times 40 \times 30$ microns in size. This study concludes that multipurpose nanorobotic manipulators 1-micron in length would cover five of the six faces of the device, forming a dense coating of ~7000 nanomechanical cilia of similar number density as might be found on the outer surface of a microbivore (Section 23.6.2.1) or the underside of a vasculocyte (Section 23.6.2.3). These utility appendages would serve many ancillary functions including sensing/mapping, wound debridement, individual locomotion, stationkeeping (by handholding with neighboring nanorobots), volume management of the collective, and binding to tissue walls. Actual repair work would be performed by larger manipulators on the sixth face located on the underbelly of each zippocyte, using derivatives of cell milling and tissue repair methods described elsewhere (Section "Tissue Printers, Cell Mills and Organ Mills"). The entire wound repair sequence, as seen from the viewpoint of a working dermal nanorobot, would occur in twelve sequenced mission steps including: (1) activation, (2) entry, (3) immobilization and anti-inflammation, (4) scan surface, (5) debridement, (6) muscle repair, (7) areolar (loose connective) tissue repair, (8) fatty tissue repair, (9) dermis repair, (10) germinative layer restoration, (11) corneum repair, and (12) exit and shutdown.

23.6.3.5 Internal Injury and Nanosurgery

Internal injuries are more serious and may include internal bleeding, crushed or damaged organs, electrical or burn injuries, and other serious physical traumas. This area of emergency medicine will demand some of the most sophisticated medical nanorobots available, with large numbers of devices of many different nanorobot types acting in concert under the most difficult conditions. In most cases some form of surgical intervention will be required, using nanorobotic surgical tools such as those described below.

Vascular Gates

Still only conceptual, the vascular gate (Freitas 2003r) will be a basic nanorobotic tool analogous to hemostats to allow surgeons to rapidly enable or disable free flow through whole sections of the vascular tree ranging from individual capillaries to entire capillary beds, all the way up to larger vessels the size of major arteries or veins. The most direct application in emergency medicine would be to allow the surgeon to quickly but reversibly seal off the open ends of hundreds or thousands of

broken blood vessels simultaneously, to immediately stanch massive blood losses at the outset of trauma surgery and to provide reversible wide-area hemostasis in the surgical region by temporarily blockading all vessels. More complex vascular gates could also act as real-time content filters to choose which population of bloodborne objects can pass through any targeted section of the vasculature. For example, red cells could be allowed to pass but not platelets, or the gate might pass all formed blood elements but no nanorobots (or vice versa), or all fluids but no solid objects. Content filtration could be sensor-, time-, event-, or command-driven. In other non-emergency applications, gate nanorobots could be employed as intelligent embolic particles that would be directed to a specific organ or tumor within an organ, then triggered to halt flow in blood vessels supporting these structures for the purpose of selectively blocking organ perfusion or clogging tumor inputs.

The simplest gating nanorobots can be externally administered onto or into a wound area by the emergency surgeon; bloodborne ones not involved in emergency wound management can be internally administered like free-floating clottocytes (Section 23.6.3.3) or vasculomobile vasculocytes (Section 23.6.2.3). In wound scenarios the nanorobots can recognize cuts using chemotactic sensor pads (Freitas 1999cv) to detect the telltale molecular signatures of broken blood vessels much as occurs naturally by platelets (Cruz et al. 2005) and circulating vascular progenitor cells (Sata 2003), including but not limited to detection of exposed collagen (Cruz et al. 2005; O'Connor et al. 2006; Ichikawa et al. 2007) or elastin (Hinek 1997; Keane et al. 2007) from ruptured intima or media, or smooth muscle actin (Rishikof et al. 2006) and other molecular markers expressed on injured endothelial and smooth muscle cells (Takeuchi et al. 2007). Vessel recognition may be assisted by rapid advance nanoscopic mapping of the wound area with nanorobots subsequently proceeding to their assigned stations via informed cartotaxis (Freitas 1999cw). Once having arrived on site, internally administered gating nanorobots can use circumferential intraluminal pressure fit, analogous to the vasculoid design (Freitas and Phoenix 2002), to establish a leakproof seal that should easily withstand 1–2 atm exceeding the requisite maximum physiological backpressure. Externally administered nanorobots can employ a similar approach to apply anchoring pressure rings inside the undamaged section of a leaking vessel that lies nearest to the vessel's damaged terminus. Either process may be assisted by lipophilic semaphores (Freitas 1999cu) deployed on the nanorobot hull to help maintain noncovalently-bonded reversible leakproof seals to the plasma membranes of remaining undamaged endothelium or to subendothelial basement membrane.

A nanorobotic vascular gate installed across a large 6-mm diameter artery could be established using a sheet of ~10^7 micron-sized nanorobots each having a (~2 micron)^2 patrol area within the array, with each device stationkeeping in its patrol area by handholding with neighboring nanorobots (Section 23.6.3.4) and analogously as has been described elsewhere for "utility fog" (Hall 1993, 1996) (Fig. 23.25). A positive-pass gate might use contact sensor data to recognize impinging particulate matter that the physician desired to pass through, whereupon the gate would temporarily open wide enough to allow the desired particle to pass through, then quickly close again. A negative pass gate would normally allow everything

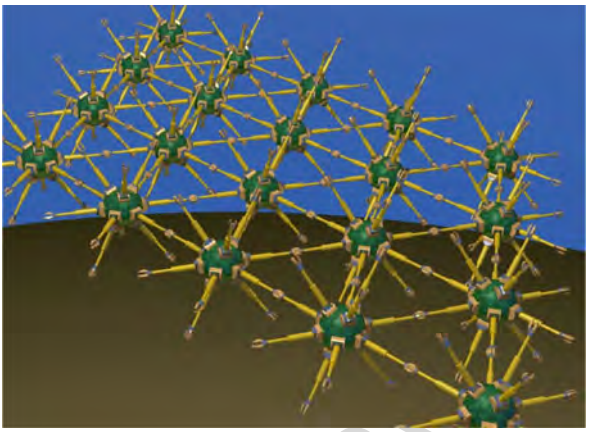

Fig. 23.25 A number of utility fog (Hall 1993) nanorobots hold hands with their neighbors, forming a strong, reconfigurable smart-matter array. Image © 1999, courtesy of J. Storrs Hall

This figure will be printed in b/w

to pass unless sensors detected an undesired particle, whereupon the gate would forcibly eject it and close up until the undesired particle had diffused away via osmotic dilution in the pulsed flow. If the vascular gate aggregate consists of vasculomobile nanorobots, then at mission's end the aggregate can disassemble itself and "walk away" much like vasculocytes (Section 23.6.2.3), then similarly be removed from the body.

Primitive but less effective analogs to vascular gates that are already in widespread surgical use include the inferior vena cava filter (Imberti et al. 2006; Dentali et al. 2006; Giannoudis et al. 2007; Patel and Patel 2007) for the prevention of pulmonary embolism as an alternative to anticoagulant therapy in high-risk patients (~100,000 cases annually in the U.S.), expandable net filters that are deployed while emplacing carotid artery stents in stroke patients (Henry et al. 2007), and the use of protective internal carotid artery flow reversal (Pipinos et al. 2006) during carotid angioplasty and stenting.

Tissue Printers, Cell Mills and Organ Mills

How can we restore severely injured organs that are too damaged to repair, or replace large chunks of missing tissue that has been excised from the body in a deep avulsive trauma? One answer is to manufacture new tissue from scratch (Mironov et al. 2003; Jakab et al. 2004). Tissue and organ printing is a very active area in biomedical research today (Box 23.2). With nanorobotic controlled precision and a massively parallel tip array, a future nanosurgical tissue printer might be used to squirt tissue matrix scaffold and tissue cells directly and accurately into a large immobilized wound, rebuilding missing tissues in situ. A sheet of finished tissue ~1 mm thick could be laid down every minute assuming a ~1 Hz scan rate and deposition layers one cell thick (~20 microns). Filling a 10 cm deep excision wound with fresh tissue would then require ~1.4 hours in an immobilized but stabilized patient. But MHC-compatible generic cells would have to be engineered for this purpose to

avoid the need for immunosuppressive drugs. Alternatively, homologous cells of the patient's own type could be manufactured, using nanorobotic "organ mills" that will also allow surgeons to manufacture whole new fully-homologous organs, and then implant them, during the surgery.

Box 23.2 Tissue and organ printing

Boland's group at Clemson University has taken the first primitive steps towards 3D printing of complex tissues (Boland et al. 2006) and ultimately entire organs (Mironov et al. 2003). In one experiment (Xu et al. 2005), Boland's team used a modified Hewlett Packard 550C computer printer to print Chinese Hamster Ovary (CHO) and embryonic motoneuron cells into a pre-defined pattern using an "ink" of cells suspended in phosphate buffered saline solution. After deposition onto several "bio-papers" made from soy agar and collagen gel, the printed cells exhibited a healthy morphology with less than 8% cell lysis observed. In another experiment by the same group (Xu et al. 2006), complex cellular patterns and structures were created by automated and direct inkjet printing of primary embryonic hippocampal and cortical neurons – which maintained basic cellular properties and functions, including normal, healthy neuronal phenotypes and electrophysiological characteristics, after being printed through thermal inkjet nozzles. 3D cellular structures also were created by layering sheets of neural cells on each other (in a layer-by-layer process) by alternate inkjet printing of NT2 cells and fibrin gels (Xu et al. 2006). Cellular attachment and proliferation have been demonstrably controlled by precise, automated deposition of collagen (a biologically active protein) to create viable cellular patterns with 350-micron resolution (Roth et al. 2004). Boland defines his ultimate objective of "organ printing" as computer-aided, jet-based 3D tissue-engineering of living human organs involving three sequential steps: pre-processing or development of "blueprints" for organs, processing or actual organ printing, and postprocessing or organ conditioning and accelerated organ maturation (Mironov et al. 2003). Another group has printed rectangular tissue blocks of several hundred microns in thickness and tubular structures several millimeters in height (Jakab et al. 2006). Private companies are getting involved too: Therics (http://www.therics.com) is solid-printing resorbable implantable bone scaffolds that are already in use by surgeons, and Sciperio (http://www.sciperio.com) is developing an in vivo "Biological Architectural Tool" by which "clinicians and tissue engineers will be able to survey, diagnose, and construct new tissues via endoscopically manipulated vision, nonthermal tissue removal, and a direct-write tissue deposition apparatus."

In our vision of future nanomedicine, a desktop-type apparatus would accept as input the patient's DNA sequence, then manufacture large complex biological

structures in a convergent assembly type process (Freitas and Merkle 2004b), as described in the following conceptual scenario.

The first module would synthesize copies of the patient's own homologous proteins and other relevant biomolecules, working from the patient's genome; as a proof of concept, functional copies of the human red cell anion exchanger, a proteinaceous transmembrane pump, have been self-assembled from sets of three, four or five complementary fragment "nanoparts" that were separately cloned in *Xenopus* oocytes (Groves et al. 1998). This process would include the manufacture of many duplicate copies of the patient's own DNA suitably methylated to match the expression pattern (e.g., the "methylome," "transcriptome," etc.) of the particular cells and organ being constructed, as described elsewhere in a lengthy technical paper (Freitas 2007). These fabricated biocomponents would then be fed to a second module which may positionally assemble them into bulk quantities of artificially fabricated organelles, membranes, vesicles, granules, and other key intracellular structures. Many such structures will self-assemble robustly (Marrink et al. 2001). As an experimental example of this, Golgi stacks (an important intracellular organelle) have been reassembled from isolated Golgi components including random assortments of vesicles, tubules, and cisternal remnants (Rabouille et al. 1995).

These mass-produced intracellular structures then serve as feedstock to the third production module, called a "cell mill," wherein these subcellular structures and materials would be assembled into complete cells of the requisite types, along with any extracellular matrix materials that might be required. This might be done using manufacturing systems analogous to 3D printing (Box 23.2). As long ago as 1970, an *Amoeba proteus* single-cell organism was reassembled from its major subcellular components – nucleus, cytoplasm, and cell membrane – taken from three different cells (Jeon et al. 1970), demonstrating the physical possibility of manually assembling living cells from more primitive parts. Others (Morowitz 1974) later reported that "cell fractions from four different animals can be injected into the eviscerated ghost of a fifth amoeba, and a living functioning organism results." Mammalian cells have also been assembled from separate nuclear and cytoplasmic parts (Veomett and Prescott 1976) and intracellular organelles have been individually manipulated both directly (Weber and Greulich 1992; Felgner et al. 1998; Bayoudh et al. 2001; Sacconi et al. 2005b) and nanosurgically (Section 23.6.4.2). Early cell assembly production systems might initially make partial use of more traditional biotechnologies such as cloning, stem cells, tissue engineering, animal cell reactors (Bliem et al. 1991; Nelson and Geyer 1991), transdifferentiation (Collas and Håkelien 2003) and nuclear reprogramming (Tada 2006).

In the fourth module, the manufactured cells are fed into a "tissue mill," which would mechanically assemble the cells into viable biological tissues using, again, positionally-controlled methods analogous to 3D printing (Box 23.2). 3D rapid prototyping has already created collagen scaffolds that can viably host human heart cells, the first step toward assembling an artificial heart valve (Taylor et al. 2006). Cells have also been manually assembled into larger artificial 3D structures such as chains, rings, and a pyramid-like tetrahedron using optical tweezers (Holmlin

et al. 2000), a potentially automatable process in which different cell types could be linked together one at a time in precisely the order and the positions necessary to assemble new tissues and organs.

Finally, the manufactured tissues would be fed to the last module, the "organ mill," that assembles the tissues into working biological organs that could be surgically implanted (Section "Endoscopic Nanosurgery and Surgical Nanorobots"). Crude estimates suggest that throughput rates of materials in such nanorobotic-based assembly modules could be on the order of minutes, with an organ-build time on the order of a few hours. This is at least several orders of magnitude faster than growing organs from tissue-engineered organoids (Poznansky et al. 2000; Saito et al. 2006; McGuigan and Sefton 2006) or via homologous organ cloning (Wood and Prior 2001; Cui 2005) in a biotech reactor apparatus. This is also fast enough to fall within the time range of oxygenation and pH buffering provided by respirocytes, which could be supplied to the nascent vascular system as it is assembled along with local nutrients. Making organs under conditions of mild hypothermia would also reduce their metabolic demands until perfusion can be instituted, and, if need be, the growing organ could be perfused from time to time during the assembly process to keep the cells within the construct in good condition.

Endoscopic Nanosurgery and Surgical Nanorobots

From the hand saws of the 19th century to the powered drills and ultrasharp diamond cutting blades of the mid 20th century, surgical tools by the end of the last century had progressed to the concept of minimally invasive surgery (MIS). Rather than carving a giant 12 inch incision in a patient's abdomen and undertaking a marathon operation, the MIS surgeon could now open a few transcutaneous centimeter-sized holes, poke several rigid endoscopic tubes through the holes, then insert miniaturized surgical cutting, suturing, and visualization tools through the tubes, thus reducing both surgical intrusiveness and patient recovery time. Flexible catheters were also introduced that could be threaded through the largest blood vessels to install stents and to remove vascular blockages or arterial wall plaques (e.g., via mechanical debridement, laser ablation, or ultrasonic ablation).

In the first few decades of the 21st century, surgical endoscopes and catheters will become even smaller but also smarter, with sensors (temperature, pressure, chemical, mechanical, shear force, force feedback, etc.) and even computers installed initially near the tips but eventually along their entire working lengths. These devices will possess complex robotic manipulators at their business end, with the surgeon having the ability to change out multiple toolheads or inject nanoliter quantities of drugs in situ. Manipulators and sensors will become more numerous on each instrument, more densely packed and more information intensive. The earliest steps down this pathway involving microrobotics (Menciassi et al. 2007) are illustrated by the great variety of MEMS (microelectromechanical systems) -based miniaturized surgical tools (Salzberg et al. 2002) already coming into use. Examples include the "data knife" scalpel produced by Verimetra, Inc. (www.verimetra.com)

which incorporates pressure and strain sensors with cautery and ultrasonic cutting edges (Kristo et al. 2003), the MicroSyringe and Micro-Infusion Catheter systems of Mercator MedSystems (www.mercatormed.com) for site-specific perivascular injection, and the MEMS-based wireless implantable blood pressure biosensor from CardioMEMS (www.cardiomems.com) (Chaer et al. 2006).

Paralleling these developments is the emergence of "robotic surgery" and telesurgery systems that soon will include force reflection to allow the surgeon to feel what he's doing and thus achieve much better results (Rizun et al. 2006). With microscale sensors he can touch the patient with tiny micron-sized hands, feeling the smallest bumps and adhesions in the tissue he's working on. Telesurgery, telemedicine, microsurgical telemanipulator systems (Li et al. 2000; Knight et al. 2005; Katz et al. 2006) and even conventional laparoscopy are getting practitioners used to the idea of operating through a machine or computer interface, rather than traditional procedures involving more direct physical contact with the patient. This process of learning how to act through a machine intermediary will continue to progress, and eventually the surgeon will become comfortable using surgical robots that accept higher-level commands. For instance, simple autonomous action sequences such as surgical knot tying have already been demonstrated experimentally by surgical robots (Bauernschmitt et al. 2005). As the next developmental step, rather than repeatedly directing the manipulators to thread a suture at various sites, the surgeon may simply indicate the positions in the tissue where he wants a series of suture loops placed using guidance virtual fixtures (Kapoor et al. 2005) and the machine will then automatically go through the motions of placing all those sutures while he watches, without the surgeon having to actively direct each suture placement site. This capability for semi-autonomous robotic surgery (Rizun et al. 2004) is foreshadowed by present-day "offline robots" or "fixed path robots" which perform subtasks that are completely automated with pre-programmed motion planning based on pre-operative imaging studies where precise movements within set confines are carried out (Sim et al. 2006).

Another outcome of the growing machine intermediation is that the surgeon will gain the ability to easily control many more than one active surgical instrument or surgical task at a time (Zhijiang et al. 2005). For example, after he has ordered the suturing device to put a series of sutures along one line, while waiting for that task to finish he can direct another surgical tool to do something else somewhere else, or he can go check some sensor readings, or he can palpate a section of nearby tissue to test its strength, and so forth. This multitasking will speed the surgical process and increase the number of in vivo interventive foci to which the individual surgeon can simultaneously attend inside his patient. Immersive virtual reality interfaces will further extend the surgeon's ability to maintain proper control of a growing number of tools simultaneously, improve his efficiency and confidence in the multitasking situation, and generally allow him to work faster and safer while doing more. Collaborative robotic surgeries (Hanly et al. 2006) will also become more commonplace. In sum, the current trends in surgery are generally these: the tools will get smaller and more complex, and the surgeon will be working increasingly through a computerized intermediary in a rich sensory and control environment, while relying

increasingly on the mechanized intermediary to carry out preprogrammed microtasks (enabling the surgeon to concentrate on the big picture and to guide the general course of the procedure) while being freed to multitask with an increasing number of tools and collaborators.

As the era of surgical nanorobotics arrives, these trends will accelerate and progress still further. Today's smallest millimeter diameter flexible catheters will shrink to 1–10 micron diameter bundles that can be steered (Glozman and Shoham 2006) through the tiniest blood vessels (including capillaries) or could even be inserted directly through the skin into organs without pain (Wang et al. 2005) or discomfort. Nanorobotic mechanisms embedded in the external surfaces of a nanocatheter or nanosyringe (Section "Nanosyringoscopy") will assist in actively propelling the telescoping apparatus gently through the tissues (Freitas 1999at), sampling the chemical environment (e.g., concentrations of oxygen, glucose, hormones, cytokines) along the way (Freitas 1999c), and providing a torrent of mechanical and optical sensory feedback along with precision positional metrology to allow the surgeon to know exactly where his tools are at all times, and also where his "virtual presence" is in relation to his targets. Internal hollow spaces inside the nanocatheter can be used to transport tools, sensors, fluids, drugs, or debridement detritus between patient and physician. The tip of the nanocatheter or nanosyringoscope may include a working head with thousands or millions of independent manipulators and sensors branching outward from the central trunk on retractile stalks, from which data can be encoded in real time and passed to external computers along an optical data bus located inside each nanocatheter. The endoscopic nanosurgeon's ability to multitask may extend to thousands of nanocatheters and millions or billions of simultaneously occurring mechanical and chemical processes during a single surgical procedure.

Populations of individual surgical nanorobots also could be introduced into the body through the vascular system or from the ends of catheters into various vessels and other cavities in the human body. Surgical microrobotics is already a thriving field of experimental research (Box 23.3). A future surgical nanorobot, programmed or guided by a human surgeon, would act as a semi-autonomous on-site surgeon inside the human body. Such devices could perform various functions such as searching for pathology and then diagnosing and correcting lesions by nanomanipulation, coordinated by an on-board computer while maintaining contact with the supervising surgeon via coded ultrasound signals.

Nanosyringoscopy

A common requirement for trauma treatment is foreign object removal. Carefully poking a needle-like 100-micron diameter nanosensor-tipped self-steering "nanosyringoscope" quickly through all intervening soft tissues to the immediate vicinity of a foreign object should cause minimal permanent damage, much like bloodless and painless microneedles (Cormier et al. 2004; Flemming et al. 2005; Coulman et al. 2006; Nordquist et al. 2007). After penetration, ~10^{10} micron^3/sec of nanorobots flowing at 1 m/sec through the tube (typical syringe rate) could surround a cubic

1 cm^3 target object to a coating thickness of 100 microns in ~10 seconds. The coating nanorobots would then dig out 1 micron wide grooves at a volumetric excavation rate of 1% nanorobot volume per second to partition the 1 cm^3 object into 10^6 100-micron microcubes in ~300 seconds, after which the foreign object microcubes are transported out of the patient in single file at 1 m/sec through the nanosyringoscope in ~100 seconds, followed by the exiting nanorobots taking ~10 seconds, completing a ~7 minute object-removal nanosyringotomy procedure through a ~100-micron diameter hole.

Box 23.3 Experimental surgical microrobotics

There have already been early attempts to build less sophisticated stand-alone microrobots for near-term in vivo surgical use. For example, Ishiyama et al. (Ishiyama et al. 2002) at Tohoku University developed tiny magnetically-driven spinning screws intended to swim along veins and carry drugs to infected tissues or even to burrow into tumors and kill them with heat. Martel's group at the NanoRobotics Laboratory of Ecole Polytechnique in Montreal has used variable MRI magnetic fields to generate forces on an untethered microrobot containing ferromagnetic particles, developing sufficient propulsive power to direct the small device through the human body (Mathieu et al. 2005). In 2007 they reported injecting, guiding via computer control, and propelling at 10 cm/sec a prototype untethered microdevice (a ferromagnetic 1.5- millimeter-diameter sphere) within the carotid artery of a living animal placed inside a clinical magnetic resonance imaging (MRI) system (Martel et al. 2007) – the first time such in vivo mobility has been demonstrated. Nelson's team at the Swiss Federal Institute of Technology in Zurich has pursued a similar approach, in 2005 reporting (Yesin et al. 2005) the fabrication of a microscopic robot small enough (~200 μm) to be injected into the body through a syringe and which they hope might someday be used to perform minimally invasive eye surgery. Nelson's simple microrobot has successfully maneuvered through a watery maze using external energy from magnetic fields, with different frequencies able to vibrate different mechanical parts on the device to maintain selective control of different functions. Sitti's group at Carnegie Mellon's NanoRobotics Laboratory is developing (Behkam and Sitti 2007) a <100-micron swimming microrobot using biomimetic flagellar motors borrowed from *S. marcescens* bacteria "having the capability to swim to inaccessible areas in the human body and perform complicated user directed tasks." Friend's group in the Micro/Nanophysics Research Laboratory at Monash University in Australia is designing a 250-micron microrobot (Cole 2007) to perform minimally invasive microsurgeries in parts of the body outside the reach of existing catheter technology – such as delivering a payload of expandable glue to the site of a damaged cranial artery, a procedure typically fraught with risk because posterior human brain

arteries lay behind a complicated set of bends at the base of the skull beyond the reach of all but the most flexible catheters. Friend's completed device, expected by 2009, will be inserted and extracted using a syringe and is driven by an artificial flagellar piezoelectric micromotor.

Tactile (Ku et al. 2003; Winter and Bouzit 2007), haptic (McColl et al. 2006) and other sensory feedback will allow emergency practitioners to steer the nanosyringoscope into a patient to remove a foreign object (Feichtinger et al. 2007), then to withdraw bloodlessly from the body. The nanosurgeon may control the procedure via hand-guided interfaces similar to various medical exoskeletal appliances (Fleischer et al. 2006; Cavallaro et al. 2006; Gordon and Ferris 2007), instrumented gloves (Castro and Cliquet 1997; Yun et al. 1997) and hand-held surgical robots (Tonet et al. 2006) that have been under development for several decades.

The nanosyringoscope could also rapidly and painlessly import macroscale quantities of cells to any location inside the body (Section 23.7.1.4).

23.6.4 Cell Repair

In suggesting the novel possibility of individual cell repair, Drexler (1986) drew inspiration from the cell's eye view to explain how medical nanorobotics could bring a fundamental breakthrough in medicine: "Surgeons have advanced from stitching wounds and amputating limbs to repairing hearts and reattaching limbs. Using microscopes and fine tools, they join delicate blood vessels and nerves. Yet even the best microsurgeon cannot cut and stitch finer tissue structures. Modern scalpels and sutures are simply too coarse for repairing capillaries, cells, and molecules. Consider 'delicate' surgery from a cell's perspective. A huge blade sweeps down, chopping blindly past and through the molecular machinery of a crowd of cells, slaughtering thousands. Later, a great obelisk plunges through the divided crowd, dragging a cable as wide as a freight train behind it to rope the crowd together again. From a cell's perspective, even the most delicate surgery, performed with exquisite knives and great skill, is still a butcher job. Only the ability of cells to abandon their dead, regroup, and multiply makes healing possible. Drug molecules are simple molecular devices [that] affect tissues at the molecular level, but they are too simple to sense, plan, and act. Molecular machines directed by nanocomputers will offer physicians another choice. They will combine sensors, programs, and molecular tools to form systems able to examine and repair the ultimate components of individual cells. They will bring surgical control to the molecular domain."

23.6.4.1 Mechanisms of Natural Cell Repair

Many so-called natural "cell repair" mechanisms are actually tissue repair mechanisms, some of which act by replacing, not repairing, existing cells. For instance,

there are stem cells that can transform into other needed (differentiated) cell types at a site where a cell of the needed type has apoptosed or been phagocytosed and reabsorbed, in which case the stem cells are effectuating a fairly direct form of "repair by replacement" (Ahn et al. 2004; Ye et al. 2006; Gersh and Simari 2006; Reinders et al. 2006). Stem cells can also fuse with somatic cells and alter them (Padron Velazquez 2006). Other "cell repair" mechanisms include chondroblasts or fibroblasts that rebuild connective tissue by extruding collagen fibers and other ECM components, and oligodendrocyte progenitor cells that extracellularly remyelinate CNS cells that have been demyelinated by exposure to toxic chemicals (Armstrong et al. 2006) or viral infection (Frost et al. 2003).

As another example, injured or apoptosed cells can be replaced by new cells produced by the replication and division of neighboring cells of the same cytotype, as occurs in, for example, epithelial "cell repair" (actually tissue regeneration) of the gastrointestinal, kidney, lung, liver, skin, prostate and muscle tissues (Nony and Schnellmann 2003; Kawashima et al. 2006; Pogach et al. 2007). The predominant mode of "repair" in biology is probably turnover, a fairly robust process in which everything from molecules to whole cells is replaced with new molecules or new cells, with the old being discarded and not repaired. Most damaged molecules other than DNA are simply degraded and replaced, and all mRNAs and their precursors are degraded after limited use whether damaged or not. Typical protein turnover half-life is ~200,000 sec (Alberts et al. 1989; Becker and Deamer 1991), membrane phospholipid half-life averages ~10,000 sec (Becker and Deamer 1991) but plasma membrane turnover rate is ~1800 sec for macrophage (Lehrer and Ganz 1995) and ~5400 sec for fibroblast (Murray et al. 1993). Glycocalyx turnover in rat uterine epithelial cells is ~430,000 sec (Jones and Murphy 1994), and enterocyte glycocalyx is renewed in 14,000–22,000 sec as vesicles with adhered bacteria are expelled into the lumen of small and large intestine (Kilhamn 2003). Cell turnover rates are equally impressive. Neutrophil lifespan is ~11,000 sec in blood and ~260,000 sec in tissue (Black 1999); blood platelet lifespan is ~860,000 sec (Stein and Evatt 1992). Some mucosal surfaces may replace their entire luminal cell population every ~10^5 sec (~1 day): Cell turnover time is ~86,000 sec in gastric body, ~200,000 sec for duodenal epithelium, ~240,000 sec for ileal epithelium, and ~400,000 sec for gastric fundus (Peacock 1984). At the other extreme is the lens of the eye, where the rate of cell turnover and repair is very low (McNulty et al. 2004) and the lens crystalline is never subject to turnover or remodeling once formed (Lynnerup et al. 2008), and tooth enamel, dentine, and cementum (other biological structures that are preserved essentially without turnover; Boyde et al. 2006; Ubelaker et al. 2006).

There are at least six examples of true "cell repair" mechanisms. Most notable is eukaryotic DNA repair including excision repair (base excision repair and nucleotide excision repair), mismatch repair, repair of double-strand breaks, and cross-link repair (Sharova 2005). These repair processes boost the fidelity of DNA replication to error rates of ~10^{-11}.

Second, there is also a limited form of protein repair in which misfolding errors are corrected after protein synthesis or in response to pathological states, mediated by molecular chaperones (Craig et al. 2003) or heat shock proteins (Chow and Brown 2007).

Third, there is autophagy in which the stressed cell digests some of its own damaged components (e.g., long-lived proteins, cytomembranes and organelles) and then replaces these missing components with newly constructed ones (Bergamini et al. 2004; Malorni et al. 2007) – an activity whose failure appears linked to the process of aging (Bergamini et al. 2004; Bergamini 2006; Kaushik and Cuervo 2006; Donati 2006). This is replacement at the subcellular level but repair at the cellular level.

Fourth, there is cell membrane self-repair in which torn plasma membrane reseals with little loss of intracellular contents (Steinhardt et al. 1994; Bi et al. 1995). One or more internal membrane compartments accumulate at the disruption site and fuse there with the plasma membrane, resulting in the local addition of membrane to the surface of the mechanically wounded cell (Miyake and McNeil 1995) and activating repair-related gene expression inside the cell (Ellis et al. 2001). Plasma membrane disruptions are resealed by changes in the cellular cytoskeleton (partial disassembly) (Xie and Barrett 1991) and by an active molecular mechanism thought to be composed of, in part, kinesin, CaM kinase, snap-25, and synaptobrevin (Miyake and McNeil 1995), with vesicles of a variety of sizes rapidly (in seconds) accumulating in large numbers within the cytoplasm surrounding the disruption site, inducing a local exocytosis (Miyake and McNeil 1995). Intracellularly, torn Golgi membrane readily reconstitutes itself from a vesiculated state (Kano et al. 2000) and the nuclear membrane is reversibly disassembled and reassembled (a form of "repair") during mitosis (Georgatos and Theodoropoulos 1999).

Fifth, some limited forms of cytoskeletal self-repair exist, most notably the coordinated remodeling of plasma membrane-associated (cortical) cytoskeleton self-repair (Bement et al. 2007), autocatalytic microfilament actin polymerization (Pantaloni et al. 2001), and recovery from mechanical disruption of cross-bridged intermediate filament networks (Wagner et al. 2007).

Sixth, there is the lysosomal system (Walkley 2007) for recycling all major classes of biological macromolecules, with soluble products of this digestion able to cross the membrane, exit the organelle, and enter the cytosol for recycling into the cellular metabolism, and there is the proteasome/ubiquitin system (Wolf and Hilt 2004) for similarly recycling damaged proteins – both of which effect "repair by replacement" since the whole macromolecule is discarded and a new one is synthesized in its place.

Medical nanorobotics will make possible comprehensive true cell repair, including, most importantly, those repairs that the cell cannot make for itself when it is relying solely on natural self-repair processes.

23.6.4.2 Cell Nanosurgery

The earliest forms of cellular nanosurgery are already being explored today. Atomic force microscopes (AFMs) have been used to observe the movement of filaments beneath the plasma membrane of living eukaryotic (Parpura et al. 1993) and bacterial (Méndez-Vilas et al. 2006) cells. Microrobotic systems are being developed for single cell nanoscale probing, injection, imaging and surgery (Li and Xi 2004), and the differing effects of intracellular surgical nanoneedles having cylindrical or

conical tips (Obataya et al. 2005), or DNA-functionalized tips (Han et al. 2005), have been explored experimentally. Optical tweezers and vortex traps (Jeffries et al. 2007) permit noncontact immobilization and manipulation of individual cells.

Basic individual cell manipulation is fairly commonplace in the laboratory. For more than four decades microbiologists have used nuclear transplantation (Gurdon 2006; Meissner and Jaenisch 2006) techniques to routinely extract or insert an entire nucleus into an enucleated cell using micropipettes without compromising cell viability. Direct microsurgical extraction of chromosomes from nuclei has been practiced since the 1970s (Korf and Diacumakos 1978, 1980; Frey et al. 1982; Maniotis et al. 1997), and microinjection of new DNA directly into the cell nuclei using a micropipette (pronuclear microinjection) is a common biotechnology procedure (Wall 2001) easily survived by the cell, though such injected DNA often eventually exits the nucleus (Shimizu et al. 2005). DNA microinjection into pronuclei of zygotes from various farm animal species has been practiced commercially since 1985 but has shown poor efficiency and involves a random integration process which may cause mosaicism, insertional mutations and varying expression due to position effects (Wolf et al. 2000).

Nanosurgery has been performed on individual whole cells by several means. For example, a rapidly vibrating (100 Hz) micropipette with a <1 micron tip diameter has been used to completely slice off dendrites from single neurons without damaging cell viability (Kirson and Yaari 2000), and individual cut nerve cells have been rejoined by microsuturing or fibrin glue welding (Zhang et al. 1998). Axotomy of roundworm neurons was performed by femtosecond laser (femtolaser) surgery, after which the axons functionally regenerated (Yanik et al. 2004). A femtolaser acts like a pair of "nano-scissors" by vaporizing tissue locally while leaving adjacent tissue unharmed. Femtolaser surgery has also performed localized nanosurgical ablation of focal adhesions adjoining live mammalian epithelial cells (Kohli et al. 2005). AFMs have dissected bacterial cell walls in situ in aqueous solution, with 26 nm thick twisted strands revealed inside the cell wall after mechanically peeling back large patches of the outer cell wall (Firtel et al. 2004). Maniotis et al. (Maniotis et al. 1997) has mechanically spooled and extracted chromatin from a nucleus, observing that "pulling a single nucleolus or chromosome out from interphase or mitotic cells resulted in sequential removal of the remaining nucleoli and chromosomes, interconnected by a continuous elastic thread."

Nanosurgery has also been reported on subcellular and even nanoscale structures deep inside individual living cells without killing them. For instance, femtolaser surgery has performed: (1) microtubule dissection inside live cells (Sacconi et al. 2005a, Colombelli et al. 2005, 2007), (2) severing a single microtubule without disrupting the neighboring microtubules less than 1 micron away (Heisterkamp et al. 2005), (3) altering depolymerization rate of cut microtubules by varying laser pulse duration (Wakida et al. 2007), (4) selective removal of sub-micron regions of the cytoskeleton and individual mitochondria without altering neighboring structures (Shen et al. 2005), (5) noninvasive intratissue nanodissection of plant cell walls and selective destruction of intracellular single plastids or selected parts of them

(Tirlapur and Konig 2002), and even (6) the nanosurgery of individual chromosomes (selectively knocking out genomic nanometer-sized regions within the nucleus of living Chinese hamster ovary cells) without perturbing the outer cell membrane (Konig et al. 1999). Zettl's group has demonstrated a nanoinjector consisting of an AFM-tip-attached carbon nanotube that can release injected quantum dots into cell cytosol, with which they plan to carry out organelle-specific nanoinjections (Chen et al. 2007). Gordon's group at the University of Manitoba has proposed magnetically-controlled "cytobots" and "karyobots" for performing wireless intracellular and intranuclear surgery. Future diamondoid medical nanorobots equipped with operating instruments and mobility will be able to perform precise and refined intracellular, intra-organelle, and nanometer-scale nanosurgical procedures which are well beyond current capabilities.

23.6.4.3 Chromosome Replacement Therapy

The chromallocyte (Freitas 2007) is a hypothetical mobile cell-repair nanorobot whose primary purpose will be to perform chromosome replacement therapy (CRT). In CRT, the entire chromatin content of the nucleus in a living cell will be extracted and promptly replaced with a new set of prefabricated chromosomes that have been artificially manufactured as defect-free copies of the originals.

The chromallocyte (Fig. 23.26) will be capable of limited vascular surface travel into the capillary bed of the targeted tissue or organ, followed by diapedesis (exiting a blood vessel into the tissues) (Freitas 1999bq), histonatation (locomotion through tissues) (Freitas 1999at), cytopenetration (entry into the cell interior) (Freitas 1999x), and complete chromatin replacement in the nucleus of the target cell. The CRT mission ends with a return to the vasculature and subsequent extraction of the nanodevice from the body at the original infusion site. This ~3 hour chromosome replacement process is expected to involve a 26-step sequence of distinct semi-autonomous sensor-driven activities, which are described at length in a comprehensive published technical paper on the subject (Freitas 2007) and in

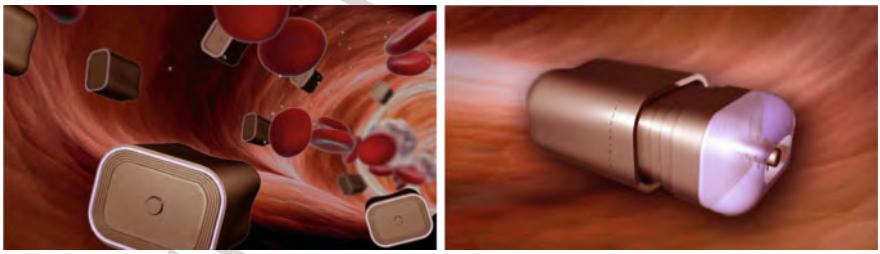

This figure will be printed in b/w

Fig. 23.26 Artist's conceptions of the basic chromallocyte (Freitas 2007) design: devices walking along luminal wall of blood vessel (*left*); schematic of telescoping funnel assembly and proboscis operation (*right*). Image © 2006 Stimulacra LLC (www.stimulacra.net) and Robert A. Freitas Jr. (www.rfreitas.com)

more detail below, and include: (1) injection, (2) extravasation, (3) ECM immigration, (4) cytopenetration, (5) inhibition of mechanotransduction (to avoid nanorobot mechanical actions triggering unwanted cell responses), (6) nuclear localization, (7) nucleopenetration, (8) blockade of apoptosis (to prevent misinterpretation of CRT processes as damage demanding cell suicide), (9) arrest of DNA repair (to prevent misinterpretation of CRT processes as damage demanding repair), (10) blockade of inflammatory signals, (11) deactivation of transcription, (12) detachment of chromatin from inner nuclear wall lamins (cortex proteins), (13) extension of the "Proboscis", (14) rotation of the Proboscis, (15) deployment of the chromosomal collection funnel, (16) digestion of stray chromatin, (17) dispensation of new chromatin, (18) decondensation of the new chromatin, (19) re-anchoring of the dispensed chromatin to inner nuclear wall lamins, (20) reactivation of transcription, (21) reactivation of DNA repair and other DNA-related maintenance and usage processes, (22) nuclear emigration, (23) cellular emigration, (24) ECM emigration, (25) return to original point of entry into the body, and (26) removal from the body. Treatment of an entire large human organ such as a liver, involving simultaneous CRT on all 250 billion hepatic tissue cells, might require the localized infusion of a ~1 terabot (10^{12} devices) or ~69 cm^3 chromallocyte dose in a 1-liter (7% v/v nanorobots) saline suspension during a ~7 hour course of therapy. This nanodevice population draws 100–200 watts which lies within estimated nanorobot thermogenic limits consistent with maintenance of constant body temperature (Freitas 1999 cm).

Replacement chromosomes would be manufactured in a desktop *ex vivo* chromosome sequencing and manufacturing facility, then loaded into the nanorobots for delivery to specific targeted cells during CRT. The new DNA is manufactured to incorporate proper methylation for the target cell type and other post-translational modifications constituting the "histone code" used by the cell to encrypt various chromatin conformations and gene expression states (Villar-Garea and Imhof 2006). A single fully-loaded lozenge-shaped 69 $micron^3$ chromallocyte will measure 4.18 microns and 3.28 microns along cross-sectional diameters and 5.05 microns in length, typically consuming 50–200 pW of power in normal operation and a maximum of 1000 pW in bursts during outmessaging, the most energy-intensive task. Onboard power can be provided acoustically from the outside in an operating-table scenario in which the patient is well-coupled to a medically-safe 1000 W/m^2 0.5 MHz ultrasound transverse-plane-wave transmitter throughout the procedure (Freitas 1999n) – the American Institute of Ultrasound in Medicine (AIUM) deems 10,000-sec exposures to 1000 W/m^2 ultrasound to be safe (Freitas 1999n). The chromallocyte design includes an extensible primary manipulator 4 microns long and 0.55 microns in diameter called the Proboscis that is used to spool up chromatin strands via slow rotation when inserted into the cell nucleus. After spooling, a segmented funnel assembly is extended around the spooled bolus of DNA, fully enclosing and sequestering the old genetic material. The new genetic material can then be discharged into the nucleus through the center of the Proboscis by pistoning from internal storage vaults, while the old chromatin that is sequestered inside the sealed leakproof funnel assembly is forced into the storage vaults as space is vacated

by the new chromatin that is simultaneously being pumped out. The chromallocyte will employ a mobility system similar to the microbivore grapple system, possibly including a solvation wave drive (Freitas 1999bx) to help ensure smooth passage through cell plasma and nuclear membranes.

Modified procedures are proposed in the full technical description published elsewhere (Freitas 2007) for special cases including (1) proliferating, pathological, multinucleate, and karyolobate cells, (2) cells in locations where access is difficult such as brain, bone, or mobile cells, and (3) cells expressing genetic mosaicism, and also for alternative missions including (1) partial- or single-chromosome replacement, (2) single-cell and whole-body CRT, and (3) mitochondrial DNA replacement.

23.6.4.4 Modifying Cellular Controls and Cycles

Another important function of cell repair nanorobots (among those specialized for the task) would be the alteration of cellular control and metabolic cycle parameters. For example, the standard cell cycle for proliferating cells includes four rigidly-controlled and sequentially-executed phases, namely: entry G1 phase (cell expands in size), S phase (DNA synthesis), G2 phase (resting), and final brief M phase (mitosis or cell division, only ~4% of total cycle duration), with nonreplicating cells said to be in the quiescent G0 phase. Section 23.6.1 of the chromallocyte paper (Freitas 2007) reviews how a cell repair nanorobot might take complete control of a cell's mitotic cycle (Guardavaccaro and Pagano 2006), giving cell repair devices the ability to exercise nominal control over cell growth. Combined with control of cell development by changing the pattern of gene expression using CRT (Section 23.6.4.3), this provides a very general ability to replace cells. One clinical implication, for example, is that after a heart attack when scar tissue has replaced dead muscle, cell repair machines could stimulate unscarred regions of the heart to grow fresh muscle by resetting cellular control mechanisms, allowing the physician to guide the in situ self-healing of the heart.

The control of gene expression (e.g., via control of transcription factors, microRNAs, shRNAs, etc.) is paramount in the control of the cell. Important classes of cellular control modification – some having temporary, some having permanent, effects – might include direct intervention in protein synthesis (e.g., examining and editing extant mRNA tapes found in the cytosol, or fabricating and releasing supplemental natural or synthetic mRNA sequences, thus altering the rate of translation of specific protein sequences by the natural cellular machinery (Grudzien et al. 2004)); sequestration of key tRNA populations to sensitively influence the rate of protein synthesis (Delgado-Olivares et al. 2006); sequestration, augmentation, or chemical modification of key cell signaling molecules or ions to modulate internal signal pathways; artificial ubiquitination or de-ubiquitination (Johnston et al. 1999), or editing nuclear (Johnson et al. 2004) and cytoplasmic (Gomord et al. 1997) compartment localization sequences, on cytosolic proteins to assert control over trafficking; direct alteration of internal mitochondrial chemistry or internal lysosomal pH levels; artificially regulating normal cell functions including metabolism and secretion;

or cytocarriage (Freitas 1999ce) by nanorobotic "pilots" inside fibroblasts to direct the deposition and placement of collagen fibers by these mobile cells to rebuild extracellular matrix. Cellular controls and cycles could also be modified at their most upstream source by directly altering transcription (synthesis of RNA on a DNA template) in the nucleus, possibly by editing promoter sequences (Wray et al. 2003) in new replacement DNA that is installed by chromallocytes (Section 23.6.4.3), or by using sorting rotors to release or sequester inhibitors or transcription factors, since promoter activity is usually controlled by transcription factors that bind to the promoters or by inhibitors that inactivate the transcription factors.

23.6.4.5 Clearing Cytoplasm of Extraneous Materials and Devices

Cell repair nanorobots could restore and maintain cellular health by removing extraneous materials from the cytosol and other intracellular compartments. Perhaps the best-known example of such extraneous material is the insoluble age-pigment lysosomal granules called "lipofuscin" that collect in many of our cells, the accumulation starting as early in life as 11 years old and rising with age (Terman and Brunk 1998), activity level (Basson et al. 1982) and caloric intake (Moore et al. 1995), and varying with cell type (Brunk et al. 1992; Harman 1989). Clumps of these yellow-brown autofluorescent granules – typically 1–3 microns in diameter – may occupy up to 10% of the volume of heart muscle cells (Strehler et al. 1959), and from 20% of brainstem neuron volume at age 20 to as much as 50% of cell volume by age 90 (West 1979). Lipofuscin concentrations as high as 75% have been reported in Purkinje neurons of rats subjected to protein malnutrition (James and Sharma 1995). Elevated concentrations in heart cells appear not to increase the risk of heart attack (Strehler et al. 1959; Roffe 1998), nor to accelerate cellular aging processes in heart muscle or liver tissues (Blackett and Hall 1981), and brain cell lipofuscin is not associated with mental (West 1979; Drach et al. 1994) or motor (McHolm et al. 1984) abnormalities or other detrimental cellular function (Davies et al. 1983). However, hereditary ceroid lipofuscinosis (Shotelersuk and Gahl 1998) or neuronal ceroid-lipofuscinosis (NCL) diseases (Kida et al. 2001) can lead to premature death, though ceroid appears to be pathological only in neurons (Kida et al. 2001) or when loaded into human fibroblasts (Terman et al. 1999). There is also evidence that A2E, a hydrophobic fluorophore component of retinal pigment epithelial lipofuscin-like material, may contribute to age-related macular degeneration (De and Sakmar 2002). Lipofuscin is an indigestible lipid peroxidation product that cannot normally be excreted or metabolized by the cell, but which cytopenetrating microbivores that had entered the cell could readily detect and harmlessly digest – as the existence of various artificial lipofuscinolytic drugs (Totaro et al. 1985; James et al. 1992) and naturally occurring lipofuscinolytic bacteria (de Grey et al. 2005) attests is possible.

Other similarly inert intracellular pigments are known (Powell et al. 1996), along with a number of pathological intracellular storage diseases [e.g., of ER (Kim and Arvan 1998) and lysosomes (Winchester et al. 2000), etc.], including Fabrey's, Gaucher's, mannosidosis, Niemann-Pick (Simons and Gruenberg

2000), Tay-Sachs, Lewy bodies (Kosaka 2000) in Hallervorden-Spatz disease, and Hirano bodies (Yagishita et al. 1979). Neurofibrillary tangles (Mattson 2004) are pathological material found in neurons and are associated with Alzheimer's disease. Accumulation of lysosomal deposits of oxidized low-density lipoproteins or cholesterol crystals (Tangirala et al. 1994) in macrophage foam cells may contribute to atherosclerosis. Intracellular crystalloid bodies have been observed in the skeletal muscle cells of patients with hypothyroid myopathy (Ho 1987) and noninert amyloid deposits average ~12% of pancreatic islet cell volume in patients with maturity onset diabetes (Westermark and Wilander 1978). (See Section 23.7.1.1 for more on amyloidosis.) Excessive intracellular crystallization of drug molecules can lead to acute renal failure (Farge et al. 1986) and intracellular crystals have been found inside chondrocytes in certain crystal deposition diseases (Dijkgraaf et al. 1995). Other intracellular crystal deposition diseases are known such as mitochondrial crystalline inclusions (Farrants et al. 1988) and intermembrane inclusion bodies (O'Gorman et al. 1997), polyglucosan bodies (Matsumuro et al. 1993), and Fardeau-Engel bodies (Vital et al. 2002) that are involved in peripheral neuropathies. Several types of inorganic particles are highly toxic to phagocytes: just 0.05 μg of silica per 10^6 macrophages (Bateman et al. 1982), or 0.002% of cell volume assuming 1166 micron^3 per rat alveolar macrophage, is cytotoxic. Finally, heavy metals, radioactive ions, and metabolic poisons can also kill cells. All of these molecules, particles and deposits could either be digested to harmless effluents in situ by cytopenetrating microbivores (Section 23.6.2.1), or loaded into the large onboard storage tanks of chromallocyte-class nanorobots (Section 23.6.4.3) and transported intact out of the patient's body for external disposal.

Cell repair nanorobots may also remove extraneous nanodevices from the intracellular spaces. The most common of such devices would be natural biological nanomachines. For example, prions are the only known infectious intracellular pathogens that are devoid of nucleic acid (Prusiner 2001), and similarly viroids (Flores 2001) and viroid-like RNAs are intracellular pathogens lacking protein – and both are beyond the ability of current medicine to remove from infected cells (although antimisfolding agents to combat protein misfolding disorders like prions are under active study (Estrada et al. 2006)). Other biota that may live inside of cells include a variety of endosymbionts (Corsaro et al. 1999), viruses, and certain other entities involved in disease-associated emperipolesis (Freitas 2003y). In human cells, the tuberculosis bacterium enters the alveolar macrophage which transports the intruder into the blood, the lymphatic system, and elsewhere. Other intracellular microorganisms such as *Listeria* (~0.25 micron^3) and *Shigella* (~2 micron^3), once free in the cytoplasm, propel through the cytosol via continuous cytoskeleton-linked actin polymerization (Freitas 1999bz); macrophages infected with *Listeria* have been observed with ~2% of their volume co-opted by the microbes (~100 organisms) (Decatur and Portnoy 2000). Some motile intracellular parasites such as *Tyzzer* (Fujiwara et al. 1981) may cause disarrangement and depopulation of host cell organelles by the movement of their peritrichous (covering entire surface) flagella. Other motile intracellular parasites such as the spotted fever-group *Rickettsiae* (Hackstadt 1996) spread rapidly from cell to cell by actin-based movement but do

not cause lysis of the host cell. Typhus-group rickettsiae (Hackstadt 1996) multiply in host cells to great numbers, though without profound damage until cell lysis finally occurs. Harmful pathogens such as malarial schizonts of *Plasmodium falciparum* may multiply to 50–70% of erythrocyte cytoplasmic volume before the red cell bursts, and other intracellular parasites have been observed at similar cytoplasmic volumetric fractions (Heydorn and Mehlhorn 1987; Abd-Al-Aal et al. 2000). Microbivore-class devices could remove all of these from intracellular spaces.

Beyond microbiological intruders, in a future era foreign nanorobots might be placed in a victim's body surreptitiously for unwanted or even malicious purposes. Chromallocyte-class personal cytosecurity nanorobots could be deployed having the ability to scavenge intracellular foreign nanodevices and either disable them in situ or transport them harmlessly out of the body, or to perform related sentinel or cytodefensive functions.

23.6.4.6 Organelle Testing, Replacement, or Repair

Another general class of cell repair machine would undertake the direct census and testing of intracellular organelle number and function, followed by appropriate corrective actions including the internal modification and repair or wholesale replacement of malfunctioning organelles. Excessive populations or damaged intracellular organelles could be removed using a cytopenetrating microbivore-class device; insufficient populations or volume of organelles can be addressed using a larger chromallocyte-class "delivery truck" type device (Section 23.6.4.3) to import supplemental organelles manufactured externally (Section "Tissue Printers, Cell Mills and Organ Mills").

Given the many thousands of unique biochemicals normally present within the cell, all having complex interactions, considerable R&D effort will be required to define the optimal testing regime for each organelle and is beyond the scope of this Chapter. However, simple tests are readily imagined as diagnostic indicators of correct organelle function. Cytosolic ATP concentrations, when combined with sensor readings for glucose and activity level indicators, can be diagnostic of proper metabolic function in the mitochondrial population. Organelle membrane breach (Freitas 2003z) is another concern – detection of free digestive enzymes in the cytosol may reveal a lysosomal or peroxisomal membrane breach, or the similar presence of cytochrome c may indicate mitochondrial wall breach. Neurons could be checked for proper ionic balance, ribosomes or mitochondria could be counted and inspected, and even vesicles, granules and vacuoles could be inventoried and sampled if deemed necessary or useful. A nonexhaustive list of general diagnostic mission classes (Freitas 1999ca) might include: (1) organelle counting, dimensional measuring, and general cytocartography (albeit somewhat ephemeral); (2) circumorganelle chemical assay; (3) organelle-specific surface membrane analysis or intracytoplasmic chemical assay; (4) dynamic functional or structural testing of cellular components; and (5) sampling, diagnosis, chemoinjection, replacement or repair operations to be performed upon an individual organelle or cytocomponent in a specific cell. Organelles could also be checked for organelle-specific storage diseases (Section 23.6.4.5) or for organelle-specific endosymbiont infestations such as

mitochondrial mitophages (Sassera et al. 2006), and any unwanted foreign matter would be removed by cell repair nanorobots (Section 23.6.4.5).

The cell nucleus is the largest and most important intracellular organelle. Besides performing CRT (Section 23.6.4.3) on intranuclear genetic material, other activities that a cell repair machine might perform without entering the nucleus (Freitas 1999cb) could include: (1) physical mapping and compositional analysis of the nuclear envelope; (2) monitoring of nuclear pore traffic; (3) near-complete regulation of nuclear pore traffic using multiple manipulators or other devices; (4) monitoring, initiating, or modifying cytoskeletally-mediated mechanical signal transduction into the nuclear interior; and (5) injection of enzymes, RNA or DNA fragments, or other bioactive materials through nuclear pores using hollow nanoinjectors. The nucleus could also be checked for the presence of nucleus-specific intranuclear microbial parasites analogous to the tachyzoites of *Toxoplasma gondii* in mouse (which may enter the nucleus using its apical secretory organelle called the rhoptry) (Barbosa et al. 2005), *Nucleospora salmonis* (an intranuclear microsporidian parasite of marine and freshwater fish) (El Alaoui et al. 2006), the merogonic and gamogonic stages of *Eimeria* parasites in the goose (Pecka 1993), and MVM parvovirus (Cohen et al. 2006) – all of which could readily be detected and removed by medical nanorobots designed specifically for this task.

Cell membrane is a related compartment that suffers various molecular derangements that could be detected by medical nanorobots. For example, improper function of transmembrane glucose transporters could be detected by measuring interior glucose levels and comparing them to extracellular levels. Chemical testing could reveal toxins or poisons in cell receptors and transport channels, and related tests could be devised for other transmembrane pumps (e.g., the lack of pumps can be associated with disease (Chambers et al. 1999)), or to detect surface glycation (Section 23.7.1.2), and so forth. Upon detecting these conditions, nanorobots could appropriately edit or replace cell membrane components to repair all identified defects.

23.6.4.7 Cytostructural Testing, Replacement, or Repair

Besides testing for proper function, cell repair nanorobots could also examine cells for proper structure. For example, from outside the cell neural dendrites and other structural extensions could be checked for acceptable gross dimensions and appropriate connectivity (Freitas 1999co), adequate physical strength (Freitas 1999bd) and general health. Muscular dystrophy may be caused by disorganization of links between the intracellular cytoskeleton (e.g., dystrophin) and the ECM (Cohn and Campbell 2000), and the disruption of proper adhesive interactions with neighboring cells can lead to fatal defects in extracellular tissue architecture (Hagios et al. 1998). The cell plasma membrane and underlying cell cortex could be checked for mechanical integrity, and also to make sure that the correct surface receptors are in place and of the correct types and numbers (Freitas 1999cn). Cell membranes are ordinarily self-sealing after a puncture wound (Section 23.6.4.1), but a severely damaged membrane might need to be quickly patched using lipophilic materials dispensed from a repair nanorobot.

The cytoskeleton is normally self-repairing in a healthy cell – a fact that will help to allow nanorobots to transit the intracellular space without causing lasting damage. But some cells may experience "cytoskeletal disease" (Box 23.4) requiring nanorobotic repair. Direct nanorobotic intervention to repair these broken or inadequate cytoskeletal elements should be possible in all cases. However, the defect often will be widespread and caused by an underlying genetic (Section 23.6.4.3) or metabolic (Sections 23.6.2.5 and 23.6.4.4) pathology which should be directly corrected by the nanorobots, permanently curing the causative disease and allowing natural self-repair processes to resume their normal functions.

Box 23.4 Disorders of cytoskeletal architecture

Disorganization of the cytoskeletal architecture has been associated with diseases as diverse as heart failure (Hein et al. 2000; Lemler et al. 2000), rotavirus infection (Brunet et al. 2000), sickle cell anemia (Kuczera 1996), lissencephaly (Sapir et al. 1997), and Alzheimer's disease (Lee 1995), and a "collapse transition" of neurofilament sidearm domains may contribute to amyotrophic lateral sclerosis (ALS) and Parkinson's disease (Kumar et al. 2002). Cytoskeletal diseases most notably involve transmembrane linkage disruptions. For instance, breakage of major cytoskeletal attachments between the plasma membrane and peripheral myofibers in cardiac myocytes predisposes the cell to further mechanical damage from cell swelling or from ischemic contracture (Sage and Jennings 1988). Elliptocytosis (Liu et al. 1990) and other inherited hemolytic disorders (Delaunay 1995) are caused by disorganization of the subsurface spectrin-actin cell cortex in the erythrocyte (Zhang et al. 2001). Deeper inside the cell, perturbations in the architecture of the intermediate filament cytoskeleton in keratinocytes and in neurons can lead to degenerative diseases of the skin, muscle cells, and nervous system (Fuchs 1996). Tissues lacking intermediate filaments fall apart, are mechanically unstable, and cannot resist physical stress, which leads to cell degeneration (Galou et al. 1997). Perinuclear clumping of fragmented keratin intermediate filaments accompanies many keratin disorders of skin, hair, and nails (Sprecher et al. 2001). Impairment of normal axonal cytoskeletal organization in Charcot-Marie-Tooth disease results in distal axonal degeneration and fiber loss (Sahenk et al. 1999). A variety of human disorders are also associated with dysfunction of cytoskeleton-based molecular motors, including, for example: (1) the motor-based diseases involving defective cellular myosin motors (Keats and Corey 1999), e.g., implicated in Griscelli syndrome (Westbroek et al. 2001), hearing loss (Avraham 2002), hypertrophic cardiomyopathy (Rayment et al. 1995), and other myosin myopathies (Seidman and Seidman 2001); (2) spindle assembly- and function-related diseases (Mountain and Compton 2000) or kinesin- and dynein-related motor molecule

diseases, e.g., implicated (Schliwa and Woehlke 2003) in Charcot-Marie-Tooth disease type 2A (Zhao et al. 2001), Kartagener syndrome (Marszalek et al. 1999) or primary ciliary dyskinesia (Olbrich et al. 2002), lissencephaly (Vallee et al. 2001), polycystic kidney disease (Qin et al. 2001), and retinitis pigmentosa (Williams 2002); and (3) other avenues for cellular malfunction (Schliwa and Woehlke 2003; Fischer 2000; Reilein et al. 2001; Schliwa 2003).

23.6.4.8 Intracellular Environmental Maintenance

Cell repair machines could also test, analyze, and restore a pathological cytoplasmic environment that has gotten too far from homeostatic equilibrium. This could be as simple as detecting and removing pathological proteins (or other damaged or unwanted biomolecules) from the cytosol, or it could involve actively manipulating intracellular pH, temperature, ionic balance, or metabolic inputs and byproduct concentrations. A nanorobot could straddle the plasma membrane of the cell, acting as a temporary artificial membrane transporter to pump out excess sodium, calcium, drug molecules, toxins, CO_2 and other waste products, or to pump in supplemental ions, O_2/glucose, or other nutrient molecules that are in short supply. These applications might require a pharmacyte-, microbivore-, or chromallocyte-class nanodevice, depending on circumstances.

As a simple example of the tremendous power of nanorobots to regulate the intracellular chemical environment, consider the Ca^{++} ion which serves as an intracellular mediator in a wide variety of cell responses including secretion, cell proliferation, neurotransmission, cellular metabolism (when complexed to calmodulin), and participates in signal cascade events that are regulated by calcium-calmodulin-dependent protein kinases and adenylate cyclases. The concentration of free Ca^{++} in the extracellular fluid or in the cell's internal calcium sequestering compartment (which is loaded with a binding protein called calsequestrin) is ~10^{-3} ions/nm^3. However, in the cytosol, free Ca^{++} concentration varies from 6×10^{-8} ions/nm^3 for a resting cell up to 3×10^{-6} ions/nm^3 when the cell is activated by an extracellular signal; cytosolic levels >10^{-5} ions/nm^3 may be toxic (Alberts et al. 1989), e.g., via apoptosis (Freitas 1999ag, cc).

To transmit an artificial Ca^{++} activation signal into a typical 20 micron cuboidal tissue cell in ~1 millisec, a single nanorobot stationed in the cytoplasm must promptly raise the cytosolic ion count from 480,000 Ca^{++} ions to 24 million Ca^{++} ions, a transfer rate of ~2.4×10^{10} ions/sec which may be accomplished using ~24,000 molecular sorting rotors (Freitas 1999o) operated in reverse, requiring a total nanorobot emission surface area of ~2.4 micron^2. Or, more compactly, pressurized venting or multiple ion diffusion nozzles may be employed (Freitas 1999 cd). Onboard storage volume of ~0.1 micron^3 can hold ~2 billion calcium atoms, enough to transmit ~100 artificial Ca^{++} signals into the cell (e.g., from $CaCl_2$) even assuming no ion recycling. In addition to the amplitude modulation (AM) of Ca^{++} signals noted above, De Koninck and Schulman (de Koninck and Schulman 1998) have

discovered a mechanism (CaM kinase II) that transduces frequency-modulated (FM) Ca^{++} intracellular signals in the range of 0.1–10 Hz. Fine tuning of the kinase's activity by both AM and FM signals (either of which should be readily detected or generated by *in cyto* nanorobots) may occur as the molecule participates in the control of diverse cellular activities.

Similarly, high cytoplasmic calcium levels can destroy mitochondria by opening the mitochondrial "megapore" and activating destructive proteases (Dong et al. 2006), and elevated calcium levels are also expected under conditions of hypoxia, ischemia, and prolonged cold storage during cryopreservation. In such cases, the nanorobot described above can equally effectively extract excess calcium from the cytoplasm – dropping Ca^{++} cytosolic levels from a toxic 10^{-5} ions/nm^3 (~3×10^6 ions/cytosol) to a modest 10^{-7} ions/nm^3 resting-cell level (~3×10^4 ions/cytosol) in ~30 millisec, given a diffusion-limited ion current to the sorting rotor binding sites of ~10^8 ions/sec at 10^{-5} ions/nm^3 falling to ~10^6 ions/sec at 10^{-7} ions/nm^3 (Freitas 1999cp). The nanorobot can perform ~1000 such extractions before it must empty its tanks extracellularly.

23.7 Control of Human Senescence using Medical Nanorobots

Senescence is the process of growing old. Over the next few decades, it seems likely that a variety of purely biotechnological solutions to many of the major types of age-related damage will be found and will enter general therapeutic practice, for example, by following the illustrative SENS program (Section 23.7.1) developed by biogerontologist Aubrey de Grey, or by following other approaches (e.g., Fahy et al. 2010). De Grey's guarded expectation (de Grey 2005a) is that "all the major types of damage will be reversed, but only partly so. In several cases this incompleteness is because the category of damage in question is heterogeneous, consisting of a spectrum of variations on a theme, some of which are harder to repair than others. In the short term it's enough to repair only the easiest variants and thereby reduce the total damage load a fair amount, but in the longer term the harder variants will accumulate to levels that are problematic even if we're fixing the easy variants really thoroughly. Hence, we will have to improve these therapies over time in order to repair ever-trickier variants of these types of damage. I predict that nanotechnological solutions will eventually play a major role in these rejuvenation therapies."

In my view, nanotechnology will play a pivotal role in the solution to the problem of human aging. It is true that purely biotechnological solutions to many, if not most, of the major classes of age-related damage may be found, and even reach the clinic, by the 2020s. However, we have no guarantee that biotechnology will find solutions to *all* the major classes of age-related damage, especially in this timeframe. If treatments for any one of the numerous major sources of aging are not found, we will continue to age – albeit at a slower rate – and possibly with little or no substantial increase in the average human lifespan.

Medical nanorobotics, on the other hand, can undoubtedly offer convenient solutions to all known causes of age-related damage (Section 23.7.1) and other aspects

of human senescence (Section 23.7.2), and most likely can also successfully address any new causes of senescence that remain undiscovered today. Medical nanorobotics is the ultimate "big hammer" in the anti-aging toolkit. Its development – as fast as humanly possible – is our insurance policy against the risk of a failure of biotechnology to provide a comprehensive solution to the problem of aging. Additionally, nanorobotic medicine, once developed, may offer superior treatments for aging, compared to the methods of biotechnology, as measured by a multitude of comparative performance metrics (Section 23.6.1). Finally, if we agree that a 16-year R&D effort costing a total of ~$1B launched today could result in a working nanofactory able to build medical nanorobots by the 2020s (Section 23.4.7), then it seems likely that by the late 2020s or early 2030s these powerful medical instrumentalities would begin to enter widespread clinical use, marking the beginning of the almost certain end to human aging (Section 23.7.1) while also providing cures for most other morbid afflictions (Section 23.6) of the human body.

23.7.1 Nanomedically Engineered Negligible Senescence (NENS)

According to Aubrey de Grey, SENS (Strategies for Engineered Negligible Senescence) (de Grey et al. 2002; de Grey 2006a, 2007a; de Grey and Rae 2007; Methuselah Foundation 2007) is a panel of proposed interventions in mammalian aging that "may be sufficiently feasible, comprehensive, and amenable to subsequent incremental refinement that it could prevent death from old age (at any age) within a time frame of decades." As explained in the foundational SENS paper (de Grey et al. 2002): "Aging is a three-stage process: metabolism, damage, and pathology. The biochemical processes that sustain life generate toxins as an intrinsic side effect. These toxins cause damage, of which a small proportion cannot be removed by any endogenous repair process and thus accumulates. This accumulating damage ultimately drives age-related degeneration. Interventions can be designed at all three stages. However, intervention in metabolism can only modestly postpone pathology, because production of toxins is so intrinsic a property of metabolic processes that greatly reducing that production would entail fundamental redesign of those processes. Similarly, intervention in pathology is a losing battle if the damage that drives it is accumulating unabated. By contrast, intervention to remove the accumulating damage would sever the link between metabolism and pathology, and so has the potential to postpone aging indefinitely. The term 'negligible senescence' (Finch 1990) was coined to denote the absence of a statistically detectable increase with organismal age in a species' mortality rate."

Seven major categories of such accumulative age-related damage have thus far been identified and targeted for anti-aging treatment within SENS. These include: removing extracellular aggregates (Section 23.7.1.1), removing extracellular crosslinks (Section 23.7.1.2), eliminating toxic death-resistant cells (Section 23.7.1.3), restoring essential lost or atrophied cells (Section 23.7.1.4), removing intracellular aggregates (Section 23.7.1.5), replacing mutant mitochondria (Section 23.7.1.6), and correcting nuclear mutations and epimutations (Section 23.7.1.7). As

late as 2007 the prospective SENS treatment protocols (de Grey 2007a; de Grey and Rae 2007; Methuselah Foundation 2007) still lacked any serious discussion of future contributions from nanotechnology, an unfortunate omission which is corrected here by adding nanomedicine (medical nanorobotics) to SENS, obtaining "NENS".

23.7.1.1 Removing Extracellular Aggregates

Extracellular aggregates are biomaterials that have accumulated and aggregated into deposits outside of the cell. These biomaterials are biochemical byproducts with no useful physiological or structural function that have proven resistant to natural biological degradation and disposal. Two primary examples are relevant to the SENS agenda (de Grey 2003, 2006b).

First, there is the acellular lipid core of mature atherosclerotic plaques – which macrophages attempt to consume, but then die when they become full of the inert indigestible material, adding their necrotic mass to the growing plaques. One proposed SENS solution is to administer a bone marrow transplant of new bone marrow stem cells (cells that produce macrophages) that have been genetically reprogrammed to encode a new artificial macrophage phenotype that incorporates more robust intracellular degradation machinery. The resulting enhanced macrophages could then completely digest the resistant plaque material in the normal manner, though the full course of treatment would require months to run to completion and would likely yield only incomplete genetic substitution of stem cell genomes. Using NENS, vasculocytes (Section 23.6.2.3) would completely remove plaque deposits in less than a day, providing immediate vascular clearance and healing the vascular walls. For protection against future plaque development, chromallocytes (Section 23.6.4.3) could be targeted to the entire population of bone marrow stem cells to install the proposed more-robust macrophage phenotype using chromosome replacement therapy, in a thorough treatment also lasting less than a day.

Second, there are amyloid plaques that form as globules of indigestible material in small amounts in normal brain tissue but in large amounts in the brain of an Alzheimer's disease patient (Finder and Glockshuber 2007). Similar aggregates form in other tissues during aging and age-related diseases, such as the islet amyloid (Hull et al. 2004) in type 2 diabetes that crowds out the insulin-producing pancreatic beta cells, and in immunoglobulin amyloid (Solomon et al. 2003). Senile Systemic Amyloidosis or SSA (Tanskanen et al. 2006), caused by protein aggregation and precipitation in cells throughout the body, is apparently (Primmer 2006) a leading killer of people who live to the age of 110 and above (supercentenarians). One proposed SENS solution being pursued by Elan Pharmaceuticals to combat brain plaque is vaccination to stimulate the immune system (specifically, microglia) to engulf the plaque material, which would then be combined with the enhanced macrophages as previously described – although anti-amyloid immunization has not had great success experimentally (Schenk 2002; Patton et al. 2006). In NENS, amyloid binding sites could be installed on the external recognition modules of tissue-mobile microbivore-class scavenging nanorobots (Section 23.6.2.1),

allowing them to quickly seek, bind, ingest, and fully digest existing plaques throughout the relevant tissues, in the manner of artificial mechanical macrophages. Chromallocytes could again be targeted to phagocyte progenitor cells to install the more robust macrophage phenotype to provide continuing protection against future plaque development.

Among the most promising investigational anti-amyloid therapies for Alzheimer's disease (Aisen 2005) is another potential SENS treatment for brain amyloid using anti-amyloid plaque peptides – one 5-residue peptide has already shown the ability, in lab rats, to prevent the formation of the abnormal protein plaques blamed for Alzheimer's and to break up plaques already formed (Soto et al. 1998), and to increase neuronal survival while decreasing brain inflammation in a transgenic mouse model (Permanne et al. 2002). However, a major challenge to the use of peptides as drugs in neurological diseases is their rapid metabolism by proteolytic enzymes and their poor blood-brain barrier (BBB) permeability (Adessi et al. 2003). In a NENS treatment model, a mobile pharmacyte-class nanorobot (Section 23.6.3.2) could steer itself through the BBB (Freitas 2003aa); release an appropriate engineered peptide antimisfolding agent (Estrada et al. 2006) in the immediate vicinity of encountered plaques so as to maintain a sufficiently high local concentration (Section 23.6.4.8) despite degradation; re-acquire the agents or their degradation products after the plaque dissolves; then exit the brain via the same entry route. Tissue-mobile microbivore-class devices could also be used to fully digest the plaques if it is deemed acceptable to ignore possible resultant localized deficits of normal soluble unaggregated amyloid-beta peptides. Nanorobots operating in the brain must be designed to accommodate the tight packing of axons and dendrites found there (Section 23.7.2(5)(a)).

23.7.1.2 Removing Extracellular Crosslinks

While intracellular proteins are regularly recycled to keep them in a generally undamaged state, many extracellular proteins are laid down early in life and are never, or only rarely, recycled. These long-lived proteins (mainly collagen and elastin) usually serve passive structural functions in the extracellular matrix and give tissue its elasticity (e.g., artery wall), transparency (e.g., eye lens), or high tensile strength (e.g., ligaments). Occasional chemical reactions with other molecules in the extracellular space may little affect these functions, but over time cumulative reactions can lead to random chemical bonding (crosslinks) between two nearby long-lived proteins that were previously unbonded and thus able to slide across or along each other (Methuselah Foundation 2007). Such crosslinking in artery walls makes them more rigid and contributes to high blood pressure.

In the SENS strategy (de Grey 2003, 2006b), it is theoretically possible to identify chemicals that can selectively dissociate crosslink bonds without breaking any other bonds, because many crosslink bonds have unusual chemical structures not found in proteins or other natural biomolecules. Some of these crosslink bonds may be unstable enough to be readily breakable by drugs, such as alagebrium chloride (aka. PMTC, ALT-711) which appeared to break one subset of glucose crosslinks

(sugar-derived alpha-diketone bridges) in clinical trials (Bakris et al. 2004), but other crosslink bonds (e.g., acid-labile glucosepane (Lederer and Bühler 1999) and K2P (Cheng et al. 2004), and the highly stable pentosidine (Sell et al. 1991)) are probably too stable to be breakable by simple catalysis. SENS research proposals include: (1) finding new or synthetic deglycating enzymes that can couple the link-breakage to the hydrolysis of ATP to ADP (the most common power source inside cells), requiring the enzyme to shuttle back and forth across the cell membrane to acquire fresh ATP for each link-breakage cycle as there is very little ATP in the extracellular matrix; (2) engineering single-use link-breaking molecules analogous in action to the DNA repair protein MGMT which reacts with a stable molecule (DNA) but thereby inactivates itself (by transferring methyl and alkyl lesions from the O6 position of guanine on damaged DNA to a cysteine in its own structure (Pieper 1997)); or (3) increasing the rate of natural ECM turnover, taking care to avoid "dire side-effects such as hemorrhage from leaky blood vessels as collagen molecules are removed and replaced" (Furber 2006).

The NENS strategy proceeds similarly but more safely, using nanorobots as the delivery vehicle for the link-breaking molecules. In the first scenario, a population of ~10^{12} (1 terabot) mobile pharmacytes would transverse the extracellular matrix in a grid pattern, releasing synthetic single-use deglycating enzymes (perhaps tethered (Craig et al. 2003; Holmbeck et al. 2004) to energy molecules, e.g., ATP) into the ECM to digest cross-linkages, then retrieving dispensed molecules before the nanorobot moves out of diffusive range. As an example, human skin and glomerular basement membrane (GBM) collagen has ~0.2 glucosepane (MW ~500 gm/mole) crosslinks per 100,000 kD strand of collagen in normally crosslinked aging tissue (Sell et al. 2005), indicating ~2×10^{18} glucosepane crosslinks in the entire human body which will require a very modest whole-body treatment chemical scission energy of ~0.2 joule per each ATP-ADP conversion event (~0.5 eV) required to energize cleavage of individual crosslink bonds. Each nanorobot would contain ~2×10^6 enzyme molecules in a ~1 micron^3 onboard tank and would travel at ~3 micron/sec through ECM, releasing and retrieving enzymes in a ~10 micron wide diffusion cloud over a ~100 sec mission duration, with 10 successive terabot waves able to process all ~32,000 cm^3 of ECM tissue in the reference 70 kg adult male body in a total treatment time of ~1000 sec. Only 1 of every 10 enzymes released and retrieved are discharged by performing a crosslink bond scission; the rest are recovered unused. This treatment would likely be complete because full saturation of the targeted tissue volume can probably be achieved via diffusion, though some enzyme molecules may exit the diffusion cloud and become lost – lost molecules that must produce no side effects elsewhere or must be safely degradable via natural processes. In the second scenario, assuming ~10^{19} collagen fibers in all ECM and allowing ~10 sec for a nanorobot to find and examine each fiber (thus removing one crosslink every ~50 sec), then ~10^{14} nanorobots (~0.3% by volume of ECM tissue) using manipulators with enzymatic end-effectors could patrol ECM tissues, seeking out unwanted crosslink bonds and clipping them off, processing ~1 cm^3/min of crosslinked tissue and finishing the entire body in ~22 days. Enzymatically active components remain tethered and cannot be lost, reducing side effects to

near-zero, but there may be some tight spaces that cannot easily be reached by the manipulator arms, possibly yielding an incomplete treatment. Further study is needed to determine the optimal combination of these two strategies.

23.7.1.3 Eliminating Toxic Death-Resistant Cells

A third source of age-related damage occurs from the accumulation of unwanted death-resistant cells that secrete substances toxic to other cells. These toxic cells are of several types: (1) fat cells (i.e., visceral adipocytes, which promote insulin resistance and lead to type 2 diabetes), (2) senescent cells (which accumulate in joint cartilage, skin, white blood cells, and atherosclerotic plaques, cannot divide when they should, and secrete abnormal amounts of certain proteins), (3) memory cytotoxic T cells (which can become too numerous, crowding out other immune cells from the useful immunological space, and which frequently become dysfunctional), (4) immune cells that have come to be hostile to endogenous antigens (autoimmune T and B cells), and (5) certain other types of immune cells which seem to become dysfunctional during aging (e.g., inability to divide, or immunosenescence) (de Grey 2006b; Methuselah Foundation 2007; Aspinall 2010).

There are several SENS strategies for reducing the number of senescent cells in a tissue: (1) conventional surgery, such as liposuction, wherein excess visceral fat tissue is simply cut out (e.g., eliminating pathology in diabetic rats (Barzilai et al. 1999)); (2) targeted apoptosis or cell suicide (Freitas 1999ag), in which only the chosen cells are induced to kill themselves in an orderly and non-necrotic manner (e.g., via immunotherapy in which immune cells would be sensitized to a diagnostic protein that is highly expressed only in the targeted cell type, or via somatic gene therapy (Campisi 2003) that would insert a suicide gene encoding a highly toxic protein controlled by a promoter that is activated only by the highly expressed diagnostic protein); and (3) de-senescing senescent cells by reversing the senescent phenotype (Beauséjour et al. 2003).

In NENS, tissue-mobile microbivore-class nanorobots (Section 23.6.2.1) would quickly and completely remove all unwanted cells, wherever located in the body, either by digesting them into harmless byproducts in situ or by sequestering their contents and transporting the compacted biomaterial out of the body for external disposal. Toxic cells could also be de-senesced using chromallocytes to wholly replace their nuclear genome with newly manufactured chromosomes (Section 23.6.4.3); alternatively, all DNA could be extracted from each toxic cell and the genome-free cell could then be flagged for natural macrophage removal (Freitas 1999cq) following the "neuter and release" protocol (Freitas 1999cr).

23.7.1.4 Restoring Essential Lost or Atrophied Cells

Cell depletion is another major source of age related damage (Methuselah Foundation 2007) that involves cell loss without equivalent replacement, most commonly in the heart, the brain, and in muscles. Missing cells leave gaps in tissues which may be filled by: (1) enlargement of adjacent similar cells (e.g., heart),

(2) invasion by dissimilar cells or fibrous acellular material (e.g., heart, brain), or (3) general tissue shrinkage (e.g., muscle).

Three SENS strategies to reverse cell depletion have been proposed (Methuselah Foundation 2007). The first two methods involve the natural stimulation of cell division by exercise (difficult in some muscles) or the injection of growth factors to artificially stimulate cell growth (Chen et al. 1995). Both methods may be of limited utility for normal dividing cells which may be robustly preprogrammed to avoid dividing excessively as a defense against cancer, but should be of greater utility in the case of stem cells, given that, for instance, marrow cells from older mice readily repopulate the irradiation-depleted marrow of young mice at least five times sequentially (Harrison and Astle, 1982) supporting the hypothesis that stem cells do not age, or age only very slowly. The third strategy would employ stem cell therapy to introduce new whole cells that have been engineered into a state where they will divide to fix the tissue even if cells already present in the body aren't doing so (Armstrong and Svendsen 2000).

The NENS approach starts with the manufacture of any needed replacement whole living cells, either very quickly with ideal quality control using external clinical cell mills (Section "Tissue Printers, Cell Mills and Organ Mills") or several orders of magnitude slower with inferior quality control using some variant of conventional mammalian cell reactors (Nelson and Geyer 1991). These replacement cells may include manufactured pluripotent stem cells. Nanosurgery is then employed to deliver the new cells to the repair site to assist the activities of vasculocytes (Section 23.6.2.3) and related nanorobots capable of controlled cell herding in vascular, ECM, or other cell-depleted tissue spaces. For example, a 1 cm^3 volume of 125 million 20-micron tissue cells, arranged in planar 10-cell slabs moving perpendicular to the slab plane through a tube, could be imported at ~1 m/sec through a 10-cm long nanosyringoscope (Section "Nanosyringoscopy") with a 100 micron inside diameter (possibly coated with mechanical cilia to facilitate efficient transport) to virtually anywhere inside the human body in ~250 sec (~4 min). A modest-sized array of 1000 safe and painless microneedles (Cormier et al. 2004; Flemming et al. 2005; Coulman et al. 2006; Nordquist et al. 2007) having a total ~10 mm^2 penetration cross-section for the array could transport ~1500 cm^3 of cells – the volume of the human liver, one of our largest organs – into the body during a ~6 minute transfer. A second nanosyringoscope can export a matching volume of body fluid or comminuted pathological tissue to precisely maintain conservation of volume/mass, if necessary. Arrival of conventionally vein-infused self-targeting stem cells at their designated destinations will take many orders of magnitude longer, and will not be 100% reliable and complete, as compared to nanosyringoscopy.

23.7.1.5 Removing Intracellular Aggregates

Intracellular aggregates are highly heterogeneous lipid and protein biomaterials that have accumulated and aggregated into clumps inside of the cell (Methuselah Foundation 2007). These biomaterials are normal intracellular molecules that have

become chemically modified so that they no longer work and are resistant to the normal processes of degradation. Intracellular aggregates most commonly accumulate inside lysosomes, organelles that contain the most powerful degradation machinery in the cell. But if the lysosomes become congested and engorged, the cell will stop working properly – crudely analogous to a house whose toilets have all backed up. Cells in the heart and in the back of the eye, motor neurons and some other nerve cells, and white blood cells trapped within the artery wall appear most susceptible – intracellular aggregates have been associated with atherosclerosis (Brown et al. 2000) (the formation of plaques in the artery wall, which eventually occlude the vessel or calve material, causing heart attacks or strokes) and appear to be a contributing factor in several types of neurodegeneration (where the aggregates accumulate elsewhere than in the lysosome) and in macular degeneration (Reinboth et al. 1997) (the main cause of blindness in the old).

The proposed SENS strategy (de Grey et al. 2005; Methuselah Foundation 2007; de Grey 2006c) is to give all cells extra enzymes (such as microbial hydrolases found in natural soil bacteria and fungi) that can degrade the relevant biomaterial, or other accessory microbial proteins such as transporters to restore lysosomal acidity. The lack of such exogenous enzymes can be regarded as a genetic deficiency that results in pathological intracellular storage disease (Section 23.6.4.5), so the SENS treatment would be analogous to replacing a natural lysosomal enzyme for which patients are congenitally deficient as in enzyme replacement therapies (ERT). The ERT treatment can be directed to all cells as a complete whole-body gene therapy, or it can be directed only to modified stem cells via a bone marrow transplant that produces enhanced macrophages (Section 23.7.1.1), a stopgap approach that still allows the intracellular storage disease to progress to full senescence in somatic cells which are then removed and successfully digested by the enhanced macrophages. Possible difficulties with both approaches include: (1) inactivity or toxicity of microbial genes introduced into mammalian cells, (2) rapid degradation of the new microbial enzymes by lysosomal proteases whose normal function is to destroy other proteins, (3) immune rejection of microbial enzymes or proteins when cells expressing or containing them are attacked by lymphocytes, and (4) the inability of therapeutic enzymes in ERT to cross the blood-brain barrier in patients with cerebral neuropathies; though it is believed that further research can overcome all these problems (de Grey et al. 2005).

The proposed NENS strategy is twofold. First, storage-diseased lysosomes and other non-lysosomal intracellular aggregates could either be digested to harmless effluents in situ by cytopenetrating microbivores (Section 23.6.2.1) or by appropriate digestive enzymes temporarily injected into organelles, or could be loaded into onboard storage tanks of chromallocyte-class nanorobots and transported intact out of the patient's body for external disposal. This method could also effectuate cell-by-cell transplants of healthy lysosomes. Second, chromallocytes (Section 23.6.4.3) could install revised genomes in every cell in the human body, with the new chromosomes expressing the novel microbial-derived lysogenic enzymes and other requisite exogenous accessory proteins borrowed from the SENS program, assuming future research can validate the use of these or similar proteins.

23.7.1.6 Replacing Mutant Mitochondria

Mitochondria are the principal source of chemical energy in the cell, metabolizing oxygen and nutrients to carbon dioxide and water, producing energy-charged molecules of ATP that provide power for many important intracellular biochemical processes. Unlike other organelles, mitochondria have their own DNA that is susceptible to mutation, causing the mutated mitochondrion to malfunction leading to respiration-driven (i.e., oxidative damage-mediated) aging (Harman 1972; de Grey 1999, 2005b).

The principal SENS stopgap strategy (Methuselah Foundation 2007; de Grey 2000, 2005c) depends on the fact that of the ~1000 proteins present in the mitochondrion, only 13 (totaling under 4000 amino acids) are encoded by its own DNA. All the rest are encoded in the cell's nuclear DNA and are manufactured in the cytosol, then transported through the mitochondrial membrane wall by a complicated apparatus called the TIM/TOM complex (Rehling et al. 2001). By adding the genes encoding the unique 13 mitochondrial proteins to the better-protected nuclear chromosome content (Zullo et al. 2005), these proteins are anticipated to be produced when the mitochondria fail to do so and will be made to be imported through the organelle wall (Gearing and Nagley 1986), thus maintaining adequate energy-producing function even in mutated organelles. Nondividing cells such as muscle fibers and neurons accumulate mutant mitochondria most severely, so these cells most urgently need gene therapy to insert the supplementary genes. This is only a stopgap strategy because the mitochondria are not really "cured" of their pathology: new untreated cell pathologies hypothetically could appear if (1) the mutated mitochondrial DNA is left in place and the mutated DNA eventually comes to produce not just dysfunctional but actually harmful proteins (Baracca et al. 2007), or (2) the mutated mitochondrial DNA involves a dosage-sensitive gene with the disease phenotype resulting from multiple copies of a normal gene (Murakami et al. 1996). Other stopgap SENS strategies, also not amounting to complete or permanent cures, have been proposed, such as the injection of an antilipolytic agent to stimulate macroautophagy (the cell repair mechanism responsible for the disposal of excess or altered mitochondria under the inhibitory control of nutrition and insulin) in a presumably small number of the most severely injured mitochondria (Donati et al. 2006).

There are many possible NENS strategies for dealing with mutant mitochondria. First, chromallocytes (Section 23.6.4.3) could deliver into the nucleus of each cell in the human body a new set of manufactured chromosomes that incorporate genes encoding the 13 unique mitochondrial proteins, thus comprehensively effectuating the (incomplete) SENS proposal in a ~7 hour therapy for a single large organ such as liver or up to ~53 hours for a continuously-performed whole-body CRT procedure (Freitas 2007). Second, chromallocytes could employ a revised CRT treatment in which mitochondrial DNA is removed from each intracellular organelle in each cell and replaced with corrected versions of mtDNA (Freitas 2007), a more time-consuming approach. Third, replacement whole mitochondria containing non-mutated DNA could be manufactured in external clinical cell mills (Section "Tissue

Printers, Cell Mills and Organ Mills"), then delivered into the cytoplasmic compartment of target cells by chromallocyte-class nanorobots. Short-lifetime marker molecules (Freitas 2007) would distinguish new mitochondria from old, facilitating subsequent deportation of the old from the cell using exiting (now-empty) nanorobots, leaving behind only the new and also ensuring the removal of any mitophages (Sassera et al. 2006) that might be present, effectuating an all-cell mitochondrial transplant operation. Finally, replacement mitochondria re-engineered to contain no endogenous DNA could be installed in all cells by chromallocytes, after other chromallocytes have replaced nuclear DNA with new DNA containing the missing mitochondrial DNA, a treatment that would constitute a complete and permanent cure for inside-mitochondrion mutation. (Nuclear mutations continue to occur, and it has been claimed by some (Hayashi et al. 1994) that the mutation rate of genes encoding mitochondrial proteins might be higher in the nucleus than in the mitochondria, in which case the aforementioned strategy would be a way of greatly delaying but not permanently curing the problem of mitochondrial mutation.)

23.7.1.7 Correcting Cancer, Nuclear Mutations and Epimutations

Despite a sophisticated DNA self-repair system, chromosomes in the cell nucleus slowly acquire two types of irreversible age-related damage. First, there can be mutations, which are changes to the DNA sequence. Second, there can be epimutations, which are changes to the chemical decorations of the DNA molecule (e.g., DNA methylation) or to the histone modifications, that control DNA's propensity to be decoded into proteins, collectively representing the "epigenetic state" of the cell. (In a given patient, different cell types have the same DNA sequence but different epigenetic states.) When DNA damage of these types leads to uncontrolled rapid cell replication, the result is rapid tumor growth, aka. cancer (Section 23.6.2.2), and other loss of gene function unrelated to cancer can also occur. DNA damage and mutation may also be a significant cause of cell toxicity (Section 23.7.1.3) and cell depletion (Section 23.7.1.4) because cells can either commit suicide or go into a senescent non-dividing state as a pre-emptive response to DNA damage that stops it from developing into cancer (Methuselah Foundation 2007).

Traditional biotechnology knows no easy way to correct in situ large numbers of randomly occurring mutations or epimutations in the DNA of large numbers of randomly chosen cells. Consequently the SENS approach uses a stopgap strategy directed only at cancer (which is proposed to be the principal negative impact of mutated nuclear DNA on health and aging (de Grey 2007b)) via "Whole-body Interdiction of Lengthening of Telomeres" or WILT (de Grey et al. 2004; de Grey 2005d, 2010).

Here's how the SENS program of WILT would work. Telomerase (Autexier and Lue 2006) is a mainly nucleus-resident enzyme that acts to increase the length of telomeres, the endcaps of chromosomes, but is not normally expressed in most cells. Telomeres normally shorten at each cell division (accelerating after age 50 (Guan et al. 2007)), eventually resulting, after enough divisions, in chromosome dysfunction and cell senescence, a natural defense to runaway cancer. Cancer cells

activate telomerase expression which removes this natural defense. WILT would forcibly reimpose the natural defense against cancer by totally eliminating the genes for telomerase and ALT (an alternative non-telomerase system for lengthening telomeres (Bryan et al. 1997)) from all cells that are able to divide. WILT would provide a permanent genetic alteration – not just a temporary improvement using drug-mediated telomerase inhibition as is currently being widely investigated (Cunningham et al. 2006) – by using gene deletion performed by comprehensive gene therapy (de Grey et al. 2002). WILT will require: (1) highly accurate gene targeting to delete the telomerase genes in tissues that don't rely on stem cells; (2) repopulating stem cells in the blood, gut, skin and any other tissues in which the stem cells divide a lot, with therapeutic infusions about once a decade (based on the apparent duration of the telomere reserve of neonatal stem cells judging (Methuselah Foundation 2007) from the age of onset of dyskeratosis congenita, a disease associated with inadequate telomere maintenance); and (3) growing engineered replacement stem cells whose telomeres have been restored in the laboratory, but which have no telomerase or ALT genes of their own. Also, cells already present in the body either must be destroyed without killing the engineered cells (in the case of stem cells for rapidly renewing tissues like the blood) or must have their telomerase and ALT genes deleted in situ (in the case of division-competent but normally quiescent cells, e.g., liver, glia) (Methuselah Foundation 2007). All this seems possible but represents a rather aggressive research agenda.

In NENS, chromallocytes (Section 23.6.4.3) could easily implement WILT, but why bother with a stopgap approach when nanorobots can fully address all nuclear mutations and epimutations, as well as cancer? Of course, cells can easily be killed by chromallocytes that extract nuclear DNA without replacing it (Freitas 1999cr), or by using cytocidal devices dramatically simpler than chromallocytes. But the optimal NENS solution to nuclear mutation and epimutation is to employ chromallocytes performing chromosome replacement therapy or CRT (Section 23.6.4.3) to replace all of the randomly damaged chromosomes with completely undamaged newly manufactured chromosome sets (Freitas 2007), in all cells of the body. As another benefit, CRT will automatically repair any somatic mutations in tumor-suppression genes, thus reinvigorating other components of the body's natural defenses against cancer – a repair that is wholly impractical using conventional biotechnology. As yet another benefit, the installed new chromosome sets can be manufactured with their telomeres re-extended to full neonatal reserve length, essentially "rolling back the clock" to birth on chromosome age and effectively implementing comprehensive cellular genetic rejuvenation (Section 23.7.2).

Because biology is highly complicated, the earliest implementations of nanorobotic CRT (perhaps in the 2030s) need not depend on knowing which DNA sequences and epigenetic states are "correct" (in the ideal functional sense), but merely on knowing which ones appear "normal" for a particular patient, with chromallocytes then reinstalling whatever is normal for each cell type. Normal can be measured by widespread sampling of DNA in the patient's native cells and statistically averaging out the observed random variations (Freitas 2007). In later implementations of CRT, we will know enough about the ideal epigenetic state of

all cell types to be able to implement it just as precisely as we will be able to edit native DNA sequences or delete foreign sequences, using the same nanorobots.

23.7.2 Nanorobot-Mediated Rejuvenation

SENS or other fundamental approaches to the biology of aging, and more powerfully nanomedical implementations thereof, will give physicians the tools to eliminate all age-related damage (Section 23.7.1), and medical nanorobotics will provide comprehensive treatments for all common causes of human morbidity (Section 23.6). In many cases, a one-shot restoration of cells to their pristine undamaged state can re-establish the ability of those cells to maintain molecular homeostasis (Wiley 2005) and to resume normal self-healing activities in response to future cell damage that may occur. But there will still remain a residuum of ongoing cell damage that cells, tissues, and organs cannot heal on their own unless they are given novel capabilities for self-repair, or are given new engineered biochemical pathways that avoid creating the damage. perhaps by augmenting and reprogramming the human genome. Until and unless we implement these augmentations, injuries that the body is incapable of repairing on its own will resume their natural rate of accumulation, allowing natural aging to reappear. Periodic rejuvenative treatments will therefore be required to reverse this accumulating new damage to the body.

Important components of such periodic rejuvenative treatments may include, among other things:

(1) *All-Cell Genetic Renatalization*. Over time, new mutations and epimutations in the nuclear genome will continue to recur, and telomeres will resume growing shorter as cells continue normal division. Chromallocytes (Section 23.6.4.3) would deliver to all cells new mutation-free chromosome sets, thus periodically "rolling back the clock" to zero chromosome age (while leaving developmental controls in adult mode) and effectively implementing comprehensive genetic cellular rejuvenation (Section 23.7.1.7). The new error-free chromosome sets will be manufactured with their telomeres re-extended to full neonatal reserve length.
(2) *Whole-Body Cytological Maintenance*. Like an old house or car, cells and their immediate environs will need periodic maintenance to keep them in showroom condition. Primarily this would involve a NENS (Section 23.7.1) sweep of every cell in the body, eliminating intracellular aggregates and extracellular aggregates and crosslinks, and removing or replacing cells within tissues or organelles within cells as required to maintain optimal tissue and organ health. It would also include repairing errant or missing intercellular connections and other malformations of the extracellular matrix other than simple crosslinking, a category of tissue damage largely ignored by SENS, using a combination of fibroblast cytocarriage to lay down fresh fiber (Section 23.6.4.4) and surgical nanorobots (Section "Endoscopic Nanosurgery and Surgical Nanorobots")

with capabilities similar to dermal zippers (Section 23.6.3.3) to rebuild and reconstruct the ECM as needed. This kind of ECM damage may occur during scarring, burning or freezing injuries, which also may pull cells out of their proper positions thus requiring mechanical repositioning. Cell membranes could be edited to remove unwanted foreign molecules or mechanisms, and poisonous chemicals and heavy metals can be extracted. In this manner, cells and the matrix surrounding them could be restored to their ideal youthful state, effectively implementing comprehensive structural and functional cellular rejuvenation.

(3) *Whole-Body Anatomical Maintenance*. Patient anatomy could be mapped and recorded down to the cellular level, then compared to the ideal state desired by the patient (in consultation with his physician), then brought into compliance with the patient's wishes by the addition or removal of specific cells, tissue masses, or even organs via nanosurgery (Section 23.6.3.5). Many age-related cosmetically undesired changes in human appearance are completely non-pathological and reflect only an extension of normal cell growth processes that could be nanorobotically blocked or reversed, e.g., by cell removal (Section 23.7.1.3). Examples of such changes include the enlarged noses and ears in older people that arise from slow growth that proceeded unimpaired from birth until old age. Changes in chin prominence and other remodeling of the skull probably fall into the same category. Pathological anatomical damage must also be repaired. Physical trauma is an obvious source of new anatomical damage that could be repaired via medical nanorobotics (Section 23.6.3), and foreign-body granulomas, wherever situated, should also be excised. Comprehensive inspection and reconditioning of the human vascular tree by vasculocytes (Section 23.6.2.3) might be an important part of a periodic rejuvenation regimen, virtually eliminating all possibility of cardiovascular disease and brain damage due to stroke. Another age-related pathology of the ECM occurs when aging fibroblasts begin producing collagenase instead of collagen (Quan et al. 2006), tearing down the ECM and causing, for example, faces to wrinkle, sag, and become softer (because the ground substance that holds the face together is being torn apart), not stiffer as would be expected if facial aging was due to crosslinking. Rejuvenating an old face might therefore require in situ redeposition of collagen and elastin fibers unless this is found to occur automatically after aging fibroblasts have been removed (Section 23.7.1.3), new fibroblasts are installed (Section 23.7.1.4), and chromallocytes have reset the telomere lengths (Section 23.7.2(1)) of dermal cells and fibroblast precursor cells (Friedenstein et al. 1976).

(4) *Systemic Deparasitization*. Analogously to computer systems, human patients should be periodically "debugged" of unwanted parasitic entities present within the body. Parasitic entities may be present at all different levels of biological organization. At the molecular level, parasitic molecules such as prions and viroids should be eliminated (Section 23.6.4.5). At the genetic level, recent or ancient retroviral insertions into our DNA should be edited out using chromallocytes (Section 23.6.4.3), except for those known to have some beneficial effect

because we've adapted to their presence. We should also periodically clean out "transposable elements" or transposons (including retrotransposons) or "jumping genes" that may contribute to aging by inserting into the middle of other genes and deactivating them. Cancer cells, cancer cell microaggregates, and cancerous tumors are parasitic at the cellular level, and could be detected by periodic scans, and then excised (Section 23.6.2.2). A great variety of microbiological parasitic entities should be deleted from the body, most notably acute viral and bacterial infections (Section 23.6.2.1) but also including granuloma-encased tuberculosis bacteria and other latent biotic reservoirs such as those that produce periodic outbreaks of herpes, shingles, etc. later in life, and any nanorobotic intruders (Section 23.6.4.5). Nonsymptomatic infestations of commensal, amensal, or other endoparasites including protozoa and worms may also be removed using medical nanorobots.

(5) *Neural Restoration*. Adult neurons generally do not reproduce and cannot replace themselves once destroyed. Early workers in the 1950s (Brody 1955) attempted the first assessment of the long-term rate of natural attrition of brain cells. Losses ranged from none at all to very many in various parts of the organ, but the brainwide average loss was ~100,000 neurons per day, a rate consistent with loss of all brain cells (in some parts of the organ) over a period of about 250–350 years. More recent work (Lopez et al. 1997) has confirmed a similar ~3%/decade cell loss rate in some areas of the brain. A sufficient loss of neural connectivity or infrastructure from this source, or from physical brain trauma, would constitute effective creeping brain death. Several possible approaches to neural restoration have been identified.

(a) *Prevent or delay random cell death* within the neuronal network by using nanogerolytic treatments on individual cells, keeping each cell healthy and avoiding DNA mutations and microdeletions (Kamnasaran et al. 2003) via nanorobot-mediated CRT (Section 23.6.4.3). Note that the brain contains only 5% extracellular space and consists for the most part of densely-packed axons and dendrites with virtually no gaps between them, so neuron-targeted motile chromallocytes will often transit plasma membranes between neighboring cells rather than intercellular spaces. Because cell bodies containing the nucleus may be relatively far apart, these specialized nanorobots must be engineered either to migrate inside the larger-diameter axons without ruining neural function or external to the axons without disturbing the local ionic environment. This may require active nanorobotic monitoring and localized remediation of the ECM chemical environment (analogous to Section 23.6.4.8) during nanorobot locomotion, given that the minimal extracellular space in the brain controls the concentrations of extracellular ions that cross and re-enter the cell membrane during and after action potentials.

To effectuate neuronal CRT, one approach might be to block apoptosis to allow more time for DNA repair, then to osmotically expand the extracellular space on a local basis to allow relatively large nanorobotic devices to migrate wherever they need to go. Considerable expansion may be tolerable: Smith's classic

hamster freezing experiments (Smith et al. 1954; Lovelock and Smith 1956; Smith 1965) showed that >60% of the water in the brain can be converted into extracellular ice without apparent brain damage, a distortion far in excess of what would be needed for nanorobot traffic. Recent unpublished observations by G. Fahy (personal communication, 2008) at 21st Century Medicine show that when ice forms in the brain even at low temperatures in the presence of cryoprotectants, neurons and nerve processes are neatly packaged and are not torn apart, supporting the idea that the extracellular space can be significantly locally expanded without lasting harm. The migration of newly-generated neurons through the brain provides additional evidence that the organ can tolerate significant local distortion of the extracellular space. For example, neurogenesis in the hippocampus is followed by neurons or their precursors migrating out of the hippocampus over large distances to other parts of the brain (Ehninger and Kempermann 2008), a mechanical process that is normal and apparently well tolerated, and microglial cells (the immune system phagocytes in the brain) have been observed (via two-photon imaging of mammalian neocortex) to have extremely motile processes and protrusions (Nimmerjahn et al. 2005).

(b) *Offset brain cell losses* by inducing compensatory regeneration and reproduction of existing neurons as in situ replacements, i.e., by stimulating endogenous neurogenesis (Tatebayashi et al. 2003). Successful neuron re-growth in response to growth factors, with associated cognitive benefits, has been reported in rats (Chen et al. 1995), and self-assembling peptide nanofiber scaffolds can create a permissive environment for axons to regenerate through the site of an acute injury and also to knit the brain tissue together, as demonstrated by the return of lost vision in one animal model (Ellis-Behnke et al. 2007).

(c) *Replace dysfunctional neurons* by infusing stem cells, allowing normal memory-reinforcing cognitive processes to provide continuous network retraining. *Ex vivo*-cultured neural stem cells have been induced to differentiate and replace lost neurons after injection into the brain (Armstrong and Svendsen 2000) and dead neurons can be replaced by introducing stem or precursor cells that differentiate appropriately (Sugaya and Brannen 2001), but patterned neuronal networks, once thoroughly disrupted to the point of serious information loss, cannot be restored by stem cells or any other means as per SENS.

(d) *Rebuild neural tissue* using a combination of tissue mills (Section "Tissue Printers, Cell Mills and Organ Mills") and nanosurgery (Section "Endoscopic Nanosurgery and Surgical Nanorobots") following blueprints assembled from a complete brain state map acquired via comprehensive in vivo nanorobotic brain scans (Fig. 23.27). Maps of neural networks and neuron activity states could be produced by nanorobots positioned outside each neuron (Freitas 1999cf), after they have passed into the brain through the BBB (Freitas 2003aa), using tactile topographic scanning (Freitas 1999co) to infer connectivity along with non-invasive neuroelectric measurements (Freitas 1999cf) including, if necessary, direct synaptic monitoring and recording (Freitas 1999cs). The key challenge in making such scans feasible is obtaining the necessary bandwidth inside the body, which should be available using an in vivo optical fiber network (Freitas

This figure will be printed in b/w

Fig. 23.27 Artist's conception of a neuron inspection nanorobot; image courtesy of Philippe van Nedervelde, © 2005 E-spaces.com. Used with permission

1999cg) distributed via nanocatheters (Section "Endoscopic Nanosurgery and Surgical Nanorobots"). Such a network could handle 10^{18} bits/sec of data traffic, capacious enough for real-time brain-state monitoring. The fiber network would have a 30 cm^3 volume and generate 4–6 watts of waste heat, both small enough for safe installation in a 1400 cm^3 25-watt human brain. Signals travel at most a few meters at nearly the speed of light, so transit time from signal origination at neuron sites inside the brain to the external computer system mediating the scanning process are ~0.00001 millisec which is considerably less than the minimum ~5 millisec neuron discharge cycle time. Neuron-monitoring chemical sensors (Freitas 1999ci) located on average ~2 microns apart can capture relevant chemical events occurring within a ~5 millisec time window, the approximate diffusion time (Freitas 1999ch) for, say, a small neuropeptide across a 2-micron distance. Thus human brain state monitoring can probably be "instantaneous", at least on the timescale of human neural response, in the sense of "nothing of significance was missed."

(e) *Avoid plethomnesia.* One theoretical additional health risk at very advanced calendar ages is that the total data storage capacity of the brain might eventually be reached. At this point, either no new memories could be stored or old memories would have to be overwritten and thus destroyed, giving rise to a hypothetical mental pathology involving forgetfulness most properly termed "plethomnesia" (from Gr. *plethos* (fullness, too full) + *mnasthai* (to remember, memory)). The data storage capacity of the human brain has been estimated using structural criteria to range from 10^{13}–10^{15} bits assuming ~1 bit per synapse (Cherniak 1990, Tipler 1994), or using functional criteria as 2.2×10^{18} bits for the information contained in a normal lifetime of experience (brain inputs) (Schwartz 1990; Tipler 1994; Baldi 2001) to ~10^{20} bits based on the accumulated total of all neural impulses conducted within the brain during a normal lifetime (von Neumann 1958). Given that experimental studies suggest a normal-lifetime limit for consciously recoverable data of only ~200 megabytes (~1.6×10^9 bits) (Landauer

1986), it appears that the human brain may have significant amounts of untapped reserve memory capacity. However, should plethomnesia occur it might most effectively be cured by employing nanomedicine via cognitive neural prosthetic implants (Berger and Glanzman 2005; Pesaran et al. 2006; Schwartz et al. 2006) linked through nanotechnology-based neural interfaces (Patolsky et al. 2006; Mazzatenta et al. 2007) to nanotechnology-based high-density read/write memory caches (Green et al. 2007; Blick et al. 2007), e.g., "brain chips".

Using perhaps annual nanorobot-mediated rejuvenative treatments such as the above, along with some occasional major repairs, it seems likely that all natural accumulative damage to the human body could be identified and eliminated on a regular basis. The net effect of these interventions will be the continuing arrest of all biological aging, along with the reduction of current biological age to whatever age-specific phenotype is deemed cosmetically desirable by the patient, severing forever the link between calendar time and biological health and appearance.

23.7.3 Maximum Human Healthspan and the Hazard Function

If all age-related causes of death and ill-health could be eliminated by medical nanorobotics and if the remaining non-medical causes of death are distributed randomly across all calendar ages, this gives a constant rate of death R_{mort} during any increment of time. The number of survivors N(t) at time t, starting from an initial population N_{pop} at time t = 0, is estimated, using the standard exponential formula for an interval-constant decay rate, as $N(t) = N_{pop} \exp(-R_{mort}\, t)$. The median healthspan T_{half} is then given by a simple half-life formula (which is generally applicable to any process having a constant event rate): $T_{half} \sim \ln(2) / R_{mort}$, where R_{mort} is the cumulative death rate from all sources, in deaths/person-year. In this case, R_{mort} is the sum of five principal components:

(1) the fatal accident rate, including motor vehicle (presently 44% of the total) and all other causes (3.62×10^{-4} yr^{-1} for 1998 in the U.S. (Census Bureau 2001c));
(2) the suicide rate (1.13×10^{-4} yr^{-1} for 1998 in the U.S. (Census Bureau 2001c));
(3) the homicide rate (6.8×10^{-5} yr^{-1} for 1998 in the U.S. (Census Bureau 2001c));
(4) the combatant war casualty rate, deaths only, as a fraction of the general population (~3.2×10^{-5} yr^{-1} for all U.S. wars in the last 100 years, relative to average (~200 million) U.S population level during that period (Almanac 1994)); and
(5) the legal execution rate (2.27×10^{-7} yr^{-1} for 1998 in the U.S. (Death Penalty Information Center 1998)).

Summing these five items gives $R_{mort} \sim 5.75 \times 10^{-4}$ yr^{-1}, yielding a median healthspan of $T_{half} \sim 1200$ years. This is consistent with an independent estimate of $T_{half,10} \sim 5300$ years based upon the actuarial death rate of children in the 10-year-old cohort ($R_{mort,10} = 1.3 \times 10^{-4}$ yr^{-1} in 1998 in U.S. (Census Bureau 2001a)), whose

death rate is the lowest for any age cohort and for whom the almost exclusive cause of death is accidents. (The death rates for children aged 1–15 is less than R_{mort} (that is, $<5.75 \times 10^{-4}$ yr^{-1}) (Census Bureau 2001a).) Note that in this model, T_{half} is the estimated median lifespan in a healthy non-aging state, with no part of that life spent in an infirm senescent state, hence the estimate reflects the anticipated length of healthy years, or *healthspan*, and not mere lifespan which today may include 25% or more time spent in a morbid condition.

It is worth pointing out (Freitas 2002) that the advances in medicine over the last two centuries have already effectively achieved a disease-related-mortality free condition for a few age cohorts of the human population in industrialized countries – our youngest children. Medical technology has had its greatest impact to date in preventing infant mortality, especially between the ages of 1 and 4. In the year 1865, a young child in this age cohort had a 6.86% probability of dying in the next year (Census Bureau 1989a), but by 1998 the probability of dying in the next year for these children had been slashed from 6.86 to 0.0345% (Census Bureau 2001a), a phenomenal 200-fold reduction. If we could keep our bodies in the same healthy condition that existed when we were young, we should have a median healthspan approaching $T_{half,10}$ ~5300 years as noted above. (This assumes the accident risks are roughly the same for adults (who drive cars, operate heavy machinery, etc.) as for children (who don't), which may seem improbable but is nonetheless approximately true: U.S. accident deaths for 1998 as a fraction of all deaths in each age cohort were 37% at 1–4 years, 42% at 5–14 years, 44% at 15–24 years, and 28% at 25–34 years (Census Bureau, 2001d).) Death would usually come from some form of non-medical accident, which is the leading cause of death up to the age range of 35–44 years (Census Bureau, 2001d). When future nanorobotic medicine is available as envisioned here, we shall extend this disease-related-mortality free condition to all age cohorts, not just to the children, and thus give all of us the potential to achieve $T_{half,10}$ ~5300 healthy years, or more.

The maximum likely healthspan in a world subject only to age-unrelated deaths can be estimated from the aforementioned exponential formula by taking N_{pop} ~6 billion, the current world population, and $N(t) = 1$, indicating the last survivor of this population, and a constant $R_{mort} = 5.75 \times 10^{-4}$ yr^{-1} as before, yielding $t = T_{max}$ ~39,200 years, the maximum healthspan of the last random survivor from this cohort.

These projected healthspans seem incredibly long by current standards. Even so, it is safe to predict that people will desire more and will seek to reduce R_{mort} still further. The simplest way to reduce nonmedical hazards is to attack the largest source of them – the accident rate – by employing nanotechnology to create a safer and more hazard-free living environment. Motorized vehicles of all kinds (land, sea, air, and space) can be made more crash resistant, new forms of "airbags" can be designed to allow survival of high-speed impact forces from any direction, and the fallibility of human operators could be eliminated by switching to automated aircraft, cars, trucks, trains and ships. Buildings (including houses) can incorporate active safety devices. Extremely fine-grained simulations of the physical world could provide more accurate risk-prediction models, allowing potential dangers

to be anticipated and avoided in advance. Implanted in vivo nanorobotic systems equivalent to respirocytes and clottocytes could greatly reduce accidental deaths from drowning and bleeding. Other basic augmentations to the human body could improve its durability and reduce its accident-proneness, including modifications to the human genome to engineer improved metabolism or increased intelligence, perhaps combined with more intrusive nanorobotic implants such as whole-body vascular replacement systems (Freitas and Phoenix 2002). Both homicide (inversely correlated with wealth and education) and suicide rates should fall as the spread of molecular manufacturing increases material prosperity (Freitas 2006b) and expands the diversity of life choices. These factors, along with greater access to knowledge, should also help to decrease the incidence of war.

The maximum speed at which R_{mort}, also known as the "hazard function," can be reduced is presently unknown but a conservative lower limit may be crudely estimated as follows. From 1933 (the first year reliable data became available) to 1998, annual accident rates fell by 50% from 71.9 per 10^5 (Census Bureau 1989b) to 36.2 (Census Bureau 2001c), suicide rates fell by 29% from 15.9 per 10^5 (Census Bureau 1989c) to 11.3 (Census Bureau 2001c), homicide rates fell by 30% from 9.7 per 10^5 (Census Bureau 1989c) to 6.8 (Census Bureau 2001c), and legal executions fell by 82% from 0.127 per 10^5 (Census Bureau 1989d) to 0.023 (Death Penalty Information Center 1998), a 65-year net decline of $\Delta R_{mort} = -0.863\%/yr$ in R_{mort}, from 1.01×10^{-3} yr^{-1} in 1933 to 5.75×10^{-4} yr^{-1} in 1998. Substituting $R(t) = R_{mort}(1-\Delta R_{mort})^{(t-1998)}$ for R_{mort} in our exponential formula to most simply represent this observed nonmedical death rate decline, T_{half} would rise from 1200 years in 1998 to 1300 years by 2009, 1500 years by 2029, and 2000 years by 2070. These figures appear conservative because if we can make our living environment as safe for adults as it currently is for our 10-year-olds, then T_{half} should more closely approximate $T_{half,10}$ ~5300 years, not 1300 years, for adults, in the present epoch.

23.8 Summary and Conclusions

This chapter has argued, I hope persuasively, that diamondoid medical nanorobotics can almost certainly achieve comprehensive control of human morbidity and aging. To the more limited extent that biotech-based instrumentalities can accomplish similar ends, nanorobot performance and safety will likely prove superior in comparison.

Some have averred that medical nanorobotics sounds like an "argument for infinity" because it appears to skeptical eyes to be a panacea that can do and cure anything. No such claim is advanced here or by any serious proponent of advanced nanomedicine. Nanorobots, no matter how capable, must always have very well-defined physical limitations. They are limited by mobility constraints, by the availability of energy, by mechanical and geometric constraints, by diffusion limits and biocompatibility requirements, and by numerous other constraints (Freitas 1999, 2003). Nanorobots cannot act instantly – they take time to effect their cure.

But because they will be constructed of superior building materials of surpassing strength and stiffness, diamondoid nanorobots will operate several orders of magnitude faster than analogous machinery built from biomaterials, and will be able to apply forces several orders of magnitude larger than those which may be applied by comparable biological- or biotech-based systems. Nanorobots will avoid almost all proximate side effects because they can operate under precise sensor-driven digital control, not drift aimlessly on the stochastic currents of the human body like nanoparticles and drug molecules. Nanorobots can be more reliable because they can report back to the physician what they are doing, both while they are doing it and after they've finished. They are safer because, unlike commonplace biotechnology-based approaches, a diamondoid nanomachine cannot be co-opted for hostile use by rapidly mutating microbes. And diamondoid nanorobots could incorporate biomaterials or biological components whenever necessary (e.g., in the design of exterior biocompatible coatings (Freitas 2003ab)), so hybrid bio-diamondoid nanorobots can assimilate any performance advantages of biotech as a subset of medical nanorobotics design.

Future clinical nanorobotic therapies will typically involve the administration of a cocktail of multiple nanorobot types, some performing the primary mission and others serving in a support role. After treatment is completed the nanorobots may be removed from the body, allowing human nature to resume its erratic but endlessly fascinating journey into the future.

Acknowledgments The author acknowledges private grant support for this work from the Life Extension Foundation, the Alcor Foundation, the Kurzweil Foundation, and the Institute for Molecular Manufacturing, and thanks Greg Fahy for extensive comments on an earlier version of this manuscript.

References

Abd-Al-Aal Z, Ramadan NF, Al-Hoot A (2000) Life-cycle of *Isospora mehlhornii* sp. Nov. (Apicomplexa: Eimeriidae), parasite of the Egyptian swallow *Hirundo rubicola savignii*. Parasitol Res 86:270–278

Adessi C, Frossard MJ, Boissard C et al. (2003) Pharmacological profiles of peptide drug candidates for the treatment of Alzheimer's disease. J Biol Chem 278:13905–13911; http://www.jbc.org/cgi/content/full/278/16/13905

Ahn JI, Terry Canale S, Butler SD et al. (2004) Stem cell repair of physeal cartilage. J Orthop Res 22:1215–1221

Aisen PS (2005) The development of anti-amyloid therapy for Alzheimer's disease: from secretase modulators to polymerisation inhibitors. CNS Drugs 19:989–996

Alberts B, Bray D, Lewis J et al. (1989) The Molecular Biology of the Cell, 2nd edn. Garland Publishing Inc., New York

Allis DG, Drexler KE (2005) Design and analysis of a molecular tool for carbon transfer in mechanosynthesis. J Comput Theor Nanosci 2:45–55; http://e-drexler.com/d/05/00/DC10C-mechanosynthesis.pdf

Almanac, U.S. Casualties in Major Wars: Total Deaths. The 1994 Information Please Almanac, Atlas and Yearbook, 47th edn. Houghton Mifflin Company, New York, p. 385

Alvarez-Chaver P, Rodríguez-Piñeiro AM, Rodríguez-Berrocal FJ et al. (2007) Identification of hydrophobic proteins as biomarker candidates for colorectal cancer. Int J Biochem Cell Biol 39:529–540

Ardekian L, Gaspar R, Peled M et al. (2000) Does low-dose aspirin therapy complicate oral surgical procedures? J Am Dent Assoc 131:331–335

Armstrong RJE, Svendsen CN (2000) Neural stem cells: from cell biology to cell replacement. Cell Transplantation 9:139–152

Armstrong RC, Le TQ, Flint NC et al. (2006) Endogenous cell repair of chronic demyelination. J Neuropathol Exp Neurol 65:245–56

Aspenberg P, Anttila A, Konttinen YT et al. (1996) Benign response to particles of diamond and SiC: bone chamber studies of new joint replacement coating materials in rabbits. Biomaterials 17:807–812

Aspinall R (2010) Chapter 15. Maintenance and Restoration of Immune System Function. In: Fahy GM et al. (eds) The Future of Aging: Pathways to Human Life Extension. Springer, Berlin Heidelberg New York, pp. 489–520

Autexier C, Lue NF (2006) The structure and function of telomerase reverse transcriptase. Annu Rev Biochem 75:493–517

Avraham KB (2002) The genetics of deafness: a model for genomic and biological complexity. Ernst Schering Res Found Workshop 36:271–297

Bakris GL, Bank AJ, Kass DA et al. (2004) Advanced glycation end-product cross-link breakers. A novel approach to cardiovascular pathologies related to the aging process. Am J Hypertens 17:23S–30S

Baldi P (2001) The Shattered Self: The End of Natural Evolution. MIT Press, Cambridge MA

Baracca A, Sgarbi G, Mattiazzi M et al. (2007) Biochemical phenotypes associated with the mitochondrial ATP6 gene mutations at nt8993. Biochim Biophys Acta 1767:913–919

Barbosa HS, Ferreira-Silva MF, Guimaraes EV et al. (2005) Absence of vacuolar membrane involving *Toxoplasma gondii* during its intranuclear localization. J Parasitol 91:182–184

Barzilai N, She L, Liu BQ et al. (1999) Surgical removal of visceral fat reverses hepatic insulin resistance. Diabetes 48:94–98

Basson AB, Terblanche SE, Oelofsen W (1982) A comparative study on the effects of ageing and training on the levels of lipofuscin in various tissues of the rat. Comp Biochem Physiol A 71:369–374

Basu S, Mehreja R, Thiberge S et al. (2004) Spatiotemporal control of gene expression with pulse-generating networks. PNAS 101:6355–6360; http://www.princeton.edu/~rweiss/papers/basu-pulse-2004.pdf

Basu S, Gerchman Y, Collins CH et al. (2005) A synthetic multicellular system for programmed pattern formation. Nature 434:1130–1134; http://www.princeton.edu/~rweiss/papers/basu-nature-2005.pdf

Bateman ED, Emerson RJ, Cole PJ (1982) A study of macrophage-mediated initiation of fibrosis by asbestos and silica using a diffusion chamber technique. Br J Exp Pathol 63:414–425

Bauernschmitt R, Schirmbeck EU, Knoll A et al. (2005) Towards robotic heart surgery: introduction of autonomous procedures into an experimental surgical telemanipulator system. Int J Med Robot 1:74–79

Baxevanis AD, Ouellette BF (eds) (1998) Bioinformatics: A Practical Guide to the Analysis of Genes and Proteins. Wiley-Interscience, New York

Bayoudh S, Mehta M, Rubinsztein-Dunlop H et al. (2001) Micromanipulation of chloroplasts using optical tweezers. J Microsc 203:214–222

Beauséjour CM, Krtolica A, Galimi F et al. (2003) Reversal of human cellular senescence: roles of the p53 and p16 pathways. EMBO J 22:4212–4222

Becker WM, Deamer DW (1991) The World of the Cell, 2nd edn. Benjamin/Cummings Publishing Company, Redwood City, CA

Behkam B, Sitti M (2007) Bacterial flagella-based propulsion and on/off motion control of microscale objects. Appl Phys Lett 90:1–3; http://nanolab.me.cmu.edu/publications/papers/Behkam-APL2007.pdf

Bement WM, Yu HY, Burkel BM et al. (2007) Rehabilitation and the single cell. Curr Opin Cell Biol 19:95–100

Berd D, Kairys J, Dunton C et al. (1998) Autologous, hapten-modified vaccine as a treatment for human cancers. Semin Oncol 25:646–653

Bergamini E (2006) Autophagy: a cell repair mechanism that retards ageing and age-associated diseases and can be intensified pharmacologically. Mol Aspects Med 27:403–410

Bergamini E, Cavallini G, Donati A et al. (2004) The role of macroautophagy in the ageing process, anti-ageing intervention and age-associated diseases. Int J Biochem Cell Biol 36:2392–2404

Berger TW, Glanzman DL (eds) (2005) Toward Replacement Parts for the Brain: Implantable Biomimetic Electronics as Neural Prostheses. MIT Press, Cambridge, MA

Bergers G, Javaherian K, Lo KM et al. (1999) Effects of angiogenesis inhibitors on multistage carcinogenesis in mice. Science 284:808–812

Bi G, Alderton JM, Steinhardt RA (1995) Calcium-regulated exocytosis is required for cell membrane resealing. J Cell Biol 131:1747–1758

Black J (1999) Biological Performance of Materials: Fundamentals of Biocompatibility, 3rd edn. Marcel Dekker, New York

Blackett AD, Hall DA (1981) Tissue vitamin E levels and lipofuscin accumulation with age in the mouse. J Gerontol 36:529–533

Blick RH, Qin H, Kim HS et al. (2007) A nanomechanical computer – exploring new avenues of computing. New J Phys 9:241; http://www.iop.org/EJ/article/1367-2630/9/7/241/njp7_7_241.html

Bliem R, Konopitzky K, Katinger H (1991) Industrial animal cell reactor systems: aspects of selection and evaluation. Adv Biochem Eng Biotechnol 44:1–26

Boland T, Xu T, Damon B et al. (2006) Application of inkjet printing to tissue engineering. Biotechnol J 1:910–917

Boyde A, Jones SJ, Robey PG (2006) Primer on the Metabolic Bone Diseases and Disorders of Mineral Metabolism. American Society for Bone and Mineral Research, Washington, DC; http://www.jbmronline.org/doi/xml/10.1359/prim.2006.0684

Bracci L, Lozzi L, Pini A et al. (2002) A branched peptide mimotope of the nicotinic receptor binding site is a potent synthetic antidote against the snake neurotoxin alpha-bungarotoxin. Biochemistry 41:10194–10199

Brody H (1955) Organization of the cerebral cortex, III. A study of aging in the human cerebral cortex. J Comp Neurol 102:511–556

Brown AJ, Mander EL, Gelissen IC et al. (2000) Cholesterol and oxysterol metabolism and subcellular distribution in macrophage foam cells. Accumulation of oxidized esters in lysosomes. J Lipid Res 41:226–237

Browne WR, Feringa BL (2006) Making molecular machines work. Nat Nanotechnol 1:25–35

Brunet JP, Jourdan N, Cotte-Laffitte J et al. (2000) Rotavirus infection induces cytoskeleton disorganization in human intestinal epithelial cells: implication of an increase in intracellular calcium concentration. J Virol 74:10801–10806

Brunk UT, Jones CB, Sohal RS (1992) A novel hypothesis of lipofuscinogenesis and cellular aging based on interactions between oxidative stress and autophagocytosis. Mutat Res 275: 395–403

Bryan TM, Englezou A, Dalla-Pozza L et al. (1997) Evidence for an alternative mechanism for maintaining telomere length in human tumors and tumor-derived cell lines. Nat Med 3: 1271–1274

Bullen D, Chung S, Wang X et al. (2002) Development of parallel dip pen nanolithography probe arrays for high throughput nanolithography. Symposium LL: Rapid Prototyping Technologies, Materials Research Society Fall Meeting; 2–6 Dec 2002; Boston, MA. Proc. MRS, Vol. 758, 2002; http://mass.micro.uiuc.edu/publications/papers/84.pdf

Cagin T, Jaramillo-Botero A, Gao G (1998) Molecular mechanics and molecular dynamics analysis of Drexler-Merkle gears and neon pump. Nanotechnology 9:143; http://www.wag.caltech.edu/foresight/foresight_1.html

Cameron CL, Fisslthaler B, Sherman A et al. (1989) Studies on contact activation: effects of surface and inhibitors. Med Prog Technol 15:53–62

Campisi J (2003) Consequences of cellular senescence and prospects for reversal. Biogerontology 4:13

Castro MC, Cliquet A (1997) A low-cost instrumented glove for monitoring forces during object manipulation. IEEE Trans Rehabil Eng 5:140–147

Cavallaro EE, Rosen J, Perry JC et al. (2006) Real-time myoprocessors for a neural controlled powered exoskeleton arm. IEEE Trans Biomed Eng 53:2387–2396

Census Bureau (1989a) Series B 201–213. Death Rate, by Age, for Massachusetts: 1865 to 1900. Vital Statistics, Historical Statistics of the United States: Colonial Times to 1970. U.S. Department of Commerce, Bureau of the Census, p. 63 (Series 203)

Census Bureau (1989b) Series B 149–166. Death Rate, for Selected Causes: 1900–1970. Vital Statistics, Historical Statistics of the United States: Colonial Times to 1970. U.S. Department of Commerce, Bureau of the Census, p. 58 (Series 163, 164, and 165)

Census Bureau (1989c) Series H 971–986. Homicides and Suicides: 1900–1970. Vital Statistics, Historical Statistics of the United States: Colonial Times to 1970. U.S. Department of Commerce, Bureau of the Census, p. 414 (Series 972 and 980)

Census Bureau (1989d) Series H 1155–1167. Prisoners Executed Under Civil Authority, by Race and Offense: 1900–1970. Vital Statistics, Historical Statistics of the United States: Colonial Times to 1970. U.S. Department of Commerce, Bureau of the Census, p. 422 (Series 1155); and Series A 6–8. Annual Population Estimates for the United States: 1790–1970. Vital Statistics, Historical Statistics of the United States: Colonial Times to 1970. U.S. Department of Commerce, Bureau of the Census, p. 8 (Series 7)

Census Bureau (2001a) Table 98. Expectation of Life and Expected Deaths by Race, Sex, and Age: 1998. Vital Statistics, Statistical Abstract of the United States: 2001. U.S. Census Bureau, p. 74

Census Bureau (2001b) The 2000 U.S. GDP was $9.896 trillion in constant year 2000 dollars, according to: Table 1340. Gross Domestic Product (GDP) by Country: 1995 to 2000. Comparative International Statistics, Statistical Abstract of the United States: 2001. U.S. Census Bureau, p. 841

Census Bureau (2001c) Table 105. Deaths and Death Rates by Selected Causes: 1990 to 1998. Vital Statistics, Statistical Abstract of the United States: 2001. U.S. Census Bureau, p. 79

Census Bureau (2001d) Table 107. Death by Selected Causes and Selected Characteristics: 1998. Vital Statistics, Statistical Abstract of the United States: 2001. U.S. Census Bureau, p. 81

Chaer RA, Trocciola S, DeRubertis B et al. (2006) Evaluation of the accuracy of a wireless pressure sensor in a canine model of retrograde-collateral (type II) endoleak and correlation with histologic analysis. J Vasc Surg 44:1306–1313

Chambers EJ, Bloomberg GB, Ring SM et al. (1999) Structural studies on the effects of the deletion in the red cell anion exchanger (band 3, AE1) associated with South East Asian ovalocytosis. J Mol Biol 285:1289–1307

Chen KS, Masliah E, Mallory M et al. (1995) Synaptic loss in cognitively impaired aged rats is ameliorated by chronic human nerve growth factor infusion. Neuroscience 68:19–27

Chen X, Kis A, Zettl A et al. (2007) A cell nanoinjector based on carbon nanotubes. Proc Natl Acad Sci USA 104:8218–8222

Cheng R, Feng Q, Argirov OK et al. (2004) Structure elucidation of a novel yellow chromophore from human lens protein. J Biol Chem 279:45441–45449

Cherniak C (1990) The bounded brain: toward quantitative neuroanatomy. J Cognitive Neurosci 2:58–68

Chesnokov SA, Nalimova VA, Rinzler AG et al. (1999) Mechanical energy storage in carbon nanotube springs. Phys Rev Lett 82:343–346

Chow AM, Brown IR (2007) Induction of heat shock proteins in differentiated human and rodent neurons by celastrol. Cell Stress Chaperones 12:237–244

Chrusch DD, Podaima BW, Gordon R (2002) Cytobots: intracellular robotic micromanipulators. In: Kinsner W, Sebak A (eds) Conference Proceedings, 2002 IEEE Canadian Conference on Electrical and Computer Engineering; 2002 May 12–15; Winnipeg, Canada,

IEEE, Winnipeg;http://www.umanitoba.ca/faculties/medicine/radiology/Dick_Gordon_papers/Chrusch,Podaima,Gordon2002

Clark LD, Clark RK, Heber-Katz E (1998) A new murine model for mammalian wound repair and regeneration. Clin Immunol Immunopathol 88:35–45

Cleveland LR, Grimstone AV (1964) The fine structure of the flagellate *Mixotricha* and its associated microorganisms. Proc Roy Soc London B 159:668–686

Cohen S, Behzad AR, Carroll JB et al. (2006) Parvoviral nuclear import: bypassing the host nuclear-transport machinery. J Gen Virol 87:3209–3213

Cohn RD, Campbell KP (2000) Molecular basis of muscular dystrophies. Muscle Nerve 23: 1456–1471

Cole E (2007) Fantastic Voyage: Departure 2009. Wired Magazine, 18 January 2007; http://www.wired.com/medtech/health/news/2007/01/72448

Collas P, Håkelien AM (2003) Teaching cells new tricks. Trends Biotechnol 21:354–361

Collins PG, Arnold MS, Avouris P (2001) Engineering carbon nanotubes and nanotube circuits using electrical breakdown. Science 292:706–709

Colombelli J, Reynaud EG, Rietdorf J et al. (2005) In vivo selective cytoskeleton dynamics quantification in interphase cells induced by pulsed ultraviolet laser nanosurgery. Traffic 6:1093–1102

Colombelli J, Reynaud EG, Stelzer EH (2007) Investigating relaxation processes in cells and developing organisms: from cell ablation to cytoskeleton nanosurgery. Methods Cell Biol 82:267–291

Committee to Review the National Nanotechnology Initiative, National Materials Advisory Board (NMAB), National Research Council (NRC) (2006) A Matter of Size: Triennial Review of the National Nanotechnology Initiative. The National Academies Press, Washington, DC; http://www.nap.edu/catalog/11752.html#toc

Cormier M, Johnson B, Ameri M et al. (2004) Transdermal delivery of desmopressin using a coated microneedle array patch system. J Control Release 97:503–511

Corsaro D, Venditti D, Padula M et al. (1999) Intracellular life. Crit Rev Microbiol 25:39–79

Costerton JW, Stewart PS, Greenberg EP (1999) Bacterial biofilms: a common cause of persistent infections. Science 284:1318–1322

Coulman S, Allender C, Birchall J (2006) Microneedles and other physical methods for overcoming the stratum corneum barrier for cutaneous gene therapy. Crit Rev Ther Drug Carrier Syst 23:205–258

Craig EA, Eisenman HC, Hundley HA (2003) Ribosome-tethered molecular chaperones: the first line of defense against protein misfolding? Curr Opin Microbiol 6:157–162

Cruz MA, Chen J, Whitelock JL et al. (2005) The platelet glycoprotein Ib-von Willebrand factor interaction activates the collagen receptor alpha2beta1 to bind collagen: activation-dependent conformational change of the alpha2-I domain. Blood 105:1986–1991

Cui KH (2005) Three concepts of cloning in human beings. Reprod Biomed Online 11:16–17

Cumings J, Zettl A (2000) Low-friction nanoscale linear bearing realized from multiwall carbon nanotubes. Science 289:602–604

Cunningham AP, Love WK, Zhang RW et al. (2006) Telomerase inhibition in cancer therapeutics: molecular-based approaches. Curr Med Chem 13:2875–2888

Das S, Rose G, Ziegler MM et al. (2005) Architectures and simulations for nanoprocessor systems integrated on the molecular scale. In: Cuniberti G, Fagas G, Richter K (eds) Introducing Molecular Electronics. Springer, New York; http://www.mitre.org/work/tech_papers/tech_papers_05/05_0977/05_0977.pdf

Davies I, Fotheringham A, Roberts C (1983) The effect of lipofuscin on cellular function. Mech Ageing Dev 23:347–356

Davis S (1996) Chapter 16. Biomedical applications of particle engineering. In: Coombs RRH, Robinson DW (eds) Nanotechnology in Medicine and the Biosciences. Gordon & Breach Publishers, Netherlands, pp. 243–262

Day JC (1993) Table 2. Projections of the Population, by Age, Sex, Race, and Hispanic Origin, for the United States: 1993 to 2050 (Middle Series) – July 1, 2000, White Male. Population

Projections of the United States, by Age, Sex, Race, and Hispanic Origin: 1993 to 2050, Current Population Reports, Report No. P25-1104, Bureau of the Census, U.S. Department of Commerce, p. 26

De S, Sakmar TP (2002) Interaction of A2E with model membranes. Implications to the pathogenesis of age-related macular degeneration. J Gen Physiol 120:147–157

Death Penalty Information Center (1998) 1998 Year End Report: New Voices Raise Dissent, Executions Decline; http://www.deathpenaltyinfo.org/article.php?scid=45&did=542

Decatur AL, Portnoy DA (2000) A PEST-like sequence in listeriolysin O essential for *Listeria monocytogenes* pathogenicity. Science 290:992–995

de Grey ADNJ (1999) The Mitochondrial Free Radical Theory of Aging. Landes Bioscience, Austin, TX

de Grey ADNJ (2000) Mitochondrial gene therapy: an arena for the biomedical use of inteins. Trends Biotechnol 18:394–399; http://www.sens.org/allo.pdf

de Grey ADNJ (2003) Challenging but essential targets for genuine anti-ageing drugs. Exp Opin Therapeut Targets 37:1–5; http://www.sens.org/manu21.pdf

de Grey ADNJ (2005a) Developing biomedical tools to repair molecular and cellular damage. Foresight Nanotech Institute website; http://foresight.org/challenges/health002.html

de Grey ADNJ (2005b) Reactive oxygen species production in the mitochondrial matrix: implications for the mechanism of mitochondrial mutation accumulation. Rejuvenation Res 8:13–17; http://www.sens.org/AKDH.pdf

de Grey ADNJ (2005c) Forces maintaining organellar genomes: is any as strong as genetic code disparity or hydrophobicity? BioEssays 27:436–446; http://www.sens.org/HH-CDH-PP.pdf

de Grey ADNJ (2005d) Whole-body interdiction of lengthening of telomeres: a proposal for cancer prevention. Front Biosci 10:2420–2429; http://www.sens.org/WILT-FBS.pdf

de Grey ADNJ (2006a) Is SENS a farrago? Rejuvenation Res 9:436–439

de Grey ADNJ (2006b) Foreseeable pharmaceutical repair of age-related extracellular damage. Curr Drug Targets 7:1469–1477; http://www.sens.org/excellPP.pdf

de Grey ADNJ (2006c) Appropriating microbial catabolism: a proposal to treat and prevent neurodegeneration. Neurobiol Aging 27:589–595; http://www.sens.org/NBA-PP.pdf

de Grey ADNJ (2007a) The natural biogerontology portfolio: "defeating aging" as a multi-stage ultra-grand challenge. Ann NY Acad Sci 1100:409–423

de Grey ADNJ (2007b) Protagonistic pleiotropy: Why cancer may be the only pathogenic effect of accumulating nuclear mutations and epimutations in aging. Mech Ageing Dev 128:456–459; http://www.sens.org/nucmutPP.pdf

de Grey ADNJ (2010) Chapter 22. WILT: Necessity, Feasibility, Affordability. In: Fahy GM et al. (eds) The Future of Aging: Pathways to Human Life Extension. Springer, Berlin Heidelberg, New York, pp. 667–684

de Grey ADNJ, Rae M (2007) Ending Aging: The Rejuvenation Breakthroughs That Could Reverse Human Aging in Our Lifetime. St. Martin's Press, New York

de Grey ADNJ, Ames BN, Andersen JK et al. (2002) Time to talk SENS: critiquing the immutability of human aging. Ann NY Acad Sci 959:452–462

de Grey ADNJ, Campbell FC, Dokal I et al. (2004) Total deletion of in vivo telomere elongation capacity: an ambitious but possibly ultimate cure for all age-related human cancers. Annals NY Acad Sci 1019:147–170; http://www.sens.org/WILT.pdf

de Grey ADNJ, Alvarez PJJ, Brady RO et al. (2005) Medical bioremediation: Prospects for the application of microbial catabolic diversity to aging and several major age-related diseases. Ageing Res Rev 4:315–338; http://alvarez.rice.edu/emplibrary/63.pdf

De Koninck P, Schulman H (1998) Sensitivity of CaM kinase II to the frequency of Ca^{2+} oscillations. Science 279:227–230

Delaunay J (1995) Genetic disorders of the red cell membranes. FEBS Lett 369:34–37

Delgado-Olivares L, Zamora-Romo E, Guarneros G et al. (2006) Codon-specific and general inhibition of protein synthesis by the tRNA-sequestering minigenes. Biochimie 88:793–800

Delongeas JL, Netter P, Boz P et al. (1984) Experimental synovitis induced by aluminium phosphate in rabbits. Comparison of the changes produced in synovial tissue and in articular cartilage by aluminium phosphate, carrageenin, calcium hydrogen phosphate dihydrate, and natural diamond powder. Biomed Pharmacother 38:44–48

Dentali F, Ageno W, Imberti D (2006) Retrievable vena cava filters: clinical experience. Curr Opin Pulm Med 12:304–309

Department of Energy (1999) The 1999 GDP for 197 countries was $27.5769 trillion in constant 1990 dollars, according to: Table B2. World Gross Domestic Product at Market Exchange Rates, 1990–1999. Department of Energy (DOE); http://www.eia.doe.gov/emeu/iea/tableb2.html. Using Census Bureau data (Census Bureau, 2001b) to estimate the world GDP deflator, this figure for world GDP is estimated as equivalent to $33.7080 trillion in constant year 2000 dollars, for the year 2000.

Dijkgraaf LC, Liem RS, de Bont LG et al. (1995) Calcium pyrophosphate dihydrate crystal deposition disease. Osteoarthr Cartilage 3:35–45

Ding B, Seeman NC (2006) Operation of a DNA robot arm inserted into a 2D DNA crystalline substrate. Science 314:1583–1585

Donaldson VH, Wagner CJ, Mitchell BH et al. (1998) An HMG-I protein from human endothelial cells apparently is secreted and impairs activation of Hageman factor (factor XII). Proc Assoc Am Physicians 110:140–149

Donati A (2006) The involvement of macroautophagy in aging and anti-aging interventions. Mol Aspects Med 27:455–470

Donati A, Taddei M, Cavallini G et al. (2006) Stimulation of macroautophagy can rescue older cells from 8-OHdG mtDNA accumulation: a safe and easy way to meet goals in the SENS agenda. Rejuvenation Res 9:408–412

Dong Z, Saikumar P, Weinberg JM et al. (2006) Calcium in cell injury and death. Annu Rev Pathol 1:405–434

Dowling P, Meleady P, Dowd A et al. (2007) Proteomic analysis of isolated membrane fractions from superinvasive cancer cells. Biochim Biophys Acta 1774:93–101

Drach LM, Bohl J, Goebel HH (1994) The lipofuscin content of the inferior olivary nucleus in Alzheimer's disease. Dementia 5:234–239

Drexler KE (1986) Engines of Creation: The Coming Era of Nanotechnology. Anchor Press/Doubleday, New York

Drexler KE (1992) Nanosystems: Molecular Machinery, Manufacturing, and Computation. John Wiley & Sons, New York; (a) 13.2, (b) Ch. 12, (c) 16.3.2, (d) 13.2.2, (e) 13.4.1, (f) 10.4.7, (g) 10.7.8, (h) Ch. 8, (i) 8.3.4, (j) Fig. 5.9

Drexler KE (1995) Introduction to Nanotechnology. In: Krummenacker M, Lewis J (eds) Prospects in Nanotechnology: Toward Molecular Manufacturing. John Wiley & Sons, New York, pp. 1–19

Drexler KE, Merkle RC (1996) Simple pump selective for neon. Institute for Molecular Manufacturing website; http://www.imm.org/Parts/Parts1.html or http://www.imm.org/Images/pumpApartC.jpg

Drexler KE, Peterson C, Pergamit G (1991) Unbounding the Future: The Nanotechnology Revolution. William Morrow/Quill Books, New York

Dunn GP, Bruce AT, Ikeda H et al. (2002) Cancer immunoediting: from immunosurveillance to tumor escape. Nat Immunol 3:991–998

Dutt MVG, Childress L, Jiang L et al. (2007) Quantum register based on individual electronic and nuclear spin qubits in diamond. Science 316:1312–1316

Ehninger D, Kempermann G (2008) Neurogenesis in the adult hippocampus. Cell Tissue Res 331:243–250

El Alaoui H, Gresoviac SJ, Vivares CP (2006) Occurrence of the microsporidian parasite *Nucleospora salmonis* in four species of salmonids from the Massif Central of France. Folia Parasitol (Praha) 53:37–43

Elgue G, Sanchez J, Egberg N et al. (1993) Effect of surface-immobilized heparin on the activation of adsorbed factor XII. Artif Organs 17:721–726

Ellis PD, Hadfield KM, Pascall JC et al. (2001) Heparin-binding epidermal-growth-factor-like growth factor gene expression is induced by scrape-wounding epithelial cell monolayers: involvement of mitogen-activated protein kinase cascades. Biochem J 354:99–106

Ellis-Behnke RG, Liang YX, Tay DKC et al. (2007) Using nanotechnology to repair the body. Strategies for Engineered Negligible Senescence (SENS), Third Conference, Queens' College, Cambridge, England, 6–10 September 2007; http://www.sens.org/sens3/abs/Ellis-Behnke.htm

Estrada LD, Yowtak J, Soto C (2006) Protein misfolding disorders and rational design of antimisfolding agents. Methods Mol Biol 340:277–293

Fahy GM (1993) Molecular nanotechnology and its possible pharmaceutical implications. In: Bezold C, Halperin JA, Eng JL (eds) 2020 Visions: Health Care Information Standards and Technologies. U.S. Pharmacopeial Convention Inc., Rockville MD, pp. 152–159

Fahy GM (2003) Apparent induction of partial thymic regeneration in a normal human subject: a case report. J Anti Aging Med 6:219–227

Fahy GM (2007) Method for the prevention of transplant rejection. U.S. Patent No. 7,166,569

Fahy GM (2010) Chapter 6. Precedents for the biological control of aging: Experimental postponement, prevention, and reversal of aging processes. In: Fahy GM et al. (eds) The Future of Aging: Pathways to Human Life Extension. Springer, Berlin Heidelberg, New York, pp. 127–223

Farge D, Turner MW, Roy DR et al. (1986) Dyazide-induced reversible acute renal failure associated with intracellular crystal deposition. Am J Kidney Dis 8:445–449

Farrants GW, Hovmoller S, Stadhouders AM (1988) Two types of mitochondrial crystals in diseased human skeletal muscle fibers. Muscle Nerve 11:45–55

Fauque J, Borgna JL, Rochefort H (1985) A monoclonal antibody to the estrogen receptor inhibits in vitro criteria of receptor activation by an estrogen and an anti-estrogen. J Biol Chem 260:15547–15553

Federal Reserve System (2007) Flow of Funds Accounts of the United States, Flows and Outstandings, Third Quarter 2007, Federal Reserve Statistical Release Z.1, Board of Governors of the Federal Reserve System, Washington DC, 6 December 2007; http://www.federalreserve.gov/releases/z1/Current/z1.pdf. (Net worth 2007 QIII: Household $58.6T, Nonfarm Nonfinancial Corporate Business $15.5T, Nonfarm Noncorporate Business $6.2T.)

Feichtinger M, Zemann W, Kärcher H (2007) Removal of a pellet from the left orbital cavity by image-guided endoscopic navigation. Int J Oral Maxillofac Surg 36:358–361

Felgner H, Grolig F, Muller O et al. (1998) In vivo manipulation of internal cell organelles. Methods Cell Biol 55:195–203

Feng Y, Tian ZM, Wan MX et al. (2007) Protein profile of human hepatocarcinoma cell line SMMC-7721: identification and functional analysis. World J Gastroenterol 13:2608–2614

Fennimore AM, Yuzvinsky TD, Han WQ et al. (2003) Rotational actuators based on carbon nanotubes. Nature 424:408–410

Feynman RP (1960) There's plenty of room at the bottom. Eng Sci (CalTech) 23:22–36

Finch CE (1990) Longevity, Senescence and the Genome. University of Chicago Press, Chicago, IL

Fincher EF, Johannsen L, Kapas L et al. (1996) Microglia digest *Staphylococcus aureus* into low molecular weight biologically active compounds. Am J Physiol 271:R149–R156

Finder VH, Glockshuber R (2007) Amyloid-beta aggregation. Neurodegener Dis 4:13–27

Firtel M, Henderson G, Sokolov I (2004) Nanosurgery: observation of peptidoglycan strands in *Lactobacillus helveticus* cell walls. Ultramicroscopy 101:105–109

Fischer JA (2000) Molecular motors and developmental asymmetry. Curr Opin Genet Dev 10:489–496

Fleischer C, Wege A, Kondak K et al. (2006) Application of EMG signals for controlling exoskeleton robots. Biomed Tech (Berl) 51:314–319

Flemming JH, Ingersoll D, Schmidt C et al. (2005) In vivo electrochemical immunoassays using ElectroNeedles. 2005 NSTI Nanotechnology Conference; http://www.nsti.org/Nanotech2005/showabstract.html?absno=1112

Flores R (2001) A naked plant-specific RNA ten-fold smaller than the smallest known viral RNA: the viroid. CR Acad Sci III 324:943–952

Franke R, Hirsch T, Overwin H et al. (2007) Synthetic mimetics of the CD4 binding site of HIV-1 gp120 for the design of immunogens. Angew Chem Int Ed Engl 46:1253–1255

Freitas RA Jr (1996a) Dermal zippers. Institute for Molecular Manufacturing, internal design study

Freitas RA Jr (1996b) The End of Heart Disease. Institute for Molecular Manufacturing, internal design study

Freitas RA Jr (1998) Exploratory design in medical nanotechnology: A mechanical artificial red cell. Artif Cells Blood Subst Immobil Biotech 26:411–430; http://www.foresight.org/Nanomedicine/Respirocytes.html

Freitas RA Jr (1999) Nanomedicine, Volume I: Basic Capabilities. Landes Bioscience, Georgetown, TX; http://www.nanomedicine.com/NMI.htm; (a) 2.1, (b) Ch. 3, (c) Ch. 4, (d) Ch. 5, (e) Ch. 6, (f) Ch. 7, (g) Ch. 8, (h) 9.3, (i) 9.4, (j) 10.1, (k) 10.2, (m) 8.5.1, (n) 6.4.1, (o) 3.4.2, (p) 3.5, (q) 4.2, (r) 4.3, (s) 4.4, (t) 4.5, (u) 4.6, (v) 4.7, (w) 4.8.2, (x) 9.4.5, (y) 10.4.2, (z) 9.3.5.3.6, (aa) Table 9.3, (ab) 10.5, (ac) 6.3.1, (ad) 6.3.7, (ae) 9.3.1, (af) 5.3.1.4, (ag) 10.4.1.1, (ah) 7.3, (ai) 10.2.3, (aj) 10.4.2.4.2, (ak) 8.5.2.2, (am) 9.3.1.4, (an) 9.3.5.1, (ao) 6.4.3.4, (ap) 7.2.5.4, (aq) 6.3.4.4, (ar) 6.3.4.5, (as) 3.4.1, (at) 9.4.4, (au) 9.4.4.2, (av) 8.4.1.4, (aw) 8.4.3, (ax) 5.2.1, (ay) 8.2.1.2, (az) 5.4, (ba) 5.3.3, (bb) 5.2.4.2, (bc) 9.4.3, (bd) 9.4.3.2, (be) 9.3.2, (bf) 9.4.3.5, (bg) 5.4.2, (bh) 10.3, (bi) 6.3.4, (bj) 4.2.1, (bk) 7.2.2, (bm) 10.3.6, (bn) 9.2.6, (bo) 9.2.4, (bp) 9.2.5, (bq) 9.4.4.1, (br) 8.5.2.1, (bs) 8.2.1.1, (bt) 9.4.1.4, (bu) 5.2.5, (bv) 9.4.4.4, (bw) 9.4.2.6, (bx) 9.4.5.3, (by) 9.4.4.3, (bz) 9.4.6, (ca) 8.5.3.12, (cb) 8.5.4.7, (cc) 10.4.2.1, (cd) 9.2.7, (ce) 9.4.7, (cf) 4.8.6, (cg) 7.3.1, (ch) Table 3.4, (ci) 7.4.5.2, (cj) 4.2.3, (ck) 6.3.3, (cm) 6.5.2, (cn) 4.2.9, (co) 4.8.1, (cp) 4.2.5, (cq) 10.4.1.2, (cr) 10.4.2.5.2, (cs) 4.8.6.4, (ct) 1.3.3, (cu) 5.3.6, (cv) 4.2.8, (cw) 8.3.2

Freitas RA Jr (2000a) Clottocytes: artificial mechanical platelets. IMM Report No. 18, Foresight Update No. 41, pp. 9–11; http://www.imm.org/Reports/Rep018.html

Freitas RA Jr (2000b) Nanodentistry. J Amer Dent Assoc 131:1559–1566; http://www.rfreitas.com/Nano/Nanodentistry.htm

Freitas RA Jr (2002) "Death is an Outrage!" invited lecture, 5th Alcor Conference on Extreme Life Extension, 16 November 2002, Newport Beach, CA; http://www.rfreitas.com/Nano/DeathIsAnOutrage.htm

Freitas RA Jr (2003) Nanomedicine, Volume IIA: Biocompatibility. Landes Bioscience, Georgetown, TX, 2003; http://www.nanomedicine.com/NMIIA.htm; (a) 15.4.3.1, (b) 15.2.3.6, (c) 15.2.4, (d) 15.4.3.6, (e) 15.4.3.1, (f) 15.4.3.6.1, (g) 15.4.3.6.2, (h) 15.4.3.6.3, (i) 15.4.3.6.4, (j) 15.4.3.6.5, (k) 15.4.3.6.6, (m) 15.4.3.6.7, (n) 15.4.3.6.8, (o) 15.4.3.6.9, (p) 15.4.3.6.10, (q) 15.4.3.5, (r) 15.4.2.3, (s) 15.4.2, (t) 15.6.2, (u) 15.5.7.2.3, (v) 15.5.2.1, (w) 15.2.2.4, (x) 15.5.2.3, (y) 15.6.3.5, (z) 15.5.7.2.4, (aa) 15.3.6.5, (ab) 15.2.2

Freitas RA Jr (2005a) "What is Nanomedicine?" Nanomedicine: Nanotech Biol Med 1:2–9; http://www.nanomedicine.com/Papers/WhatIsNMMar05.pdf

Freitas RA Jr (2005b) Microbivores: Artificial mechanical phagocytes using digest and discharge protocol. J Evol Technol 14:1–52; http://www.jetpress.org/volume14/freitas.html

Freitas RA Jr (2005c) Current status of nanomedicine and medical nanorobotics. J Comput Theor Nanosci 2:1–25; http://www.nanomedicine.com/Papers/NMRevMar05.pdf

Freitas RA Jr (2005d) A simple tool for positional diamond mechanosynthesis, and its method of manufacture. U.S. Provisional Patent Application No. 60/543,802, filed 11 February 2004; U.S. Patent Pending, 11 February 2005; http://www.MolecularAssembler.com/Papers/DMSToolbuildProvPat.htm

Freitas RA Jr (2006a) Pharmacytes: an ideal vehicle for targeted drug delivery. J Nanosci Nanotechnol 6:2769–2775; http://www.nanomedicine.com/Papers/JNNPharm06.pdf

Freitas RA Jr (2006b) Economic impact of the personal nanofactory. Nanotechnol Perceptions Rev Ultraprecision Eng Nanotechnol 2:111–126; http://www.rfreitas.com/Nano/NoninflationaryPN.pdf

Freitas RA Jr (2007) The ideal gene delivery vector: Chromallocytes, cell repair nanorobots for chromosome replacement therapy. J Evol Technol 16:1–97; http://jetpress.org/v16/freitas.pdf

Freitas RA Jr (2009) Computational tasks in medical nanorobotics. In: Eshaghian-Wilner MM (ed) Bio-inspired and Nano-scale Integrated Computing. Wiley, New York; http://www.nanomedicine.com/Papers/NanorobotControl2009.pdf

Freitas RA Jr, Merkle RC (2004) Kinematic Self-Replicating Machines. Landes Bioscience, Georgetown, TX; http://www.molecularassembler.com/KSRM.htm; (a) Section 5.7, (b) 5.9.4, (c) 3.8, (d) 4.20

Freitas RA Jr, Merkle RC (2008) A minimal toolset for positional diamond mechanosynthesis. J Comput Theor Nanosci 5: 760–861; http://www.molecularassembler.com/Papers/MinToolset.pdf

Freitas RA Jr, Phoenix CJ (2002) Vasculoid: A personal nanomedical appliance to replace human blood. J Evol Technol 11:1–139; http://www.jetpress.org/volume11/vasculoid.pdf

Freitas RA Jr, Allis DG, Merkle RC (2007) Horizontal Ge-substituted polymantane-based C_2 dimer placement tooltip motifs for diamond mechanosynthesis. J Comput Theor Nanosci 4:433–442; http://www.MolecularAssembler.com/Papers/DPTMotifs.pdf

Frey M, Koller T, Lezzi M (1982) Isolation of DNA from single microsurgically excised bands of polytene chromosomes of *Chironomus*. Chromosoma 84:493–503

Friedenstein AJ, Gorskaja JF, Kulagina NN (1976) Fibroblast precursors in normal and irradiated mouse hematopoietic organs. Exp Hematol 4:267–274

Frost EE, Nielsen JA, Le TQ et al. (2003) PDGF and FGF2 regulate oligodendrocyte progenitor responses to demyelination. J Neurobiol 54:457–472

Fuchs E (1996) The cytoskeleton and disease: genetic disorders of intermediate filaments. Annu Rev Genet 30:197–231

Fuhrer G, Gallimore MJ, Heller W (1990) FXII. Blut 61:258–266

Fujiwara K, Takahashi K, Shirota K et al. (1981) Fine pathology of mouse spinal cord infected with the Tyzzer organism. Jpn J Exp Med 51:171–178

Furber JD (2006) Extracellular glycation crosslinks: prospects for removal. Rejuvenation Res. 9:274–278

Galou M, Gao J, Humbert J (1997) The importance of intermediate filaments in the adaptation of tissues to mechanical stress: evidence from gene knockout studies. Biol Cell 89:85–97

Garibotti AV, Liao S, Seeman NC (2007) A simple DNA-based translation system. Nano Lett 7:480–483

Gearing DP, Nagley P (1986) Yeast mitochondrial ATPase subunit 8, normally a mitochondrial gene product, expressed in vitro and imported back into the organelle. EMBO J 5:3651–3655

Georgatos SD, Theodoropoulos PA (1999) Rules to remodel by: what drives nuclear envelope disassembly and reassembly during mitosis? Crit Rev Eukaryot Gene Expr 9:373–381

Gersh BJ, Simari RD (2006) Cardiac cell-repair therapy: clinical issues. Nat Clin Pract Cardiovasc Med 3:S105-S109

Giannoudis PV, Pountos I, Pape HC et al. (2007) Safety and efficacy of vena cava filters in trauma patients. Injury 38:7–18

Glozman D, Shoham M (2006) Flexible needle steering for percutaneous therapies. Comput Aided Surg 11:194–201

Goddard WA III (1995) Computational Chemistry and Nanotechnology. Presentation at the 4th Foresight Conference on Molecular Nanotechnology, November 1995

Gomord V, Denmat LA, Fitchette-Lainé AC et al. (1997) The C-terminal HDEL sequence is sufficient for retention of secretory proteins in the endoplasmic reticulum (ER) but promotes vacuolar targeting of proteins that escape the ER. Plant J 11:313–325

Gordon KE, Ferris DP (2007) Learning to walk with a robotic ankle exoskeleton. J Biomech 40:2636–2644

Gouaux E, Mackinnon R (2005) Principles of selective ion transport in channels and pumps. Science 310:1461–1465

Gouverneur M, Berg B, Nieuwdorp M et al. (2006) Vasculoprotective properties of the endothelial glycocalyx: effects of fluid shear stress. J Intern Med 259:393–400

Green JE, Choi JW, Boukai A et al. (2007) A 160-kilobit molecular electronic memory patterned at 10(11) bits per square centimetre. Nature 445:414–417

Grobbee DE, Bots ML (2004) Atherosclerotic disease regression with statins: studies using vascular markers. Int J Cardiol 96:447–459

Groves JD, Wang L, Tanner MJ (1998) Functional reassembly of the anion transport domain of human red cell band 3 (AE1) from multiple and non-complementary fragments. FEBS Lett 433:223–227

Grudzien E, Stepinski J, Jankowska-Anyszka M et al. (2004) Novel cap analogs for in vitro synthesis of mRNAs with high translational efficiency. RNA 10:1479–1487

Guan JZ, Maeda T, Sugano M et al. (2007) Change in the telomere length distribution with age in the Japanese population. Mol Cell Biochem 304:353–360

Guardavaccaro D, Pagano M (2006) Stabilizers and destabilizers controlling cell cycle oscillators. Mol Cell 22:1–4

Guet CC, Elowitz MB, Hsing W (2002) Combinatorial synthesis of genetic networks. Science 296:1466–1470; http://www.aph.caltech.edu/people/CombinatorialNetworks.pdf

Gurdon JB (2006) Nuclear transplantation in *Xenopus*. Methods Mol Biol 325:1–9

Hackstadt T (1996) The biology of rickettsiae. Infect Agents Dis 5:127–143

Hadi HA, Carr CS, Al Suwaidi J (2005) Endothelial dysfunction: cardiovascular risk factors, therapy, and outcome. Vasc Health Risk Manag 1:183–198

Hagios C, Lochter A, Bissell MJ (1998) Tissue architecture: the ultimate regulator of epithelial function? Philos Trans R Soc Lond B Biol Sci 353:857–870

Hall JS (1993) Utility fog: A universal physical substance. Vision-21: Interdisciplinary Science and Engineering in the Era of Cyberspace, Westlake OH. NASA Conference Publication CP-10129, pp. 115–126

Hall JS (1996) Utility fog: The stuff that dreams are made of. In: Crandall BC (ed) Nanotechnology: Molecular Speculations on Global Abundance. MIT Press, Cambridge, MA, pp. 161–184; http://www.kurzweilai.net/meme/frame.html?main=/articles/art0220.html?m%3D7

Han SW, Nakamura C, Obataya I et al. (2005) A molecular delivery system by using AFM and nanoneedle. Biosens Bioelectron 20:2120–2125

Hanly EJ, Miller BE, Kumar R et al. (2006) Mentoring console improves collaboration and teaching in surgical robotics. J Laparoendosc Adv Surg Tech A 16:445–451

Harman D (1972) The biologic clock: the mitochondria? J Am Geriatr Soc 20:145–147

Harman D (1989) Lipofuscin and ceroid formation: the cellular recycling system. Adv Exp Med Biol 266:3–15

Harrison DE, Astle CM (1982) Loss of stem cell repopulating ability upon transplantation. Effects of donor age, cell number, and transplantation procedure. J Exp Med 156:1767–1779

Hayashi JI, Ohtall S, Kagawall Y et al. (1994) Nuclear but not mitochondrial genome involvement in human age-related mitochondrial dysfunction: Functional integrity of mitochondrial DNA from aged subjects. J Biol Chem 269:6878–6883

Heath JR (2000) Wires, switches, and wiring. A route toward a chemically assembled electronic nanocomputer. Pure Appl Chem 72:11–20; http://www.iupac.org/publications/pac/2000/7201/7201pdf/2_heath.pdf

Hedenborg M, Klockars M (1989) Quartz-dust-induced production of reactive oxygen metabolites by human granulocytes. Lung 167:23–32

Hein S, Kostin S, Heling A et al. (2000) The role of the cytoskeleton in heart failure. Cardiovasc Res 45:273–278

Heinzelmann-Schwarz VA, Gardiner-Garden M, Henshall SM et al. (2004) Overexpression of the cell adhesion molecules DDR1, Claudin 3, and Ep-CAM in metaplastic ovarian epithelium and ovarian cancer. Clin Cancer Res 10:4427–4436

Heisterkamp A, Maxwell IZ, Mazur E et al. (2005) Pulse energy dependence of subcellular dissection by femtosecond laser pulses. Opt Express 13:3690–3696

Henry M, Polydorou A, Henry I et al. (2007) New distal embolic protection device the FiberNet 3 dimensional filter: first carotid human study. Catheter Cardiovasc Interv 69:1026–1035

Hertzendorf LR, Stehling L, Kurec AS et al. (1987) Comparison of bleeding times performed on the arm and the leg. Am J Clin Pathol 87:393–396

Heydorn AO, Mehlhorn H (1987) Fine structure of *Sarcocystis arieticanis Heydorn*, 1985 in its intermediate and final hosts (sheep and dog). Zentralbl Bakteriol Mikrobiol Hyg A 264: 353–362

Higson FK , Jones OT (1984) Oxygen radical production by horse and pig neutrophils induced by a range of crystals. J Rheumatol 11:735–740

Hinek A (1997) Elastin receptor and cell-matrix interactions in heart transplant-associated arteriosclerosis. Arch Immunol Ther Exp (Warsz) 45:15–29

Ho KL (1987) Crystalloid bodies in skeletal muscle of hypothyroid myopathy. Ultrastructural and histochemical studies. Acta Neuropathol (Berl) 74:22–32

Holmbeck K, Bianco P, Yamada S et al. (2004) MT1-MMP: a tethered collagenase. J Cell Physiol 200:11–19

Holmlin RE, Schiavoni M, Chen CY et al. (2000) Light-driven microfabrication: assembly of multicomponent, three-dimensional structures by using optical tweezers. Angew Chem Intl. Ed. 39:3503–3506

Huang TJ, Lu W, Tseng HR et al. (2003) Molecular shuttle switching in closely packed Langmuir films, 11th Foresight Conf. Mol. Nanotech., San Francisco, CA, 10–12 October 2003

Hull RL, Westermark GT, Westermark P et al. (2004) Islet amyloid: a critical entity in the pathogenesis of type 2 diabetes. J Clin Endocrinol Metab 89:3629–3643

Ichikawa O, Osawa M, Nishida N et al. (2007) Structural basis of the collagen-binding mode of discoidin domain receptor 2. EMBO J. 26:4168–4176

Imberti D, Ageno W, Carpenedo M (2006) Retrievable vena cava filters: a review. Curr Opin Hematol 13:351–356

Ishiyama K, Sendoh M, Arai KI (2002) Magnetic micromachines for medical applications. J Magnetism Magnetic Mater 242–245:1163–1165

Jakab K, Neagu A, Mironov V et al. (2004) Organ printing: fiction or science. Biorheology 41: 371–375

Jakab K, Damon B, Neagu A et al. (2006) Three-dimensional tissue constructs built by bioprinting. Biorheology 43:509–513

James TJ, Sharma SP (1995) Regional and lobular variation in neuronal lipofuscinosis in rat cerebellum: influence of age and protein malnourishment. Gerontology 41:213–228

James TJ, Sharma SP, Gupta SK et al. (1992) 'Dark' cell formation under protein malnutrition: process of conversion and concept of 'semi-dark' type Purkinje cells. Indian J Exp Biol 30: 470–473

Jeffries GD, Edgar JS, Zhao Y et al. (2007) Using polarization-shaped optical vortex traps for single-cell nanosurgery. Nano Lett 7:415–420

Jeon KW, Lorch IJ, Danielli JF (1970) Reassembly of living cells from dissociated components. Science 167:1626–1627

Johnson LR, Scott MG, Pitcher JA (2004) G protein-coupled receptor kinase 5 contains a DNA-binding nuclear localization sequence. Mol Cell Biol 24:10169–10179

Johnston SC, Riddle SM, Cohen RE et al. (1999) Structural basis for the specificity of ubiquitin C-terminal hydrolases. EMBO J 18:3877–3887

Jones BJ, Murphy CR (1994) A high resolution study of the glycocalyx of rat uterine epithelial cells during early pregnancy with the field emission gun scanning electron microscope. J Anat 185:443–446

Kamnasaran D, Muir WJ, Ferguson-Smith MA et al. (2003) Disruption of the neuronal PAS3 gene in a family affected with schizophrenia. J Med Genet 40:325–332

Kano F, Nagayama K, Murata M (2000) Reconstitution of the Golgi reassembly process in semi-intact MDCK cells. Biophys Chem 84:261–268

Kapoor A, Li M, Taylor RH (2005) Spatial motion constraints for robot assisted suturing using virtual fixtures. Med Image Comput Comput Assist Interv Int Conf Med Image Comput Comput Assist Interv 8:89–96

Kapyla J, Pentikainen OT, Nyronen T et al. (2007) Small molecule designed to target metal binding site in the alpha2I domain inhibits integrin function. J Med Chem 50:2742–2746

Kasirajan K, Marek JM, Langsfeld M (2001) Mechanical thrombectomy as a first-line treatment for arterial occlusion. Semin Vasc Surg 14:123–131

Katz RD, Taylor JA, Rosson GD et al. (2006) Robotics in plastic and reconstructive surgery: use of a telemanipulator slave robot to perform microvascular anastomoses. J Reconstr Microsurg 22:53–57

Kaushik S, Cuervo AM (2006) Autophagy as a cell-repair mechanism: activation of chaperone-mediated autophagy during oxidative stress. Mol Aspects Med 27:444–454

Kawashima R, Kawamura YI, Kato R et al. (2006) IL-13 receptor alpha2 promotes epithelial cell regeneration from radiation-induced small intestinal injury in mice. Gastroenterology 131: 130–141

Kay ER, Leigh DA, Zerbetto F (2007) Synthetic molecular motors and mechanical machines. Angew Chem Int Ed 46:72–191

Keane FM, Loughman A, Valtulina V et al. (2007) Fibrinogen and elastin bind to the same region within the A domain of fibronectin binding protein A, an MSCRAMM of *Staphylococcus aureus*. Mol Microbiol 63:711–723

Keats BJ, Corey DP (1999) The usher syndromes. Am J Med Genet 89:158–166

Kelly TR, De Silva H, Silva RA (1999) Unidirectional rotary motion in a molecular system. Nature 401:150–152

Kenny T (2007) Tip-Based Nanofabrication (TBN). Defense Advanced Research Projects Agency (DARPA)/Microsystems Technology Office (MTO), Broad Agency Announcement BAA 07–59; http://www.fbo.gov/spg/ODA/DARPA/CMO/BAA07-59/listing.html

Kessler N, Perl-Treves D, Addadi L et al. (1999) Structural and chemical complementarity between antibodies and the crystal surfaces they recognize. Proteins 34:383–394

Kida E, Golabek AA, Wisniewski KE (2001) Cellular pathology and pathogenic aspects of neuronal ceroid lipofuscinoses. Adv Genet 45:35–68

Kilhamn J (2003) The protective mucus and its mucins produced by enterocytes and goblet cells. Centrum for Gastroenterologisk Forskning, Goteborgs Universitet; http://www.cgf.gu.se/fouschema.html

Kim PS, Arvan P (1998) Endocrinopathies in the family of endoplasmic reticulum (ER) storage diseases: disorders of protein trafficking and the role of ER molecular chaperones. Endocr Rev 19:173–202

Kirson ED, Yaari Y (2000) A novel technique for micro-dissection of neuronal processes. J Neurosci Methods 98:119–122

Knight CG, Lorincz A, Cao A et al. (2005) Computer-assisted, robot-enhanced open microsurgery in an animal model. J Laparoendosc Adv Surg Tech A 15:182–185

Knutson KL (2002) GMK (Progenics Pharmaceuticals). Curr Opin Investig Drugs 3:159–164

Koenig W, Khuseyinova N (2007) Biomarkers of atherosclerotic plaque instability and rupture. Arterioscler Thromb Vasc Biol 27:15–26

Kohli V, Elezzabi AY, Acker JP (2005) Cell nanosurgery using ultrashort (femtosecond) laser pulses: Applications to membrane surgery and cell isolation. Lasers Surg Med 37:227–230

Konig K, Riemann I, Fischer P et al. (1999) Intracellular nanosurgery with near infrared femtosecond laser pulses. Cell Mol Biol 45:195–201

Korf BR, Diacumakos EG (1978) Microsurgically-extracted metaphase chromosomes of the Indian muntjac examined with phase contrast and scanning electron microscopy. Exp Cell Res 111: 83–93

Korf BR, Diacumakos EG (1980) Absence of true interchromosomal connectives in microsurgically isolated chromosomes. Exp Cell Res 130:377–385

Kosaka K (2000) Diffuse Lewy body disease. Neuropathology 20:S73–S78

Koumura N, Zijlstra RW, van Delden RA et al. (1999) Light-driven monodirectional molecular rotor. Nature 401:152–155

Kristo B, Liao JC, Neves HP et al. (2003) Microelectromechanical systems in urology. Urology 61:883–887; http://liaolab.stanford.edu/images/paper5_urology_2003.pdf

Ku J, Mraz R, Baker N et al. (2003) A data glove with tactile feedback for FMRI of virtual reality experiments. Cyberpsychol Behav 6:497–508

Kuczera K (1996) Free energy simulations of axial contacts in sickle-cell hemoglobin. Biopolymers 39:221–242

Kumar R, Ansell JE, Canoso RT et al. (1978) Clinical trial of a new bleeding-time device. Am J Clin Pathol 70:642–645

Kumar S, Yin X, Trapp BD et al. (2002) Role of long-range repulsive forces in organizing axonal neurofilament distributions: evidence from mice deficient in myelin-associated glycoprotein. J Neurosci Res 68:681–690; http://hohlab.bs.jhmi.edu/Hoh_lab_Media/neuro_JNR.pdf

Landauer TK (1986) How much do people remember? Some estimates of the quantity of learned information in long-term memory. Cognitive Sci 10:477–493

Lapidus IR, Schiller R (1978) A model for traveling bands of chemotactic bacteria. Biophys J 22:1–13

Lasker Foundation (2000) Exceptional Returns: The Economic Value of America's Investment in Medical Research. Funding First Reports, Lasker Medical Research Network, May 2000, p. 5; http://www.laskerfoundation.org/reports/pdf/exceptional.pdf

Lederer MO, Bühler HP (1999) Cross-linking of proteins by Maillard processes – characterization and detection of a lysine-arginine cross-link derived from D-glucose. Bioorg Med Chem 7:1081–1088

Lee HJ, Ho W (1999) Single bond formation and characterization with a scanning tunneling microscope. Science 286:1719–1722; http://www.physics.uci.edu/%7Ewilsonho/stm-iets.html

Lee S, Desai KK, Iczkowski KA et al. (2006) Coordinated peak expression of MMP-26 and TIMP-4 in preinvasive human prostate tumor. Cell Res 16:750–758

Lee VM (1995) Disruption of the cytoskeleton in Alzheimer's disease. Curr Opin Neurobiol 5: 663–668

Leferovich JM, Bedelbaeva K, Samulewicz S et al. (2001) Heart regeneration in adult MRL mice. Proc Natl Acad Sci USA 98:9830–9835; http://www.pnas.org/cgi/content/full/98/17/9830

Lehrer RI, Ganz T (1995) Chapter 87. Biochemistry and function of monocytes and macrophages. In: William's Hematology, 5th edn. McGraw-Hill, New York, pp. 869–875

Leigh DA, Wong JKY, Dehez F et al. (2003) Unidirectional rotation in a mechanically interlocked molecular rotor. Nature 424:174–179

Lemler MS, Bies RD, Frid MG et al. (2000) Myocyte cytoskeletal disorganization and right heart failure in hypoxia-induced neonatal pulmonary hypertension. Am J Physiol Heart Circ Physiol 279:H1365–H1376

Li RA, Jensen J, Bowersox JC (2000) Microvascular anastomoses performed in rats using a microsurgical telemanipulator. Comput Aided Surg 5:326–332

Li WJ, Xi N (2004) Novel micro gripping, probing, and sensing devices for single-cell surgery. Conf Proc IEEE Eng Med Biol Soc 4:2591–2594

Liang X, Zhao J, Hajivandi M et al. (2006) Quantification of membrane and membrane-bound proteins in normal and malignant breast cancer cells isolated from the same patient with primary breast carcinoma. J Proteome Res 5:2632–2641

Lind SE (1995) Chapter 33. The Hemostatic System. In: Handin RI, Stossel TP, Lux SE (eds) Blood: Principles and Practice of Hematology. J.B. Lippincott Co., Philadelphia, PA, pp. 949–972

Lipinski MJ, Fuster V, Fisher EA et al. (2004) Technology insight: targeting of biological molecules for evaluation of high-risk atherosclerotic plaques with magnetic resonance imaging. Nat Clin Pract Cardiovasc Med 1:48–55

Liu SC, Derick LH, Agre P et al. (1990) Alteration of the erythrocyte membrane skeletal ultrastructure in hereditary spherocytosis, hereditary elliptocytosis, and pyropoikilocytosis. Blood 76:198–205

Livingston P (1998) Ganglioside vaccines with emphasis on GM2. Semin Oncol 25:636–645

Lomer WM (1951) A dislocation reaction in the face-centered cubic lattice. Phil Mag 42: 1327–1331

Lopez I, Honrubia V, Baloh RW (1997) Aging and the human vestibular nucleus. J Vestib Res 7:77–85

Lovelock JE, Smith AU (1956) Studies on golden hamsters during cooling to and rewarming from body temperatures below 0 degrees C. Proc R Soc Lond B Biol Sci 145:391–442

Lu SJ, Feng Q, Caballero S et al. (2007) Generation of functional hemangioblasts from human embryonic stem cells. Nature Methods 4:501–509

Lynnerup N, Kjeldsen H, Heegaard S et al. (2008) Radiocarbon dating of the human eye lens crystallines reveal proteins without carbon turnover throughout life. PLoS ONE 3:e1529; http://www.plosone.org/article/info:doi/10.1371/journal.pone.0001529

Malorni W, Matarrese P, Tinari A et al. (2007) Xeno-cannibalism: a survival "escamotage". Autophagy 3:75–77

Malyankar UM (2007) Tumor-associated antigens and biomarkers in cancer and immune therapy. Int Rev Immunol 26:223–247

Maniotis AJ, Bojanowski K, Ingber DE (1997) Mechanical continuity and reversible chromosome disassembly within intact genomes removed from living cells. J Cell Biochem 65:114–130

Mann DJ, Peng J, Freitas RA Jr et al. (2004) Theoretical analysis of diamond mechanosynthesis. Part II. C_2 mediated growth of diamond C(110) surface via Si/Ge-triadamantane dimer placement tools. J Comput Theor Nanosci 1:71–80; http://www.MolecularAssembler.com/JCTNMannMar04.pdf

Marrink SJ, Lindahl E, Edholm O et al. (2001) Simulation of the spontaneous aggregation of phospholipids into bilayers. J Am Chem Soc 123:8638–8639

Marszalek JR, Ruiz-Lozano P, Roberts E et al. (1999) Situs inversus and embryonic ciliary morphogenesis defects in mouse mutants lacking the KIF3A subunit of kinesin-II. Proc Natl Acad Sci USA 96:5043–5048; http://www.pnas.org/cgi/content/full/96/9/5043

Martel S, Hunter I (2002) Nanofactories based on a fleet of scientific instruments configured as miniature autonomous robots. Proc 3rd Intl Workshop on Microfactories; 16–18 Sep 2002; Minneapolis, MN, pp. 97–100

Martel S, Mathieu JB, Felfoul O et al. (2007) Automatic navigation of an untethered device in the artery of a living animal using a conventional clinical magnetic resonance imaging system. Appl Phys Lett 90:114105; http://wiki.polymtl.ca/nano/fr/images/1/14/J-2007-MRSUB-APL-Sylvain2.pdf

Marty AM, Jahrling PB, Geisbert TW (2006) Viral hemorrhagic fevers. Clin Lab Med 26:345–386

Mathieu JB, Martel S, Yahia L et al. (2005) MRI systems as a mean of propulsion for a microdevice in blood vessels. Biomed Mater Eng 15:367

Matsumuro K, Izumo S, Minauchi Y et al. (1993) Chronic demyelinating neuropathy and intra-axonal polyglucosan bodies. Acta Neuropathol (Berl) 86:95–99

Mattson MP (2004) Pathways towards and away from Alzheimer's disease. Nature 430:631–639

Mayes PA (1993) Metabolism of acylglycerols and sphingolipids. In: Murray RK, Granner DK, Mayes PA, Rodwell VW (eds) (1993) Harper's Biochemistry, 23rd edn. Appleton & Lange, Norwalk, CT, pp. 241–249

Mazzatenta A, Giugliano M, Campidelli S et al. (2007) Interfacing neurons with carbon nanotubes: electrical signal transfer and synaptic stimulation in cultured brain circuits. J Neurosci 27: 6931–6936

McColl R, Brown I, Seligman C et al. (2006) Haptic rendering for VR laparoscopic surgery simulation. Australas Phys Eng Sci Med 29:73–78

McGuigan AP, Sefton MV (2006) Vascularized organoid engineered by modular assembly enables blood perfusion. Proc Natl Acad Sci USA 103:11461–11466

McHolm GB, Aguilar MJ, Norris FH (1984) Lipofuscin in amyotrophic lateral sclerosis. Arch Neurol 41:1187–1188

McNulty R, Wang H, Mathias RT et al. (2004) Regulation of tissue oxygen levels in the mammalian lens. J Physiol 559:883–898; http://jp.physoc.org/cgi/content/full/559/3/883

McQuibban GA, Gong JH, Tam EM et al. (2000) Inflammation dampened by gelatinase A cleavage of monocyte chemoattractant protein-3. Science 289:1202–1206
McWilliams A (2006) Nanotechnology: A Realistic Market Assessment. BCC Research, July 2006; http://www.bccresearch.com/nan/NAN031B.asp
Meissner A, Jaenisch R (2006) Mammalian nuclear transfer. Dev Dyn 235:2460–2469
Menciassi A, Quirini M, Dario P (2007) Microrobotics for future gastrointestinal endoscopy. Minim Invasive Ther Allied Technol 16:91–100
Méndez-Vilas A, Gallardo-Moreno AM, González-Martín ML (2006) Nano-mechanical exploration of the surface and sub-surface of hydrated cells of *Staphylococcus epidermidis*. Antonie Van Leeuwenhoek 89:373–386
Merkle RC (1997) A proposed 'metabolism' for a hydrocarbon assembler. Nanotechnology 8: 149–162; http://www.zyvex.com/nanotech/hydroCarbonMetabolism.html
Merkle RC, Freitas RA Jr (2003) Theoretical analysis of a carbon-carbon dimer placement tool for diamond mechanosynthesis. J Nanosci Nanotechnol 3:319–324; http://www.rfreitas.com/Nano/JNNDimerTool.pdf
Methuselah Foundation (2007); http://www.sens.org
Miettinen M, Lasota J (2006) Gastrointestinal stromal tumors: review on morphology, molecular pathology, prognosis, and differential diagnosis. Arch Pathol Lab Med 130:1466–1478
Mironov V, Boland T, Trusk T et al. (2003) Organ printing: computer-aided jet-based 3-D tissue engineering. Trends Biotechnol 21:157–161
Miyake K, McNeil PL (1995) Vesicle accumulation and exocytosis at sites of plasma membrane disruption. J Cell Biol 131:1737–1745
Monash University (2006) Micro-robots take off as ARC announces funding. Press release, 11 October 2006; http://www.monash.edu.au/news/newsline/story/1038
Moore WA, Davey VA, Weindruch R et al. (1995) The effect of caloric restriction on lipofuscin accumulation in mouse brain with age. Gerontology 41:173–185
Morowitz HJ (1974) Manufacturing a living organism. Hospital Practice 9:210–215
Moskovits M (2007) Nanoassemblers: A likely threat? Nanotech. Law & Bus. 4:187–195
Mountain V, Compton DA (2000) Dissecting the role of molecular motors in the mitotic spindle. Anat Rec 261:14–24
Murakami T, Garcia CA, Reiter LT et al. (1996) Charcot-Marie-Tooth disease and related inherited neuropathies. Medicine (Baltimore) 75:233–250
Mureebe L, McKinsey JF (2006) Infrainguinal arterial intervention: is there a role for an atherectomy device? Vascular 14:313–318
Murphy KM, Topel R (1999) The economic value of medical research. Funding First Reports, Lasker Medical Research Network, Lasker Foundation, March 1998, revised September 1999; http://www.laskerfoundation.org/reports/pdf/economicvalue.pdf
Murray RK, Granner DK, Mayes PA, Rodwell VW (1993) Harper's Biochemistry, 23rd edn. Appleton & Lange, Norwalk, CT
Nagahara L, Tao N, Thundat T (2008) Introduction to Nanosensors. Springer, New York
Nanofactory Collaboration website (2007a); http://www.MolecularAssembler.com/Nanofactory
Nanofactory Collaboration website (2007b) Remaining technical challenges for achieving positional diamondoid molecular manufacturing and diamondoid nanofactories; http://www.MolecularAssembler.com/Nanofactory/Challenges.htm
Nelson KL, Geyer S (1991) Bioreactor and process design for large-scale mammalian cell culture manufacturing. Bioprocess Technol 13:112–143
Nimmerjahn A, Kirchhoff F, Helmchen F (2005) Resting microglial cells are highly dynamic surveillants of brain parenchyma in vivo. Science 308:1314–1318
Nony PA, Schnellmann RG (2003) Mechanisms of renal cell repair and regeneration after acute renal failure. J Pharmacol Exp Ther 304:905–912
Nordquist L, Roxhed N, Griss P et al. (2007) Novel microneedle patches for active insulin delivery are efficient in maintaining glycaemic control: an initial comparison with subcutaneous administration. Pharm Res 24:1381–1388

Normanno N, De Luca A, Bianco C et al. (2006) Epidermal growth factor receptor (EGFR) signaling in cancer. Gene 366:2–16

Obataya I, Nakamura C, Han S et al. (2005) Mechanical sensing of the penetration of various nanoneedles into a living cell using atomic force microscopy. Biosens Bioelectron 20: 1652–1655

O'Connor MN, Smethurst PA, Farndale RW et al. (2006) Gain- and loss-of-function mutants confirm the importance of apical residues to the primary interaction of human glycoprotein VI with collagen. J Thromb Haemost 4:869–873

O'Gorman E, Piendl T, Muller M et al. (1997) Mitochondrial intermembrane inclusion bodies: the common denominator between human mitochondrial myopathies and creatine depletion, due to impairment of cellular energetics. Mol Cell Biochem 174:283–289

Oh JO (1985) Immunology of viral infections. Int Ophthalmol Clin 25:107–116

Olbrich H, Haffner K, Kispert A et al. (2002) Mutations in DNAH5 cause primary ciliary dyskinesia and randomization of left-right asymmetry. Nature Genet 30:143–144

Olson AL, Pessin JE (1996) Structure, function, and regulation of the mammalian facilitative glucose transporter gene family. Annu Rev Nutr 16:235–256

Oyabu N, Custance O, Yi I et al. (2003) Mechanical vertical manipulation of selected single atoms by soft nanoindentation using near contact atomic force microscopy. Phys Rev Lett 90:176102; http://link.aps.org/abstract/PRL/v90/e176102

Padron Velazquez JL (2006) Stem cell fusion as an ultimate line of defense against xenobiotics. Med Hypotheses 67:383–387

Paleri V, Stafford FW, Sammut MS (2005) Laser debulking in malignant upper airway obstruction. Head Neck 27:296–301

Pantaloni D, Le Clainche C, Carlier MF (2001) Mechanism of actin-based motility. Science 292:1502–1506

Parpura V, Haydon PG, Henderson E (1993) Three-dimensional imaging of living neurons and glia with the atomic force microscope. J Cell Sci 104:427–432; http://jcs.biologists.org/cgi/reprint/104/2/427.pdf

Patel SH, Patel R (2007) Inferior vena cava filters for recurrent thrombosis: current evidence. Tex Heart Inst J 34:187–194

Patolsky F, Timko BP, Yu G et al. (2006) Detection, stimulation, and inhibition of neuronal signals with high-density nanowire transistor arrays. Science 313:1100–1104

Patton RL, Kalback WM, Esh CL et al. (2006) Amyloid-beta peptide remnants in AN-1792-immunized Alzheimer's disease patients: a biochemical analysis. Am J Pathol 169:1048–1063

Peacock EE Jr (1984) Wound Repair. WB Saunders Company, Philadelphia, PA

Pecka Z (1993) Intranuclear development of asexual and sexual generations of *Eimeria hermani* Farr, 1953, the coccidian parasite of geese. Zentralbl Bakteriol 278:570–576

Peng J, Freitas RA Jr., Merkle RC et al. (2006) Theoretical analysis of diamond mechanosynthesis. Part III. Positional C_2 deposition on diamond C(110) surface using Si/Ge/Sn-based dimer placement tools. J Comput Theor Nanosci 3:28–41; http://www.MolecularAssembler.com/Papers/JCTNPengFeb06.pdf

Perez LC (1999) Septic arthritis. Baillieres Best Pract Res Clin Rheumatol 13:37–58

Permanne B, Adessi C, Saborio GP et al. (2002) Reduction of amyloid load and cerebral damage in a transgenic mouse model of Alzheimer's disease by treatment with a beta-sheet breaker peptide. FASEB J 16:860–862

Pesaran B, Musallam S, Andersen RA (2006) Cognitive neural prosthetics. Curr Biol 16:R77–R80

Pieper RO (1997) Understanding and manipulating O6-methylguanine-DNA methyltransferase expression. Pharmacol Ther 74:285–297

Pipinos II, Bruzoni M, Johanning JM et al. (2006) Transcervical carotid stenting with flow reversal for neuroprotection: technique, results, advantages, and limitations. Vascular 14:245–255

Pogach MS, Cao Y, Millien G et al. (2007) Key developmental regulators change during hyperoxia-induced injury and recovery in adult mouse lung. J Cell Biochem 100:1415–1429

Powell JJ, Ainley CC, Harvey RS et al. (1996) Characterisation of inorganic microparticles in pigment cells of human gut associated lymphoid tissue. Gut 38:390–395

Poznansky MC, Evans RH, Foxall RB et al. (2000) Efficient generation of human T cells from a tissue-engineered thymic organoid. Nat Biotechnol 18:729–734

Primmer S (2006) First Public Meeting of the Supercentenarian Research Foundation: Meeting Report by Stan Primmer, President of the SRF. GRG Breaking News Items [2006], 4 June 2006; http://www.grg.org/breakingnews2006.htm

Protiveris Corp. (2003) Microcantilever arrays; http://www.protiveris.com/cantilever_tech/microcantileverarrays.html

Prusiner SB (2001) Shattuck lecture – neurodegenerative diseases and prions. New Engl J Med 344:1516–1526

Qin H, Rosenbaum JL, Barr MM (2001) An autosomal recessive polycystic kidney disease gene homolog is involved in intraflagellar transport in *C. elegans* ciliated sensory neurons. Curr Biol 11:457–461

Quan T, He T, Shao Y et al. (2006) Elevated cysteine-rich 61 mediates aberrant collagen homeostasis in chronologically aged and photoaged human skin. Am J Pathol 169:482–490; http://ajp.amjpathol.org/cgi/content/full/169/2/482

Rabouille C, Misteli T, Watson R et al. (1995) Reassembly of Golgi stacks from mitotic Golgi fragments in a cell-free system. J Cell Biol 129:605–618

Rajnoch C, Ferguson S, Metcalfe AD et al. (2003) Regeneration of the ear after wounding in different mouse strains is dependent on the severity of wound trauma. Dev Dyn 226:388–397; http://www3.interscience.wiley.com/cgi-bin/fulltext/102525230/PDFSTART

Rayment I, Holden HM, Sellers JR et al. (1995) Structural interpretation of the mutations in the beta-cardiac myosin that have been implanted in familial hypertrophic cardiomyopathy. Proc Natl Acad Sci USA 92:3864–3868

Reed MA, Lee T (eds) (2003) Molecular Nanoelectronics. American Scientific Publishers, Stevenson Ranch, CA

Rehling P, Wiedemann N, Pfanner N et al. (2001) The mitochondrial import machinery for preproteins. Crit Rev Biochem Mol Biol 36:291–336

Reilein AR, Rogers SL, Tuma MC et al. (2001) Regulation of molecular motor proteins. Int Rev Cytol 204:179–238

Reinboth JJ, Gautschi K, Munz K et al. (1997) Lipofuscin in the retina: quantitative assay for an unprecedented autofluorescent compound (pyridinium bis-retinoid, A2-E) of ocular age pigment. Exp Eye Res 65:639–643

Reinders ME, Rabelink TJ, Briscoe DM (2006) Angiogenesis and endothelial cell repair in renal disease and allograft rejection. J Am Soc Nephrol 17:932–942

Rishikof DC, Lucey EC, Kuang PP et al. (2006) Induction of the myofibroblast phenotype following elastolytic injury to mouse lung. Histochem Cell Biol 125:527–534

Rizun PR, McBeth PB, Louw DF et al. (2004) Robot-assisted neurosurgery. Semin Laparosc Surg 11:99–106

Rizun P, Gunn D, Cox B et al. (2006) Mechatronic design of haptic forceps for robotic surgery. Int J Med Robot 2:341–349

Robson B (1998) Doppelganger proteins as drug leads. Nature Biotechnol 14:892–893

Robson B, Pseudoproteins: Non-protein protein-like machines. Paper presented at 6th Foresight Conference on Molecular Nanotechnology, November 1998

Roemer A, Schwettmann L, Jung M et al. (2004) The membrane proteases adams and hepsin are differentially expressed in renal cell carcinoma. Are they potential tumor markers? J Urol 172:2162–2166

Roffe C (1998) Ageing of the heart. Br J Biomed Sci 55:136–148

Rohs R, Bloch I, Sklenar H et al. (2005) Molecular flexibility in *ab initio* drug docking to DNA: binding-site and binding-mode transitions in all-atom Monte Carlo simulations. Nucleic Acids Res 33:7048–7057

Roth EA, Xu T, Das M et al. (2004) Inkjet printing for high-throughput cell patterning. Biomaterials 25:3707–3715

Royer RJ, Delongeas JL, Netter P et al. (1982) Inflammatory effect of aluminium phosphate on rat paws. Pathol Biol (Paris) 30:211–215

Sacconi L, Tolic-Norrelykke IM, Antolini R et al. (2005a) Combined intracellular three-dimensional imaging and selective nanosurgery by a nonlinear microscope. J Biomed Opt 10:14002

Sacconi L, Tolić-Nørrelykke IM, Stringari C et al. (2005b) Optical micromanipulations inside yeast cells. Appl Opt 44:2001–2007

Sage MD, Jennings RB (1988) Cytoskeletal injury and subsarcolemmal bleb formation in dog heart during in vitro total ischemia. Am J Pathol 133:327–337

Sahenk Z, Chen L, Mendell JR (1999) Effects of PMP22 duplication and deletions on the axonal cytoskeleton. Ann Neurol 45:16–24

Sahni SK (2007) Endothelial cell infection and hemostasis. Thromb Res 119:531–549

Saito M, Matsuura T, Masaki T et al. (2006) Reconstruction of liver organoid using a bioreactor. World J Gastroenterol 12:1881–1888

Salzberg AD, Bloom MB, Mourlas NJ et al. (2002) Microelectrical mechanical systems in surgery and medicine. J Am Coll Surg 194:463–476

Sapir T, Elbaum M, Reiner O (1997) Reduction of microtubule catastrophe events by LIS1, platelet-activating factor acetylhydrolase subunit. EMBO J 16:6977–6984; http://emboj.oupjournals.org/cgi/content/full/16/23/6977

Sassera D, Beninati T, Bandi C et al. (2006) '*Candidatus Midichloria mitochondrii*', an endosymbiont of the tick *Ixodes ricinus* with a unique intramitochondrial lifestyle. Int J Syst Evol Microbiol 56:2535–2540

Sata M (2003) Circulating vascular progenitor cells contribute to vascular repair, remodeling, and lesion formation. Trends Cardiovasc Med 13:249–253

Satoa F, Togoa M, Islamb MK et al. (2005) Enzyme-based glucose fuel cell using Vitamin K3-immobilized polymer as an electron mediator. Electrochem Commun 7:643–647

Scaffidi P, Misteli T, Bianchi ME (2002) Release of chromatin protein HMGB1 by necrotic cells triggers inflammation. Nature 418:191–195

Schell WD, Myers JN (1997) Regression of atherosclerosis: a review. Prog Cardiovasc Dis 39: 483–496

Schenk D (2002) Amyloid-beta immunotherapy for Alzheimer's disease: the end of the beginning. Nat Rev Neurosci 3:824–828

Schewe PF, Stein B, Riordon J (2001) A carbon nanotube integrated circuit. American Institute of Physics Bulletin of Physics News No. 531, 22 March 2001; http://newton.ex.ac.uk/aip/physnews.531.html

Schliwa M (ed) (2003) Molecular Motors. VCH-Wiley, Weinheim

Schliwa M, Woehlke G (2003) Molecular motors. Nature 422:759–765

Schönbeck U, Libby P (2001) CD40 signaling and plaque instability. Circ Res 89:1092–1103

Schwartz AB, Cui XT, Weber DJ et al. (2006) Brain-controlled interfaces: movement restoration with neural prosthetics. Neuron 52:205–220

Schwartz JT (1990) The new connectionism: Developing relationships between neuroscience and artificial intelligence. In: Graubard SR (ed) The Artificial Intelligence Debate. MIT Press, Cambridge, MA

Schwartz M, Madariaga J, Hirose R et al. (2004) Comparison of a new fibrin sealant with standard topical hemostatic agents. Arch Surg 139:1148–1154

Seidman JG, Seidman C (2001) The genetic basis for cardiomyopathy: from mutation identification to mechanistic paradigms. Cell 104:557–567

Sell DR, Nagaraj RH, Grandhee SK et al. (1991) Pentosidine: a molecular marker for the cumulative damage to proteins in diabetes, aging, and uremia. Diabetes Metab Rev 7:239–251

Sell DR, Biemel KM, Reihl O et al. (2005) Glucosepane is a major protein cross-link of the senescent human extracellular matrix. Relationship with diabetes. J Biol Chem 280:12310–12315; http://www.jbc.org/cgi/content/full/280/13/12310

Shankaran V, Ikeda H, Bruce AT et al. (2001) IFNgamma and lymphocytes prevent primary tumour development and shape tumour immunogenicity. Nature 410:1107–1111

Sharom FJ (1997) The P-glycoprotein efflux pump: how does it transport drugs? J Membr Biol 160:161–175

Sharova NP (2005) How does a cell repair damaged DNA? Biochemistry (Mosc) 70:275–291

Shen N, Datta D, Schaffer CB et al. (2005) Ablation of cytoskeletal filaments and mitochondria in live cells using a femtosecond laser nanoscissor. Mech Chem Biosyst 2:17–25

Shimizu N, Kamezaki F, Shigematsu S (2005) Tracking of microinjected DNA in live cells reveals the intracellular behavior and elimination of extrachromosomal genetic material. Nucleic Acids Res 33:6296–6307

Shirai Y, Osgood AJ, Zhao Y et al. (2005) Directional control in thermally driven single-molecule nanocars. Nano Lett 5:2330–2334. See images at: "Rice scientists build world's first single-molecule car," 20 October 2005; http://www.media.rice.edu/media/NewsBot.asp?MODE=VIEW&ID=7850

Shirai Y, Morin JF, Sasaki T et al. (2006) Recent progress on nanovehicles. Chem Soc Rev 35:1043–1055

Shotelersuk V, Gahl WA (1998) Hermansky-Pudlak syndrome: models for intracellular vesicle formation. Mol Genet Metab 65:85–96

Sim HG, Yip SK, Cheng CW (2006) Equipment and technology in surgical robotics. World J Urol 24:128–135

Simoni P, Peters GE, Magnuson JS (2003) Use of the endoscopic microdebrider in the management of airway obstruction from laryngotracheal carcinoma. Ann Otol Rhinol Laryngol 112:11–13

Simons K, Gruenberg J (2000) Jamming the endosomal system: lipid rafts and lysosomal storage diseases. Trends Cell Biol 10:459–462

Smith AU (1965) Problems in freezing organs and their component cells and tissues. Fed Proc 24:S196–S203

Smith AU, Lovelock JE, Parkes AS (1954) Resuscitation of hamsters after supercooling or partial crystallization at body temperature below 0 degrees C. Nature 173:1136–1137

Solomon A, Weiss DT, Wall JS (2003) Immunotherapy in systemic primary (AL) amyloidosis using amyloid-reactive monoclonal antibodies. Cancer Biother Radiopharm 18:853–860

Soto C, Sigurdsson EM, Morelli L et al. (1998) Beta-sheet breaker peptides inhibit fibrillogenesis in a rat brain model of amyloidosis: implications for Alzheimer's therapy. Nat Med 4:822–826

Sprecher E, Ishida-Yamamoto A, Becker OM et al. (2001) Evidence for novel functions of the keratin tail emerging from a mutation causing ichthyosis hystrix. J Invest Dermatol 116: 511–519

Stefanadis C, Diamantopoulos L, Vlachopoulos C et al. (1999) Thermal heterogeneity within human atherosclerotic coronary arteries detected in vivo: A new method of detection by application of a special thermography catheter. Circulation 99:1965–1971

Stegner AR, Boehme C, Huebl H et al. (2006) Electrical detection of coherent ^{31}P spin quantum states. Nature Phys 2:835–838

Stein SF, Evatt B (1992) Chapter 13–2. Thrombocytopenia. In: Hurst JW, Medicine for the Practicing Physician, 3rd edn. Butterworth-Heinemann, Boston, MA, pp. 769–771

Steinhardt RA, Bi G, Alderton JM (1994) Cell membrane resealing by a vesicular mechanism similar to neurotransmitter release. Science 263:390–393

Stenger S, Hanson DA, Teitelbaum R et al. (1998) An antimicrobial activity of cytolytic T cells mediated by granulysin. Science 282:121–125

Strange C, Sahn SA (1999) The definitions and epidemiology of pleural space infection. Semin Respir Infect 14:3–8

Street SE, Hayakawa Y, Zhan Y et al. (2004) Innate immune surveillance of spontaneous B cell lymphomas by natural killer cells and gammadelta T cells. J Exp Med 199:879–884

Strehler BL, Mark DD, Mildvan AS et al. (1959) Rate and magnitude of age pigment accumulation in the human myocardium. J Gerontol 14:430–439

Subat M, Borovik AS, Konig B (2004) Synthetic creatinine receptor: imprinting of a Lewis acidic zinc(II)cyclen binding site to shape its molecular recognition selectivity. J Am Chem Soc 126:3185–3190

Sugaya K, Brannen CL (2001) Stem cell strategies for neuroreplacement therapy in Alzheimer's disease. Med Hypotheses 57:697–700

Swann JB, Smyth MJ (2007) Immune surveillance of tumors. J Clin Invest 117:1137–1146

Tada T (2006) Nuclear reprogramming: an overview. Methods Mol Biol 348:227–236

Takeuchi T, Adachi Y, Ohtsuki Y et al. (2007) Adiponectin receptors, with special focus on the role of the third receptor, T-cadherin, in vascular disease. Med Mol Morphol 40:115–120

Tamm SL (1982) Flagellated ectosymbiotic bacteria propel a eukaryotic cell. J Cell Biol 94: 697–709

Tangirala RK, Jerome WG, Jones NL et al. (1994) Formation of cholesterol monohydrate crystals in macrophage-derived foam cells. J Lipid Res 35:93–104

Tanskanen M, Kiuru-Enari S, Tienari P et al. (2006) Senile systemic amyloidosis, cerebral amyloid angiopathy, and dementia in a very old Finnish population. Amyloid 13:164–169

Tardif JC, Gregoire J, L'Allier PL et al. (2006) Effect of atherosclerotic regression on total luminal size of coronary arteries as determined by intravascular ultrasound. Am J Cardiol 98:23–27

Tatebayashi Y, Lee MH, Li L et al. (2003) The dentate gyrus neurogenesis: a therapeutic target for Alzheimer's disease. Acta Neuropathol (Berl) 105:225–232

Taylor PM, Sachlos E, Dreger SA et al. (2006) Interaction of human valve interstitial cells with collagen matrices manufactured using rapid prototyping. Biomaterials 27:2733–2737

Temelso B, Sherrill CD, Merkle RC, Freitas RA Jr (2006) High-level *ab initio* studies of hydrogen abstraction from prototype hydrocarbon systems. J Phys Chem A 110:11160–11173; http://www.MolecularAssembler.com/Papers/TemelsoHAbst.pdf

Temelso B, Sherrill CD, Merkle RC, Freitas RA Jr (2007) *Ab initio* thermochemistry of the hydrogenation of hydrocarbon radicals using silicon, germanium, tin and lead substituted methane and isobutane. J Phys Chem A 111:8677–8688; http://www.MolecularAssembler.com/Papers/TemelsoHDon.pdf

Terman A, Brunk UT (1998) Lipofuscin: mechanisms of formation and increase with age. APMIS 106:265–276

Terman A, Dalen H, Brunk UT (1999) Ceroid/lipofuscin-loaded human fibroblasts show decreased survival time and diminished autophagocytosis during amino acid starvation. Exp Gerontol 34:943–957

Thompson TE, Bennett I (1969) Physalia nematocysts utilized by mollusks for defense. Science 166:1532–1533

Tipler FJ (1994) The Physics of Immortality. Doubleday, New York

Tirlapur UK, Konig K (2002) Femtosecond near-infrared laser pulses as a versatile non-invasive tool for intra-tissue nanoprocessing in plants without compromising viability. Plant J 31: 365–374

Todar K (2003) Evasion of host phagocytic defenses. University of Wisconsin-Madison website; http://www.bact.wisc.edu/microtextbook/disease/evadephago.html

Tonet O, Focacci F, Piccigallo M et al. (2006) Comparison of control modes of a hand-held robot for laparoscopic surgery. Int Conf Med Image Comput Comput Assist Interv 9:429–436

Totaro EA, Pisanti FA, Continillo A et al. (1985) Morphological evaluation of the lipofuscinolytic effect of acetylhomocysteine thiolactone. Arch Gerontol Geriatr 4:67–72

Tse RL, Phelps P (1970) Polymorphonuclear leukocyte motility in vitro. V. Release of chemotactic activity following phagocytosis of calcium pyrophosphate crystals, diamond dust, and urate crystals. J Lab Clin Med 76:403–415

Tseng GY, Ellenbogen JC (2001) Toward nanocomputers. Science 294:1293–1294

Ubelaker DH, Buchholz BA, Stewart JEB (2006) Analysis of artificial radiocarbon in different skeletal and dental tissue types to evaluate date of death. J Forensic Sci 51:484–488

Vallee RB, Tai C, Faulkner NE (2001) LIS1: cellular function of a disease-causing gene. Trends Cell Biol 11:155–160

Vaupel JW, Carey JR, Christensen K et al. (1998) Biodemographic trajectories of longevity. Science 280:855–860
Veomett G, Prescott DM (1976) Reconstruction of cultured mammalian cells from nuclear and cytoplasmic parts. Methods Cell Biol 13:7–14
Vettiger P, Cross G, Despont M et al. (2002) The Millipede – nanotechnology entering data storage. IEEE Trans Nanotechnol 1:39–55
Villar-Garea A, Imhof A (2006) The analysis of histone modifications. Biochim Biophys Acta 1764:1932–1939
Vital C, Bouillot S, Canron MH et al. (2002) Schwannian crystalline-like inclusions bodies (Fardeau-Engel bodies) revisited in peripheral neuropathies. Ultrastruct Pathol 26:9–13
Vogel S (1998) Cats' Paws and Catapults: Mechanical Worlds of Nature and People. W.W. Norton and Company, New York
von Neumann J (1958) The Computer and the Brain. Yale University Press, New Haven CT
Wagner OI, Rammensee S, Korde N et al. (2007) Softness, strength and self-repair in intermediate filament networks. Exp Cell Res 313:2228–2235
Wakida NM, Lee CS, Botvinick ET et al. (2007) Laser nanosurgery of single microtubules reveals location-dependent depolymerization rates. J Biomed Opt 12:024022
Wall RJ (2001) Pronuclear microinjection. Cloning Stem Cells 3:209–220
Walski M, Chlopicki S, Celary-Walska R et al. (2002) Ultrastructural alterations of endothelium covering advanced atherosclerotic plaque in human carotid artery visualised by scanning electron microscope. J Physiol Pharmacol 53:713–723
Walkley SU (2007) Pathogenic mechanisms in lysosomal disease: a reappraisal of the role of the lysosome. Acta Paediatr Suppl 96:26–32
Wang PM, Cornwell M, Prausnitz MR (2005) Minimally invasive extraction of dermal interstitial fluid for glucose monitoring using microneedles. Diabetes Technol Ther 7:131–141
Wang X, Song J, Liu J et al. (2007) Direct-current nanogenerator driven by ultrasonic waves. Science 316:102–105
Weatherbee CW, Freitas RA Jr (2010) The structure of the human kidney as applicable to nanoscale robot navigation. In preparation.
Weber G, Greulich KO (1992) Manipulation of cells, organelles, and genomes by laser microbeam and optical trap. Int Rev Cytol 133:1–41
West C (1979) A quantitative study of lipofuscin accumulation with age in normals and individuals with Down's syndrome, phenylketonuria, progeria and transneuronal atrophy. J Comp Neurol 186:109–116
Westbroek W, Lambert J, Naeyaert JM (2001) The dilute locus and Griscelli syndrome: gateways towards a better understanding of melanosome transport. Pigment Cell Res 14:320–327
Westermark P, Wilander E (1978) The influence of amyloid deposits on the islet volume in maturity onset diabetes mellitus. Diabetologia 15:417–421
Wiley C (2005) Nanotechnology and molecular homeostasis. J Amer Geriatrics Soc 53:S295–S298
Williams DS (2002) Transport to the photoreceptor outer segment by myosin VIIa and kinesin II. Vision Res 42:455–462
Winchester B, Vellodi A, Young E (2000) The molecular basis of lysosomal storage diseases and their treatment. Biochem Soc Trans 28:150–154
Winter SH, Bouzit M (2007) Use of magnetorheological fluid in a force feedback glove. IEEE Trans Neural Syst Rehabil Eng 15:2–8
Wissler RW, Vesselinovitch D (1990) Can atherosclerotic plaques regress? Anatomic and biochemical evidence from nonhuman animal models. Am J Cardiol 65:33F–40F
Wolf DH, Hilt W (2004) The proteasome: a proteolytic nanomachine of cell regulation and waste disposal. Biochim Biophys Acta 1695:19–31
Wolf E, Schernthaner W, Zakhartchenko V et al. (2000) Transgenic technology in farm animals – progress and perspectives. Exp Physiol 85:615–625
Wood KJ, Prior TG (2001) Gene therapy in transplantation. Curr Opin Mol Ther 3:390–398

Wray GA, Hahn MW, Abouheif E et al. (2003) The evolution of transcriptional regulation in eukaryotes. Mol Biol Evol 20:1377–1419; http://mbe.oxfordjournals.org/cgi/content/full/20/9/1377

Wright LM, Brzozowski AM, Hubbard RE et al. (2000) Structure of fab hGR-2 F6, a competitive antagonist of the glucagon receptor. Acta Crystallogr D Biol Crystallogr 56:573–580

Wu JT (2002) C-erbB2 oncoprotein and its soluble ectodomain: a new potential tumor marker for prognosis early detection and monitoring patients undergoing Herceptin treatment. Clin Chim Acta 322:11–19

Xie XY, Barrett JN (1991) Membrane resealing in cultured rat septal neurons after neurite transection: evidence for enhancement by Ca(2+)-triggered protease activity and cytoskeletal disassembly. J Neurosci 11:3257–3267

Xu T, Jin J, Gregory C et al. (2005) Inkjet printing of viable mammalian cells. Biomaterials 26: 93–99

Xu T, Gregory CA, Molnar P et al. (2006) Viability and electrophysiology of neural cell structures generated by the inkjet printing method. Biomaterials 27:3580–3588

Yagishita S, Itoh Y, Nakano T et al. (1979) Crystalloid inclusions reminiscent of Hirano bodies in autolyzed peripheral nerve of normal Wistar rats. Acta Neuropathol (Berl) 47:231–236

Yan L, Zucker S, Toole BP (2005) Roles of the multifunctional glycoprotein, emmprin (basigin; CD147), in tumour progression. Thromb Haemost 93:199–204

Ye L, Haider HK, Sim EK (2006) Adult stem cells for cardiac repair: a choice between skeletal myoblasts and bone marrow stem cells. Exp Biol Med 231:8–19

Yanik MF, Cinar H, Cinar HN et al. (2004) Neurosurgery: functional regeneration after laser axotomy. Nature 432:822

Yesin KB, Exner P, Vollmers K et al. (2005) Biomedical micro-robotic system. 8th Intl. Conf. on Medical Image Computing and Computer Assisted Intervention (MICCAI 2005 / www.miccai2005.org), Palm Springs CA, 26–29 October 2005, p. 819

Yokobayashi Y, Weiss R, Arnold FH (2002) Directed evolution of a genetic circuit. Proc Natl Acad Sci USA 99:16587–16591; http://www.pnas.org/cgi/content/abstract/99/26/16587

Yun MH, Cannon D, Freivalds A et al. (1997) An instrumented glove for grasp specification in virtual-reality-based point-and-direct telerobotics. IEEE Trans Syst Man Cybern B Cybern 27:835–846

Zhang C, Gu Y, Chen L (1998) Study on early frozen section after nerve repair with cell surgery technique. Chin J Traumatol 1:45–48

Zhang H, Li N, Chen Y et al. (2007) Protein profile of human lung squamous carcinoma cell line NCI-H226. Biomed Environ Sci 20:24–32

Zhang S, Cordon-Cardo C, Zhang HS et al. (1997) Selection of tumor antigens as targets for immune attack using immunohistochemistry: I. Focus on gangliosides. Int J Cancer 73:42–49

Zhang Z, Weed SA, Gallagher PG et al. (2001) Dynamic molecular modeling of pathogenic mutations in the spectrin self-association domain. Blood 98:1645–1653

Zhao C, Takita J, Tanaka Y et al. (2001) Charcot-Marie-Tooth disease type 2A caused by mutation in a microtubule motor KIF1Bbeta. Cell 105:587–597

Zhijiang D, Zhiheng J, Minxiu K (2005) Virtual reality-based telesurgery via teleprogramming scheme combined with semi-autonomous control. Conf Proc IEEE Eng Med Biol Soc 2: 2153–2156

Zullo SJ, Parks WT, Chloupkova M et al. (2005) Stable transformation of CHO Cells and human NARP cybrids confers oligomycin resistance (oli(r)) following transfer of a mitochondrial DNA-encoded oli(r) ATPase6 gene to the nuclear genome: a model system for mtDNA gene therapy. Rejuvenation Res 8:18–28